EVIDENCE FOR IMPACT-GENERATED DEPOSITION

ON THE LATE EOCENE SHORES OF GEORGIA

by

ROBERT SCOTT HARRIS

(Under the direction of Michael F. Roden)

ABSTRACT

Modeling demonstrates that the Late Eocene Chesapeake Bay impact would have been capable of depositing ejecta in east-central Georgia with thicknesses exceeding thirty centimeters. A coarse sand layer at the base of the Upper Eocene Dry Branch Formation was examined for shocked minerals. Universal stage measurements demonstrate that planar fabrics in some fine to medium sand-size quartz grains are parallel to planes commonly exploited by planar deformation features (PDF's) in shocked quartz. Possible PDF's are observed parallel to {10-13}, {10-11}, {10-12}, {11-22} and {51-61}. Petrographic identification of shocked quartz is supported by line broadening in X-ray diffraction experiments. Other impact ejecta recognized include possible ballen quartz, maskelynite, and reidite-bearing zircon grains. The layer is correlative with an unusual diamictite that contains goethite spherules similar to altered microkrystites. It may represent an impact-generated debris flow. These discoveries suggest that the Chesapeake Bay impact horizon is preserved in Georgia. The horizon also should be the source stratum for Georgia tektites.

INDEX WORDS: Chesapeake Bay impact, Upper Eocene, Shocked quartz, Impact shock, Shocked zircon, Impact, Impact ejecta, North American tektites, Tektites, Georgiaites, Georgia Tektites, Planar deformation features, PDF's, Georgia, Geology, Coastal Plain, Stratigraphy, Impact stratigraphy, Impact spherules, Goethite spherules, Diamictite, Twiggs Clay, Dry Branch Formation, Clinchfield Sand, Irwinton Sand, Reidite, Microkrystite, Cpx Spherules, Impact debris flow

EVIDENCE FOR IMPACT-GENERATED DEPOSITION

ON THE LATE EOCENE SHORES OF GEORGIA

by

ROBERT SCOTT HARRIS

B. S., Arizona State University, 2000

A Thesis Submitted to the Graduate Faculty of the University of Georgia in Partial Fulfillment of the Requirement for the Degree

MASTER OF SCIENCE

ATHENS, GEORGIA

2003

EVIDENCE FOR IMPACT-GENERATED DEPOSITION

ON THE LATE EOCENE SHORES OF GEORGIA

by

ROBERT SCOTT HARRIS

Major Professor: Michael Roden

Committee: Steven Holland
Paul Schroeder

Electronic Version Approved:

Maureen Grasso
Dean of the Graduate School
The University of Georgia
August, 2003

Dedicated to the Memory of

Dr. Robert S. Dietz

A pioneer in impact studies and a trusted mentor

who taught me the value of taking risks

in the pursuit of science

ACKNOWLEDGEMENTS

Scientific research, like most of life's pursuits, engages some degree of risk. Yet when this project was conceived, it arguably embraced more than its share. It was indeed a search for a needle in a haystack (or more precisely, a very large pile of sand). I am not certain whether in the beginning there was any real expectation of success. To be candid, had it not been for a few turns of extraordinary chance, I would have not found any evidence of the impact horizon. Without the advise, assistance, expertise, and encouragement of a huge number of people, I would have never found my way to those rare moments when luck had an opportunity to strike. I would like to express my deepest appreciation to all my friends, family, and colleagues who have influenced this work.

This endeavor would not have been possible without the counsel of Mike Roden. Mike gave me an opportunity to take my passion for planetary geology in a direction that I had never anticipated. I am grateful for his guidance, patience, and constant belief in my ability to pursue this research.

Paul Schroeder's observations provided the initial motivation for this project (see pages 8 and 9). Paul has been a valuable source of encouragement and assistance. His many hours of instruction, aid, and collaboration, particularly in stretching the limits of X-ray diffraction, are most appreciated. I also would like to thank Steve Holland for his critical comments and advice regarding Coastal Plain stratigraphy and depositional processes.

Mack Duncan (J. M. Huber Corporation) granted access to the Purvis School and Bracewell kaolin mines. Mack also has given valuable field assistance and insights into the local stratigraphy. Dennis Parmley (Georgia College and State University) arranged access to the Hardie Mine in Wilkinson County. Charles Jordan (Thiele Kaolin Company) provided access to diamictite exposures in Glascock County.

Glenn Izett (College of William and Mary) donated examples of shocked quartz from the K-T boundary of Colorado. Sarah Chadima (South Dakota Geological Survey) provided samples of Manson impact ejecta from the Crow Creek sand. Philippe Claeys (Free University of Brussels) contributed examples of goethite spherules collected from the K-T boundary at Agost, Spain. Wright Horton (United States Geological Survey, Reston), Bill Hames and David King (Auburn University), and John McHone (Arizona State University) have offered advice concerning the identification of shocked quartz and other impact materials and deposits.

Lucy Edwards and David Powars (USGS, Reston) have shared valuable information about the Chesapeake Bay impact structure and southeastern Coastal Plain stratigraphy. Tim Chowns (State University of State Georgia), Burt Carter (Georgia Southwestern State University), and John Anderson (Georgia Perimeter College) have improved my understanding of the Eocene geology of Georgia. Hal Povenmire and Robert Strange have provided useful discussions concerning the locations of Georgia tektites. Other timely comments and encouragement have come from Cecelia McHugh and Dallas Abbott (Columbia University), Peter Schultz (Brown University), Shaobin Liu (University of Delaware), and Gilles Allard, O. Isik Ece, Susan Goldstein, Norman Herz, Vernon Hurst, Bruce Railsback, and Sally Walker (University of Georgia). I would also like to thank John Allen (UGA), who presently is attempting to unravel the sequence stratigraphy across the impact horizon, for assistance in the field and for lengthy discussions about the Upper Eocene sediments. Chris Fleischer (UGA Electron Microprobe Facility) and John Shields and Mark Farmer (UGA Center for Advanced Ultrastructural Research) assisted with electron microscopy.

I am especially grateful to Christian Koeberl (University of Vienna) and Billy Glass (University of Delaware) for allowing me to constantly pester them for their critical input. And I am indebted to Bevan French (Smithsonian Institution) for sharing his wisdom and hospitality and for being a reliable source of information on shock metamorphism and impact processes.

This research has been funded in part by the Miriam Watts-Wheeler Howard Scholarship Fund (UGA) and by the Geological Society of America (Grant #7408-03). Additional funding for travel expenses associated with presenting the results has been provided by the Southeastern Section of GSA and by the Clay Minerals Society.

I would like to add a special dedication to three individuals. Ed Albin (Fernbank Science Center) laid the foundation for my research. The task of finding the impact horizon would have been monumental, if not impossible, without his dissertation. Ron Greeley (Arizona State University) taught both Ed and I the fundamentals of planetary geology. Without his continuing support, I would never have had most of the opportunities that I have been blessed with to pursue my professional interests. Finally, none of this would have been possible without the love, support, and understanding of Karen Black, who recently undertook the greatest risk of all ─ becoming my bride.

TABLE OF CONTENTS

CHAPTER 1

INTRODUCTION

For centuries inhabitants and visitors to east-central Georgia have collected small pebbles of greenish-black glass from streambeds, roadsides, and backyards (Povenmire, 1975; Povenmire, 1985). These Georgia tektites, or georgiaites (Figure 1), are believed to have been produced and deposited as a result of the Chesapeake Bay impact (Figure 2) (Poag et al., 1994; Albin et al., 2000; Montanari and Koeberl, 2000) during the Late Eocene approximately 35.2 to 35.5 Ma (Poag and Aubry, 1995). Albin and Wampler (1996; Albin, 1997a) have determined an average georgiaite age of 35.2 (± 0.7) Ma from potassium-argon dating.

Although more than 1700 georgiaites have been discovered across 18 counties (Figure 3) (Povenmire, 2002), none of those have been recovered from Upper Eocene sediments. Most, if not all, of the georgiaites have been found in recently deposited alluvium (McCall, 2001), with one of the newest finds coming from a gravel bar in the middle of the Savannah River (H. Povenmire and R. Strange, personal communication, 2003). The radiometric ages and typically water-worn appearances of the georgiaites (Albin, 1997a,b) attest that these objects must have been eroded and transported from Eocene sediments exposed to the north and northeast (King, 1962; Storzer et al., 1973; Albin, 1997b) (see Figure 4).

Figure 1. A photograph displaying several examples of Georgia tektites, or georgiaites, believed to have been ejected from the Chesapeake Bay impact structure approximately 35.2 to 35.5 Ma (Poag and Aubry, 1995). Photograph courtesy of Edward Albin (Fernbank Science Center).

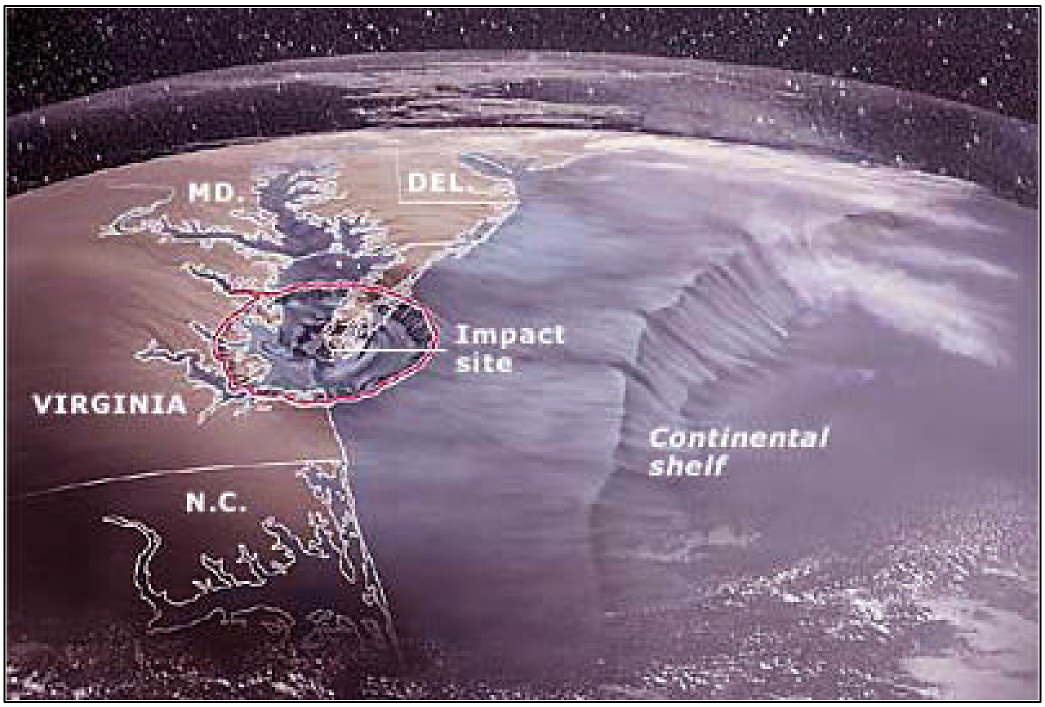

Figure 2. An illustration showing the location of the 90-kilometer wide (Poag, 1997) Chesapeake Bay impact structure, a peak-ring crater formed during the Late Eocene (Poag et al., 1994). Today the crater is buried beneath 300 to 500 meters of sediment (Powars and Bruce, 2000). Artwork by Michael Hall (©*The Virginian-Pilot*, 2001; used with permission).

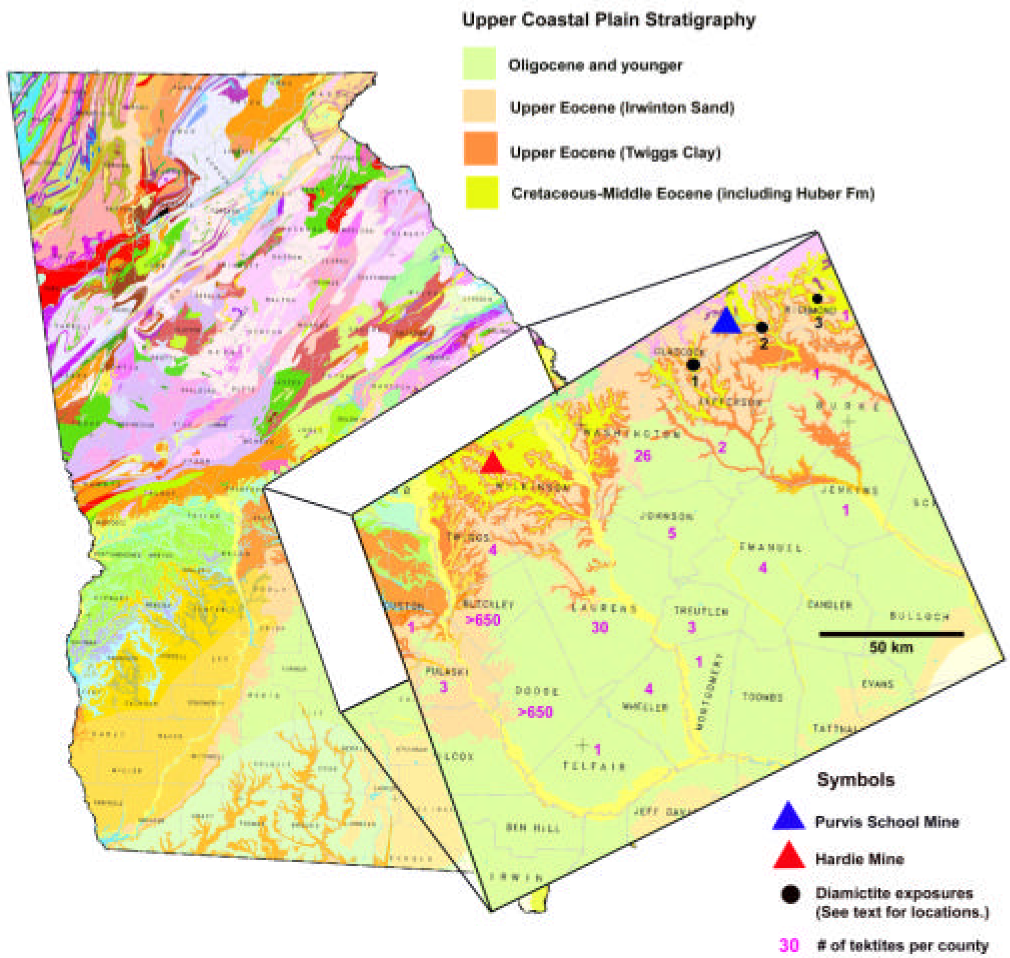

Figure 3. Geologic map of Georgia showing the major lithostratigraphic divisions in the upper Coastal Plain and the number of georgiaite finds by county. The locations of specific sites discussed in the text are shown. Tektite data from Povenmire (1995, 2003). Base geologic map is a product of the Georgia Geologic Survey (1999).

For at least four decades, geologists and tektite collectors alike have pondered the nature and location of the georgiaite source stratum. Because some georgiaites are found "on" gravels associated with the Tobacco Road Sand (Povenmire, 1985), a formation considered by some workers to have been deposited during the Late Eocene (Huddlestun and Hetrick, 1986), Povenmire (2002) has proposed that the Tobacco Road Sand holds the tektite reservoir. His proposal has been supported by the failure to identify tektites in older Upper Eocene units (i.e. the Irwinton Sand, Twiggs Clay, or Clinchfield Sand — see Figure 4.) However, Hurst and Pickering (1989) concluded that the Tobacco Road Sand postdates the Eocene-Oligocene boundary, and Albin (1997a) reported biostratigraphic evidence and glauconite ages that seem to indicate that sediments older than the Tobacco Road Sand, specifically the Twiggs Clay and Irwinton Sand, were deposited approximately 33 to 34 Ma and are significantly younger than the georgiaites.

Using biostratigraphic data and potassium-argon ages of glauconite, which he considered to give at least reliable *minimum* ages for the sediments, Albin (1997a) presented a straightforward set of constraints on the position of an approximately 35 Ma horizon in the Coastal Plain sequence (summarized in Figure 4). Albin and Wampler (1996; Albin, 1997a) reasoned that the tektite layer should lie near the base of the Twiggs Clay and Irwinton Sand (sometimes collectively referred to as the Dry Branch Formation).

L. E. Edwards (personal communication, 2003; Parmley and Holman, 2003) recently completed a study of the microfossils and nannofossils in a one meter-thick fossiliferous

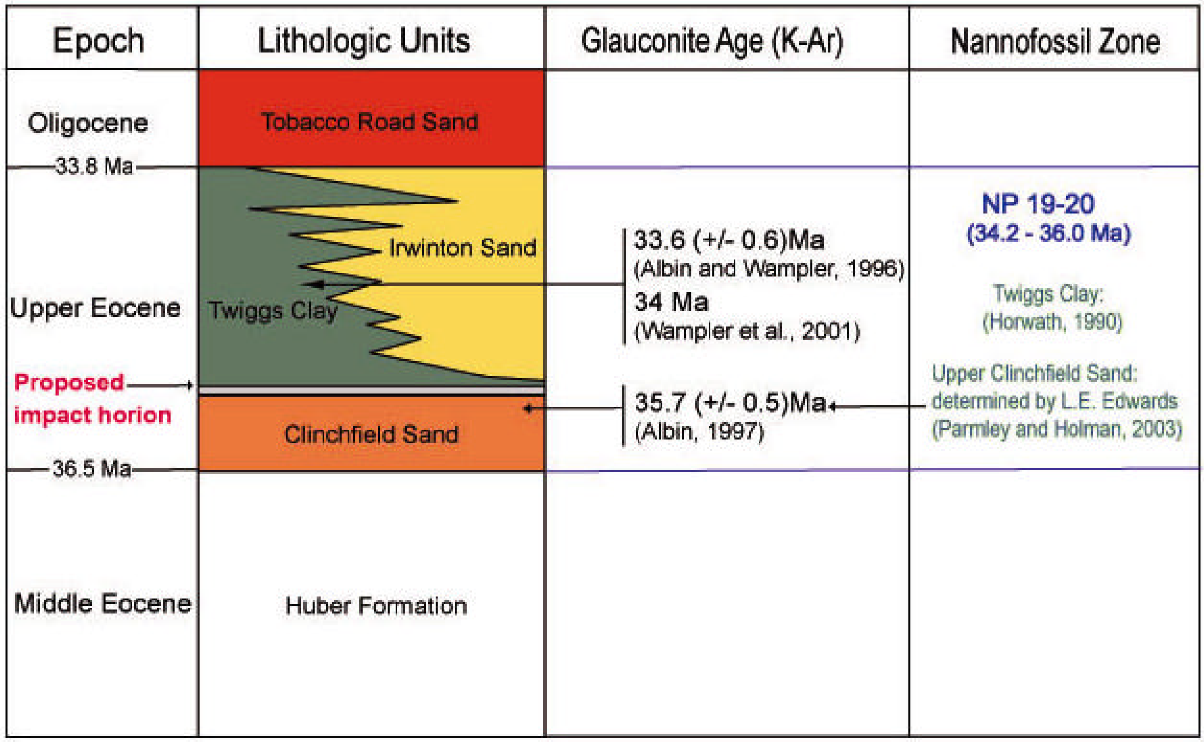

Figure 4. Lower Tertiary stratigraphy of the upper Georgia Coastal Plain. Based on Albin (1997a), the diagram outlines the important biostratigraphic and radiometric data constraining the location of a 35.2 to 35.5 Ma impact horizon. The horizon (colored gray) is expected to lie at or just below the base of the Twiggs Clay and Irwinton Sand. Nannofossil Zone NP 19-20 correlates to an age of 34.2 to 36.0 Ma on the Berggren et al. (1995) timescale (Parmley and Holman, 2003); therefore, the upper portion of the Clinchfield Sand has a maximum age of 36.0 Ma. Absolute ages are after Berggren et al. (1995) unless otherwise indicated.

sand unit below the base of the Twiggs Clay in Wilkinson County. She determined that the sand, commonly referred to as the Clinchfield Sand (Westgate, 2001), lies in nannofossil zones NP19-20, indicative of an age ranging from 34.2 to 36.0 Ma on the Berggren et al. (1995) timescale (Parmley and Holman, 2003). These results are entirely consistent with the conclusions presented by Albin and Wampler (1996). The georgiaite source stratum should occur within the base of the Dry Branch Formation or in those sands immediately below the Twiggs and Irwinton members. It is important to note that Ward (1989), prior to the discovery of the Chesapeake Bay impact structure, asserted that the Twiggs Clay is correlative with the Chickahominy Formation in Virginia. Later it was shown that the Chickahominy Formation is the first undisturbed marine unit that overlies the crater-filling breccias produced by the impact (Powars and Bruce, 2000).

Following the discovery of the Chesapeake Bay impact structure in the early 1990's and the realization that georgiaites probably are connected to its formation, the search for the tektite source stratum took on new dimensions both in terms of its scientific importance and in terms of new ideas that might be applied toward discovering its location. Chief among the points to consider is that the tektite source stratum should contain other ejecta products, including shocked minerals. The proximity of Georgia to the impact site (≈700 kilometers) could mean that ejecta were deposited with volumes and thicknesses at least large enough to make finding the materials in the sedimentary record feasible. As demonstrated in the next chapter, eastern Georgia may have been within the range covered by discontinuous ejecta. Although ejecta in that part of the field probably was patchy (Melosh, 1989), the distribution of shocked and fragmented debris might be somewhat more evenly distributed across the region than the tektites which likely jetted away from the target following discrete ray paths (Koeberl, 1989).

Albin (1997a) recognized the potential value of searching for shocked minerals, particularly quartz, and conducted a brief search along the contact between the Clinchfield Sand and Twiggs Clay in Bleckley and Dodge Counties. He chose those counties because the largest concentrations of tektite finds occur there. Previously, Zwart and Glass (Zwart, 1978) had looked for microtektites in the same vicinity. Horwath (1990) also scanned the Twiggs Clay for microtektites. Each of these efforts failed to discover impact debris, and the location of the georgiaite source stratum has remained an enigma.

A more recent report of disrupted sediments near the base of the Upper Eocene section in Jefferson County sparked new interest in the location of the Chesapeake Bay impact horizon in Georgia. P. A. Schroeder and S. M. Holland (personal communication to M. F. Roden, 2001) described a clay clast, approximately two meters in length, "floating" in a layer of coarse quartz sand (Figure 5)[1]. Their observation prompted M. F. Roden and the author to renew the search for mineralogical evidence of the impact in Coastal Plain sediments (Harris et al., 2002).

In addition to opening new directions of research into impact processes, ejecta dynamics, ejecta preservation, and the cataclysmic effects of the Chesapeake Bay impact on geological and ecological systems, discovery of the layer would establish a 35 Ma *key*

---

[1] As a result of active mining, the exposure shown in Figure 5 has been destroyed and its exact relationship to the proposed impact horizon has not been established. Although the sediments shown are not similar to the shocked quartz-bearing sands described in Chapter 4 or the diamictite described in Chapter 5, they may be similar to some sediments at the base of the Irwinton Sand in J. M Huber's Bracewell mine (see Figure 41), approximately 50 centimeters above the diamictite. The clast could represent very high-energy deposition resulting from an impact-generated tsunami, but this hypothesis has not been examined.

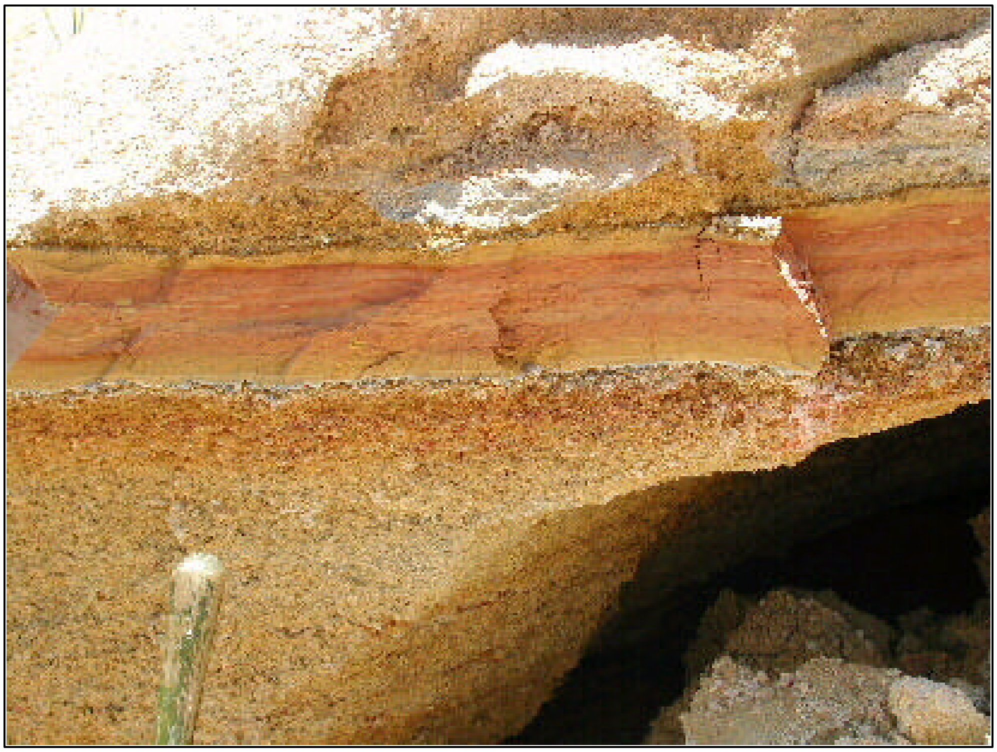

Figure 5. Photograph showing a clay clast "floating" in a layer of coarse quartz-rich sand. According to M. Duncan (personal communication, 2002) the image represents a sand unit approximately one meter above the base of the Upper Eocene sediments in J. M. Huber Corporation's Bracewell mine. The unusual clast, suggestive of very high-energy emplacement, sparked the search for Chesapeake Bay impact horizon reported in this thesis. Frame is approximately two meters wide. Photograph courtesy of Steven M. Holland (University of Georgia).

bed in Coastal Plain stratigraphy that could be used to improve regional and global correlation models. It eventually might lead to more complete characterizations of depositional environments along the Eocene shoreline of Georgia and could refine our understanding of the valuable kaolin deposits that underlie the Upper Eocene sediments (i.e., the Huber Formation in Figure 4).

The chapters that follow report the approach, methods, and results of a comprehensive investigation aimed at identifying impact ejecta at the base of the Twiggs Clay in east-central Georgia. Chapter 2 outlines four criteria that are critical for locating ejecta associated with georgiaites and the Chesapeake Bay event. Previous unsuccessful studies – Zwart (1978), Horwath (1990), and Albin (1997a) – overlooked one or more of those criteria. The brief discussion raises some important considerations applicable to any endeavor to locate distal ejecta deposits in coastal plain settings. Chapter 3 describes shocked quartz and the methods used to identify shocked grains in unconsolidated sandy sediments. Sample collection, processing, and preparation are discussed in addition to the analytical techniques used to characterize quartz micro-fabrics diagnostic of impact metamorphism. Chapter 4 reports the discovery of possible shocked quartz grains and other ejecta from two sites in east-central Georgia. Finally, Chapter 5 addresses the nature of an unusual Upper Eocene diamictite that may have an impact-related origin.

CHAPTER 2

APPROACH

Criteria for locating ejecta deposits from the Chesapeake Bay impact

1. Select sediments close to the correct age.

Investigations by Albin (1997a), Horwath (1990), and Zwart (1978) each fell short of locating the impact horizon, probably because each effort failed to account for at least one of four critical criteria. The most obvious, the most important, and yet by no means the easiest requirement to meet is limiting the search to sediments of approximately the correct age. The search for the impact horizon can be narrowed to the base of the Twiggs Clay and Irwinton Sand only after a significant number of stratigraphic, biostratigraphic, and radiometric constraints have been compiled (Figure 4). Unless one wishes to exhaust an incredible amount of time, limiting the hunt to just Upper Eocene strata is not sufficient. Horwath (1990) searched only within the body of the Twiggs Clay thus excluding sediments old enough to host a 35.2 to 35.5 Ma horizon.

Where reliable age constrains are not complied, or are not available, successful searches rely on the recognition of "unusual" or out-of-place deposits in a sedimentary sequence (Montanari and Koeberl, 2000) or on the identification of geochemical signatures indicative of an extraterrestrial bolide (Alvarez et al., 1990). Although future geochemical analyses may help test the conclusions reached as a result of this study, screening the Coastal Plain column for an Upper Eocene iridium anomaly has not been attempted because the normal cycling of platinum group elements (PGE's) in those sediments has not been studied. Establishing an accurate background PGE profile for Coastal Plain sediments, necessary to demonstrate a true anomaly, would require tremendous time and expense that may be difficult to justify given that an iridium anomaly associated with the Chesapeake Bay event has never been identified (Montanari and Koeberl, 2000). However, a 35.7 Ma global iridium anomaly has been attributed to the Popigai (Siberia) impact (Alvarez et al., 1982; Montanari et al., 1993; Kyte, 2001) and might be inherited in Chesapeake-related deposits that reworked slightly older sediments.

2. *Search for resilient materials.*

Zwart (1978) and Horwath (1990) both searched for microtektites in Georgia. Tektite glass eventually alters to smectitic clays (Bauluz et al., 2000). B. Glass (personal communication, 2003) has suggested that tiny microtektites may transform completely in Coastal Plain sediments. However, quartz is resilient in most environments. Despite some evidence that shocked silicate minerals may dissolve more rapidly than unshocked varieties (Boslough and Cygan, 1988; Boslough, 1991), quartz typically is highly resistant to chemical weathering and probably provides the best opportunity to identify the impact layer. This strategy assumes that quartzose materials are available in the target area. Fortunately, the Chesapeake Bay bolide excavated 650 meters of Early Tertiary and Cretaceous quartz-rich sediments and probably more than one kilometer of crystalline basement (Powers et al, 1993). Consequently, a large volume of quartz was available to be ejected.

3. *Maximize the amount of primary ejecta in the search area.*

Focusing on where the most *primary* ejecta, in terms of both volume and thickness, might have landed in Georgia maximizes the opportunity to find impact debris. *Primary* ejecta are materials excavated from the main crater or derived from the bolide as opposed to secondary ejecta which are derived from ejecta-surface interactions beyond the crater rim (Melosh, 1989). Generally the closer one can search to the target area, the better are the chances of finding primary ejecta. The thickness of sand-size ejecta expected to accumulate at various distances from the target may be estimated from equations derived from explosion experiments (McGetchin, 1973) and simulated hypervelocity impacts (Stöffler, 1975). The important relationships are expressed by the following equation:

$$T = K R^{a} (r/R)^{b} , \quad (1)$$

where T is the thickness of the ejecta at a distance, r, from the center of the impact and R is the radius of the transient crater (all in meters). K is a scaling coefficient. *a* and *b* are exponents, where *a* ranges from 0.74 to 1 and *b* ranges from –3.5 to –2.8 (Melosh, 1989). Setting *a* equal to 1, b *equal* to –2.8, K equal to 0.06 (Stöffler, 1975), and assuming the maximum transient crater formed by the Chesapeake Bay impact had a radius of 30 kilometers (for complex craters the diameter of the transient crater is ≈ 0.65 times the diameter of the final structure (Melosh, 1989), in this case 45 kilometers (Poag et al., 1994), the thickness of quartz-rich ejecta that might have been deposited in east-central Georgia is calculated. Figure 6 illustrates the relationship of ejecta thickness to distance from the target and to the position of the Late Eocene shoreline. The calculation suggests that between 15 and 30 centimeters of ejecta might have fallen in east-central Georgia.

As a measure of how thick an impact-generated unit might be, the results from Equation 1 probably should be considered too low (Melosh, 1989). The relationship ignores the contribution of secondary cratering to the final thickness of the impact deposit, yet locally derived material resulting from secondary events may comprise more than 60% of the deposit's final volume (Hörz et al., 1983; Melosh, 1989).

As a measure of how much *primary* ejecta was deposited, Equation 1 also likely leads to an underestimate because the relationship assumes an impact in dry sand. The Chesapeake Bay impact occurred into 100 to 300 meters of water (Powars and Bruce, 2000) overlying water-rich sediments (Poag, 1997). Impacts in saturated target materials are poorly understood, but it is generally assumed that saturation results in fluidization of the ejecta and may dramatically increase the radial distribution (Melosh, 1989). Ejection angles increase (Melosh, 1989; Melosh, 2002); therefore, a greater volume of ejecta is expelled to greater distances. The volume of continuous ejecta (within 5 crater radii of the impact) may increase by 20% (Stewart et al., 2000). Additionally, very fluid ground-hugging debris flows may develop (Melosh, 1989). Finally, Montanari and Koeberl (2000) suggest that the asymmetry of the North American tektite strewn field (Figure 7), indicates that the impact might have been oblique. In addition to launching most of the tektites down range of the collision, obliquity might have increased the volume of ejecta

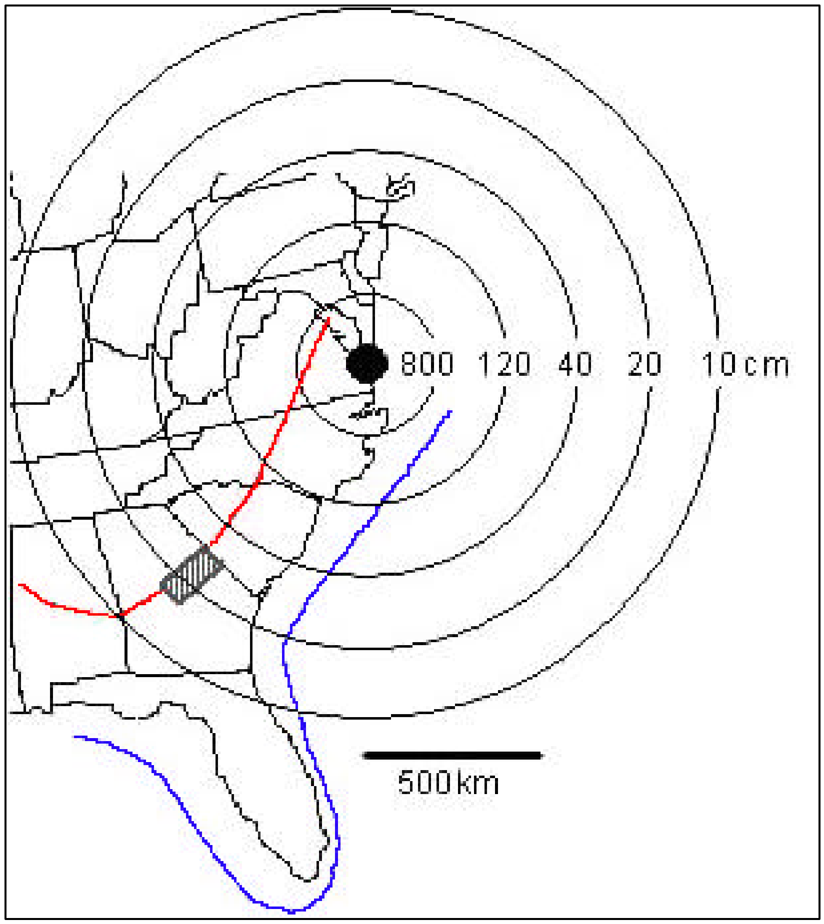

Figure 6. Isopach map illustrating the estimated minimum thickness (in centimeters) of *primary* ejecta that may have accumulated at 200, 400, 600, 800, and 1000 kilometers away from the Chesapeake Bay impact (see text for calculation and discussion). The shaded box approximately outlines the region of interest during the current study. The red and blue curves outline the approximate locations of the shoreline and shelf margin, respectively, during the Late Eocene [after Poag (1998) and Carter et al (1995)].

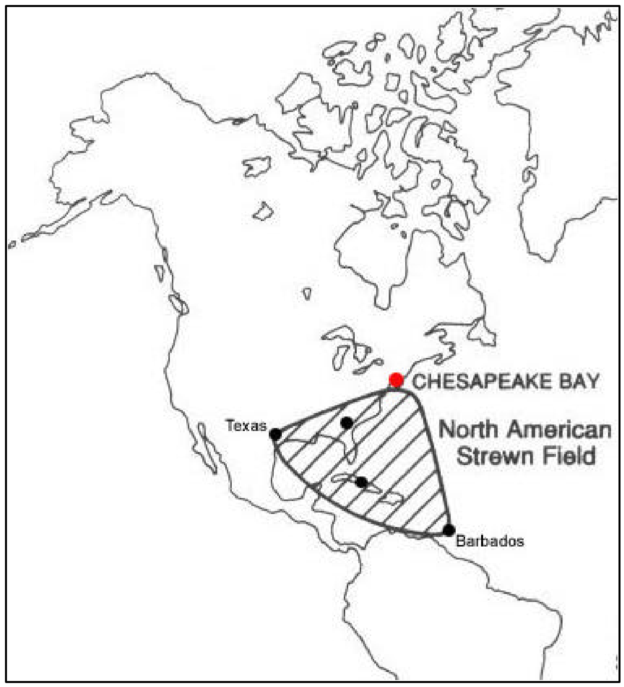

Figure 7. Map illustrating the limits of Late Eocene tektite distribution relative to the location of the Chesapeake Bay impact structure. Most of the tektites appear to have fallen south and southwest of the impact site suggesting that the bolide may have struck obliquely from the north-northeast Black dots indicate the major regions where tektites have been recovered. After Montanari and Koeberl (2000).

carried south of the crater significantly. These last three points will become important in Chapter 5.

Calculations based on Equation 1 ignore atmospheric interactions that conceivably could attenuate ejecta velocities and lead to an overestimate of distal ejecta thickness. However, atmosphere-ejecta interactions — and atmosphere-bolide interactions — are more complex than can be imagined using a simple model (Melosh, 1989; Schultz, 1992; Barnouin-Jha, and Schultz, 1998). Although Equation 1 may not be useful for predicting final ejecta thickness with great accuracy, it still may be handy for illustrating general trends in how thickness varies throughout the ejecta field and where it may or may not be reasonable to search for ejecta in sediments.

In the only two previously reported systematic searches for the impact horizon in Georgia, Albin (1997a) and Zwart (1978) both confined their observations to Bleckley and Dodge Counties. The model illustrated in Figure 6 suggests that they could have increased their chances of finding ejecta significantly if they had conducted their investigation closer to the South Carolina border.

4. *Analyze the appropriate size fraction of sediment.*

The maximum size of ballistically transported quartz grains generally diminishes as a function of distance from the crater (Claeys et al., 2002). Shocked quartz grains in distal deposits from the Chesapeake Bay impact have been identified in several Ocean Drilling Program (ODP) cores including sites 903C and 904A, approximately 330 kilometers northeast of the crater (Glass et al., 1998). These grains are found in the fine sand-size fraction (125 μm to 250 μm) of the sediment. In Georgia, 700 kilometers away from the crater, one might expect that most shocked quartz grains would, therefore, be fine sand-size or smaller. Albin (1997a) limited his search for shocked quartz to the coarse sand fraction (0.5 to 1.0 mm) and, perhaps, could have overlooked shocked grains in his samples.

Summary of strategy

The best strategy for successfully locating the Chesapeake Bay impact horizon in the Georgia Coastal Plain should consist of looking for shocked quartz grains in the very fine to fine sand-size fraction (63 μm to 250 μm) of sediments at the base of the Upper Eocene Twiggs Clay or Irwinton Sand relatively close to the South Carolina border. Natural exposures of the appropriate stratigraphic level can be identified approximately on the geologic map (Figure 3) by tracing the contacts between the greenish-yellow unit (Cretaceous-Paleocene) and the orange (Twiggs Clay) or buff-colored (Irwinton Sand) units. More accessible exposures are available near the floors of the many open-pit kaolin mines that occur throughout the region.

CHAPTER 3

METHODS

Shocked quartz: Key facts and distinguishing characteristics

During a hypervelocity impact, strain rates on the order of 10^6 s^{-1} to 10^8 s^{-1} accompany pressures as high as 5 to >50 GPa (French, 1998; Montanari and Koeberl, 2000). Sets of parallel planar fractures (PF's) develop in quartz at pressures exceeding 5 to 8 GPa (Stöffler and Langenhorst, 1994). PF's are open fissures that typically are 5 to 10 μm wide and are spaced 15 to 20 μm apart (French, 1998). PF's are typically aligned parallel to (0001) and {10-11}. Tectonic deformation may produce similar fractures, so PF's alone are not unequivocal shock indicators (Montanari and Koeberl, 2000). Above approximately 8 GPa, mechanical Brazil twins develop parallel to (0001) (Leroux et al., 1994). Although Brazil twins are common in non-shocked quartz, they typically form parallel to {10-11} (Spry et al., 1969). Basal sets have been observed only in naturally and experimentally shocked quartz (French, 1998). Therefore, basal Brazil twins appear to provide reliable evidence of impact.

The features used most often to diagnose shocked quartz are planar deformation features, or PDF's (Figure 8), which form between 8 and 35 GPa (Stöffler and Langenhorst, 1994). PDF's are thin zones of amorphous silica that form parallel to

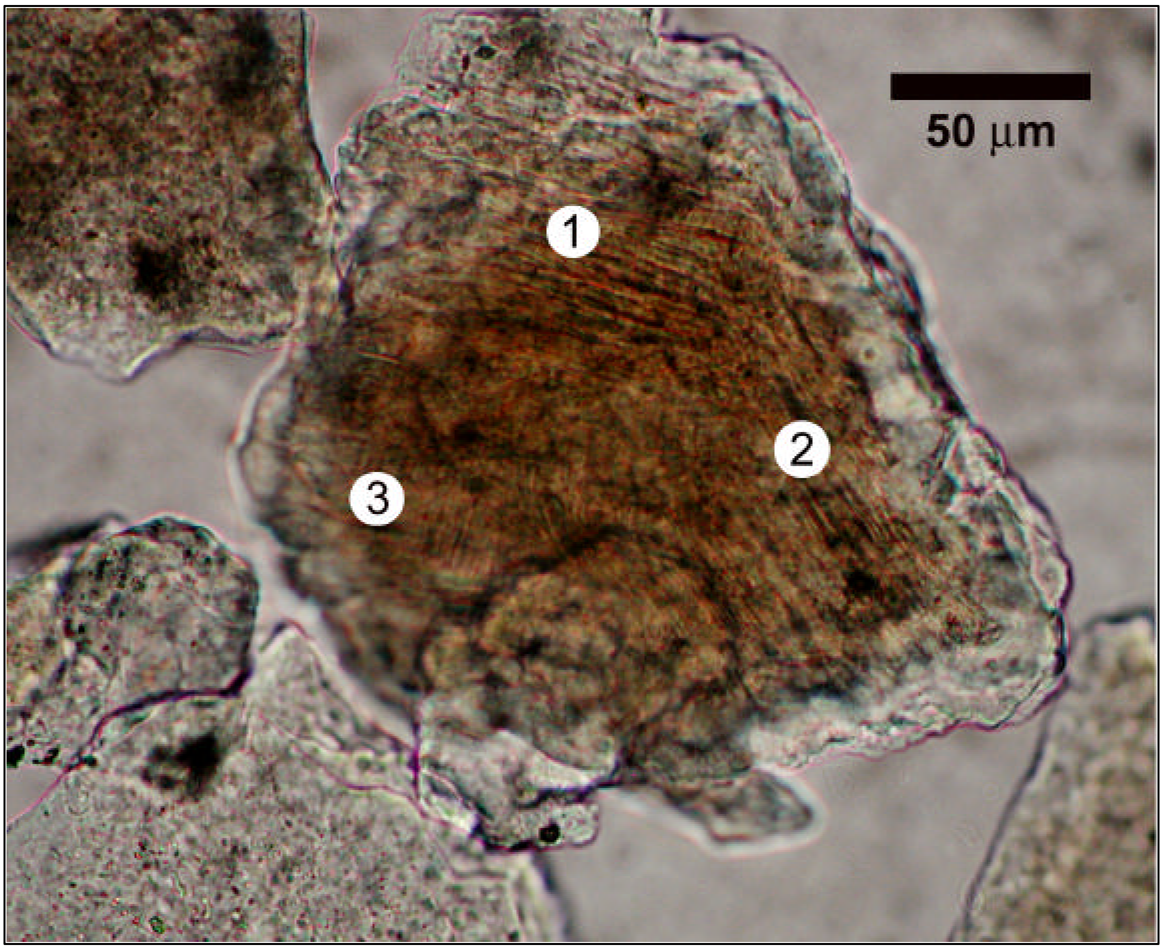

Figure 8. Photomicrograph of a classic shocked quartz grain exhibiting at least three sets of planar deformation features, or PDF's. Grain is from the K-T boundary layer in Colorado (Clear Creek North). Plane-polarized light (PPL).

Shock stage	Main orientations[a]	Additional orientations	Optical properties
1. Very weakly shocked	PFs: (0001)	PFs: rarely $\{10\bar{1}1\}$ PDFs: none	normal
2. Weakly shocked	PDFs: $\{10\bar{1}3\}$	PFs: $\{10\bar{1}1\}$, (0001) PDFs: rare	normal
3. Moderately shocked	PDFs: $\{10\bar{1}3\}$	PFs: $\{10\bar{1}1\}$, (0001) rare PDFs: $\{11\bar{2}2\}$, $\{11\bar{2}1\}$, (0001), $\{10\bar{1}0\}$+$\{11\bar{2}1\}$, $\{10\bar{1}1\}$, $\{213\bar{1}\}$, $\{516\bar{1}\}$	normal or slightly reduced refractive indices
4. Strongly shocked	PDFs: $\{10\bar{1}2\}$ $\{10\bar{1}3\}$	PFs: rare or absent PDFs: $\{11\bar{2}2\}$, $\{11\bar{2}1\}$, (0001), $\{10\bar{1}0\}$+$\{11\bar{2}1\}$, $\{10\bar{1}1\}$, $\{21\bar{3}1\}$, $\{51\bar{6}1\}$	reduced refractive indices (1.546–1.48)
5. Very strongly shocked	PDFs: $\{10\bar{1}2\}$ $\{10\bar{1}3\}$	none	reduced refractive indices (<1.48)

Figure 9. Table of common planar features and optical anomalies observed in quartz subjected to increasing stages of shock metamorphism. PF (planar fracture); PDF (planar deformation feature). From Montanari and Koeberl (2000) after Stöffler and Langenhorst (1994).

rational crystallographic planes of low Miller indices, most commonly the rhombohedral forms {10-13}, {10-12}, and {10-11} (Goltrant et al, 1992), although additional orientations may be observed (Figure 9). PDF's frequently occur in multiple sets, but single sets often are observed (French, 1998). Fresh amorphous PDF's cannot be resolved using an optical microscope (Goltrant et al, 1991). Fortunately, post-shock annealing and alteration decorate the planes with tiny quartz crystallites and bubbles that can be seen and measured (Goltrant et al, 1991; Grieve et al, 1996). These studded planes typically are 1 to 3 μm wide and are spaced 2 to 10 μm apart (French, 1998; Montanari and Koeberl, 2000). PDF's generally exhibit a high degree of planarity (Montanari and Koeberl, 2000), but some show subtle curvature (Engelhadt and Bertsch, 1969; Stöffler and Langenhorst, 1994) (e.g. planes 1 and 2 shown in Figure 8). Sometimes, especially in thin section, PDF's appear diffuse and curved because the features are viewed as they are projected onto the plane of the slide. Not until the grain is rotated around the horizontal axis of a spindle or universal stage do the PDF's appear sharp and linear.

Tectonic compression may create sets of sub-planar to planar, sub-parallel features in quartz, including frequently observed Böhm lamellae (Figure 10). Böhm lamellae typically are thicker (10 to 20 μm) and more widely spaced (>10 μm) than PDF's, and they very rarely occur in more than one set per grain (French, 1998). Unlike PDF's, which usually extend through greater than 90% of the host grain, Böhm lamellae commonly are observed to cross less than 75% of the grain (Alexopoulos, et al., 1988). Böhm lamellae also are misaligned slightly relative to the host grain. As a result, the extinction positions for the host and the lamellae may be observed to lie slightly out of phase (Engelhadt and Bertsch, 1969; French, 1998).

Another important difference between grains displaying Böhm lamellae and many grains containing PDF's is that the amorphous phase generated within shocked grains reduces the refractive index of each grain (see Figure 9) (Bohor, 1990). The refractive index, n, of quartz ranges from 1.543 to 1.554 depending on the orientation in which the crystal is observed. The mean refractive index is about 1.549. If a normal quartz grain is mounted in immersion oil or epoxy with $n \approx 1.54$ and the focus is raised, a white Becke line will move into the quartz grain (i.e. toward the material with the higher refractive index) (Phillips, 1971) (Figure 11). Similar Becke line behavior is observed in tectonically deformed grains (Figure 12). However, if $n < 1.54$, as one might expect for moderately to strongly shocked grains, then the Becke line should move into the epoxy (Figure 13). [2]

Finally, most authors (e.g. Alexopoulos et al., 1988; Grieve et al, 1996) comment on the orientations of Böhm lamellae. Typically the lamellae are close to the basal plane. The angle between the c-axis and the poles to tectonic lamellae averages less than about 15° (Alexopoulos, et al., 1988). The pole to the plane of the most frequently occurring PDF's, {10-13}, is 23° (French, 1998). Orientation measurements recorded from a universal stage have an associated error of ± 5° (Montanari and Koeberl, 2000), so some overlap and ambiguity is possible when using polar angles to discriminate between Böhm

[2] The epoxy used to prepare the grain mounts and thin sections in this study has a factory rating of $n = 1.54$. The exact refractive index may vary depending on the environment and how well the resin is mixed with the curing agent. Therefore, it is worth noting that the Becke line tests demonstrated in Figures 11, 12, 25, 27, and 29 were performed on grains in the same thin section. The identical mixture was used to prepare the grain mounts shown in Figures 26 and 28. The shocked grain shown in Figure 13 was mounted in a separate mix prepared from the same resin. Although they are not shown here, undeformed quartz grains in the same thin section were observed to show the opposite Becke line behavior.

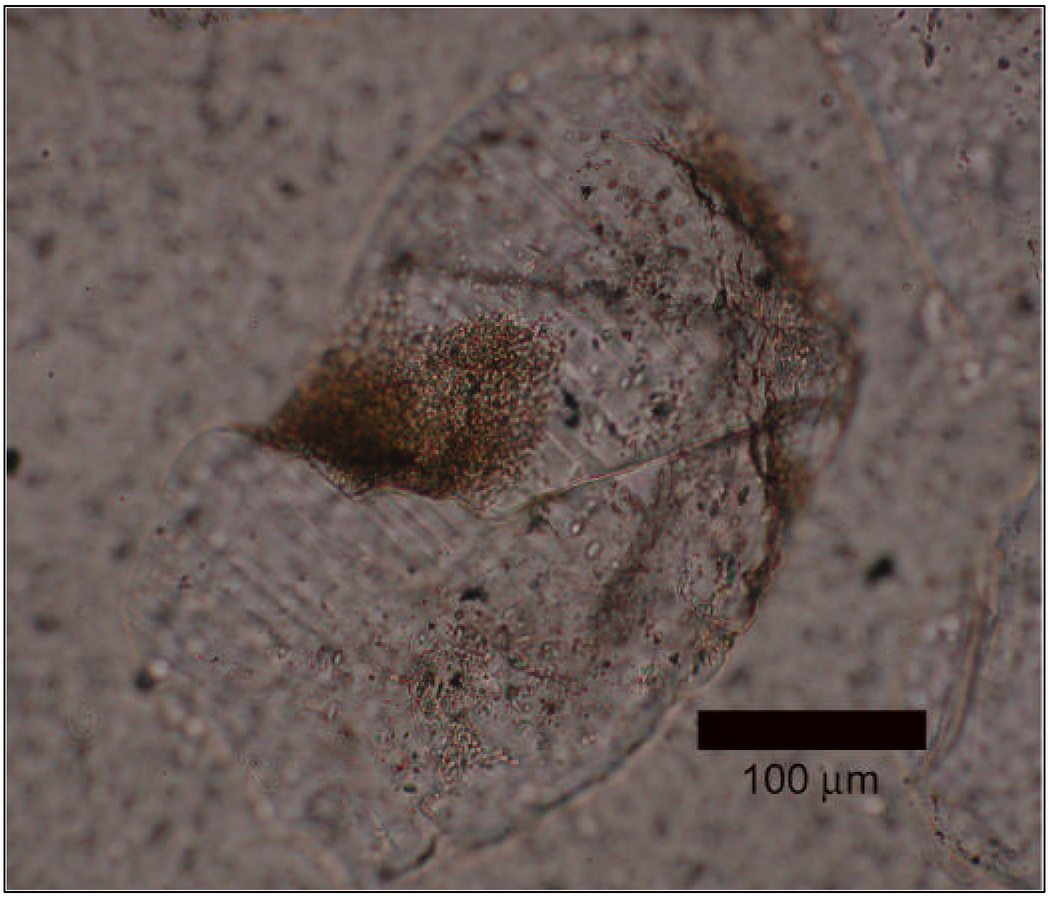

Figure 10. Photomicrograph of quartz grain exhibiting Böhm, or tectonic, lamellae. The sub-planar features are relatively thick and widely spaced compared to PDF's. They occur in a single set, and many of the planes do not extend across the entire grain. PPL.

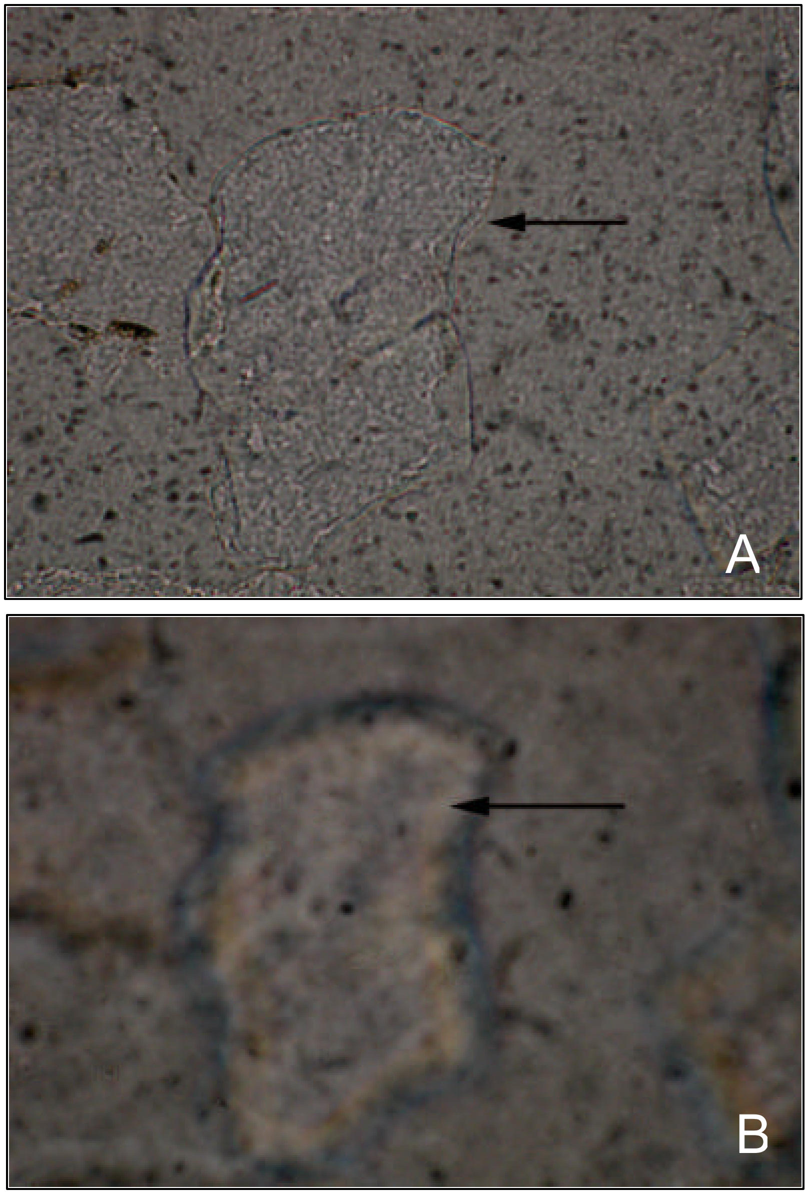

Figure 11. Demonstration of Becke line test performed on an undeformed quartz grain. A) The arrow points to the Becke line, a thin white line at the edge of the focused grain. B) As the focus is raised, the Becke line moves into the material with the higher refractive index, the quartz grain in the case. The observed behavior is expected because the quartz grain (*n* = 1.543 to 1.554) is mounted in an epoxy with *n* ≈ 1.54. PPL.

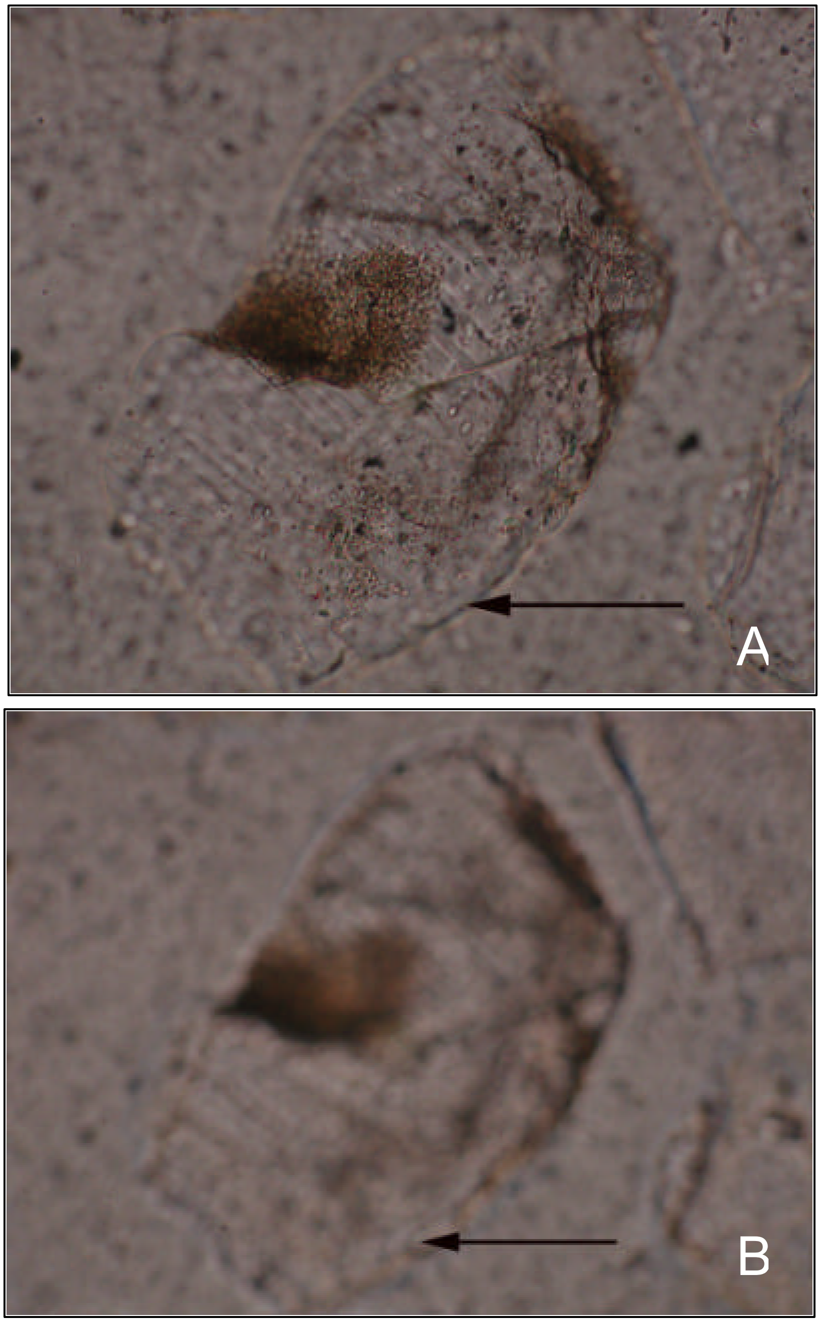

Figure 12. Demonstration of Becke line test performed on a tectonically deformed quartz grain exhibiting Böhm lamellae. A) The arrow points to the Becke line. B) As the focus is raised, the Becke line moves into the quartz; therefore, the refractive index of the grain is greater than about 1.54 (the index of the epoxy). PPL.

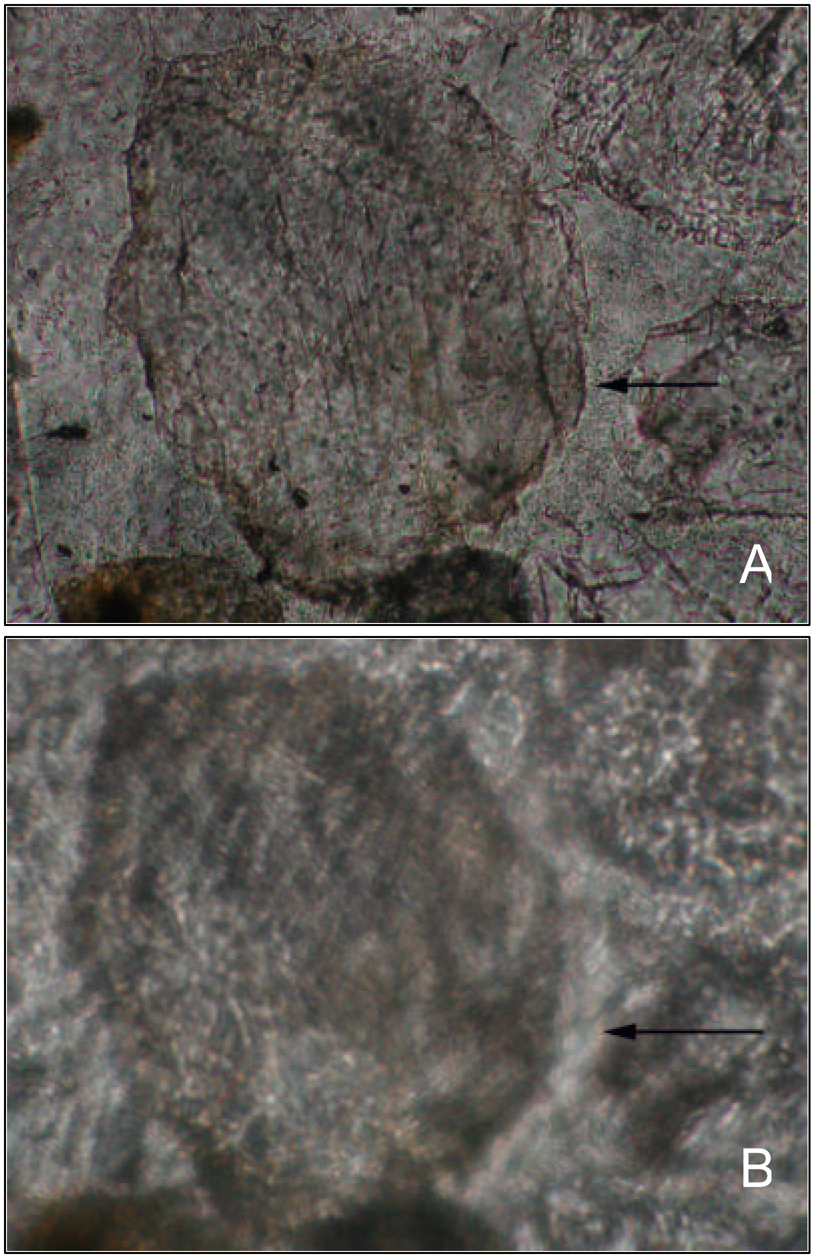

Figure 13. Demonstration of Becke line test performed on a shocked quartz grain from the Crow Creek Member of the Pierre Shale [Manson impact ejecta (Izett et al., 1993)] exhibiting at least two sets of planar fractures and possibly PDF's. A) The arrow points to the Becke line. B) As the focus is raised, the Becke line moves into the surrounding epoxy; therefore, the refractive index of the grain is less than 1.54. An anomalously low refractive index coupled with the presence of PF's and PDF's is indicative of impact deformation. PPL.

lamellae and PDF's. The best way to manage this problem is to identify grains that display more than one set of planar features. Universal stage measurements taken from at least two sets of planes allow their orientations to be compared to rational crystallographic planes in the quartz lattice. Not only do Böhm lamellae rarely occur in multiple sets, they are not crystallographically controlled and do not have a preference for rational crystallographic planes (Grieve et al, 1996). It is very unlikely that a statically deformed grain will contain two or more sets of lamellae corresponding to lattice planes.

There are some other crystallographically controlled planes that may be encountered in quartz, including twinning and growth planes. As mentioned before, Brazil twins prefer {10-11}, also a common PDF orientation. Alexopoulos et al. (1988) raise a crucial point to help avoid problems caused by the myriad of non-shock fabrics that may exist in quartz. PDF's parallel to {10-13}, if they are indexed correctly, and preferably if they coexist with additional sets, are the key because {10-13} is the only primary PDF orientation that is not known to be shared by twin planes or cleavages. They note that {10-13} very rarely serves as a growth plane.

Indexing planar elements in quartz using a universal stage or spindle stage remains the most commonly used method for demonstrating the presence of PDF's in *bona fide* shocked quartz (Montanari and Koeberl, 2000). Despite the emerging popularity of transmission electron microscopy (TEM) to supplement and verify petrographic results, the high cost, primarily of sample preparation, continues to keep TEM studies something of a luxury rather than the primary diagnostic tool. Therefore, two recent claims that TEM analyses had reversed petrographic interpretations of shocked quartz made the future course of petrographic studies unclear. However, in both cases where TEM results reportedly "overturned" petrographic results (Cordier et al., 1994; Mossman et al., 1998), the initial petrographic interpretations (Vrana, 1987; Mossman et al., 1998) were based on observations that were already suspicious, most notably for their failure to identify planes parallel to {10-13} in any grains and the diffuse appearance of the proposed PDF's. Montanari and Koeberl (2000) report that Mossman et al. (1998) questioned the identification of PDF's by Bice et al. (1992) at the Triassic-Jurassic boundary in Italy as if Mossman's TEM study directly challenged Bice's rigorous petrographic characterization of PDF's. In fact, Mossman et al. (1998) never analyzed the shocked quartz reported by Bice et al. (1992), or even grains from Italy! Instead they identified some faint lamellae in quartz from the Triassic-Jurassic boundary in Nova Scotia, determined them to be consistent with PDF's based on universal-stage measurements, and debunked their own assertion using TEM, all in the same study. Although the lamellae turned out to be sub-grain boundaries roughly parallel to rational crystallographic planes, the most obvious lamellae did not belong to the common rhombohedral forms seen in shocked quartz. Ideally, TEM work should eventually be incorporated into any search for shocked quartz, but petrographic studies that identify shocked quartz on the basis of PDF's parallel to {10-13} planes, in addition to {10-11} and/or {10-12}, and low refractive indices, should be robust.

Shocked quartz: Analytical determination of possible PDF orientations

Possible PDF orientations were measured using a universal stage (Figure 14) according to the procedures outlined by Phillips (1971), Engelhadt and Bertsch (1969),

Figure 14. Photograph of a Ziess four-axis universal stage used to measure the orientation of quartz micro-fabrics. A thin section or grain mount is placed flat between two glass hemispheres (the upper hemisphere is visible near the center of the photograph).

and Montanari and Koeberl (2000). The position of the c-axis and the poles to the observed planes are plotted on a Wulff stereonet (e.g. Figure 15A). The c-axis is rotated to the center of the stereonet and the poles are replotted (Figure 15B). The angle between the c-axis and each pole is measured (Figure 15C). Taken alone these polar angles may provide a quick estimate of the orientations that are observed (see French (1998) p. 46); but in order to demonstrate that the features correspond to rational crystallographic planes, the positions of the poles must be compared to a template illustrating the low-index lattice planes of quartz (Figure 16A). Because universal stage measurements do not determine the a_1, a_2, and a_3 quartz axes uniquely, the stereonet may be rotated to obtain a best fit with the template (Figure 16C). Poles that lie within ± 5° of ideal positions (indicated by circles on the template) can be indexed and compared to common PDF orientations (Montanari and Koeberl, 2000). Thus the orientation of a specific plane in quartz is determined from two parameters: 1) the difference between its pole and the c-axis, 2) the azimuth between its pole and the pole of another plane (see Figure 16C). Accurate indexing requires that at least two sets of planar features be present in the same grain. A single set of possible PDF's can be described only by the polar angle; and even when that angle exceeds 15°, other criteria must be used to distinguish PDF's from tectonic lamellae, twin planes, etc. For loose sand grains, a Wilcox spindle stage (Figure 18) may be used to measure the polar angles with an accuracy of ± 1° (Grieve et al. 1996). The spindle stage may be used in place of the universal stage when dealing with loose grains; however, the spindle stage lacks one horizontal axis of rotation that may be critical for accurately seeing and measuring some PDF's, especially when multiple sets are present (Grieve et al., 1996).

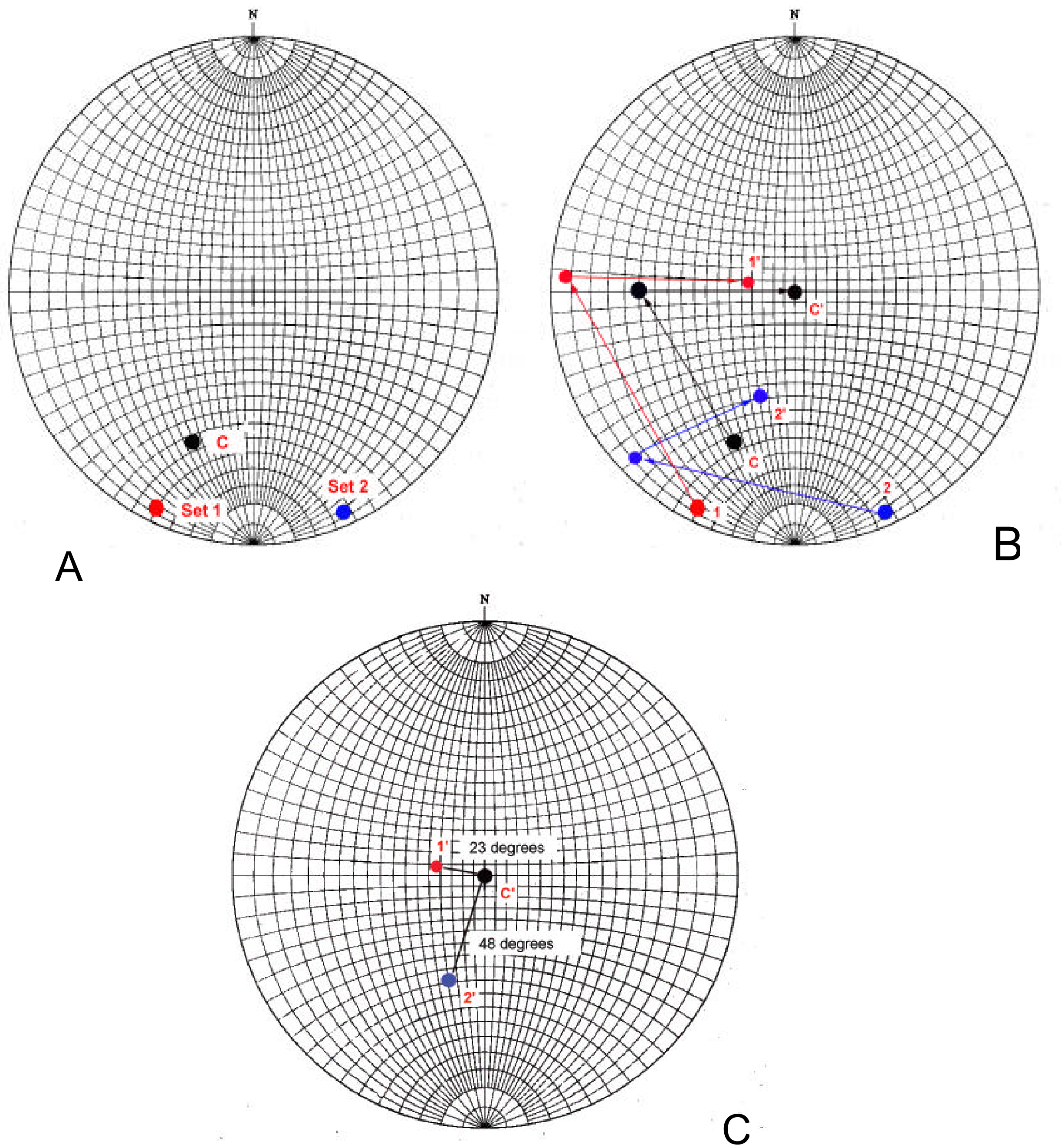

Figure 15. A series of stereographic plots illustrating the procedures for determining the angle between the c-axis and the poles to two planar elements in a quartz grain. A) The c-axis (C) and poles to the two planes (1 and 2) are plotted from universal stage data. B) The points are rotated around the center of the stereonet until C lies on the equator. C is rotated around the N-S axis and into to the center of the net (C'). 1 and 2 rotate with C and those poles are replotted at points 1' and 2'. C) The angles measured between each replotted pole and C' gives the angle between the c-axis and the poles to each planar element, in this case 23° and 48°.

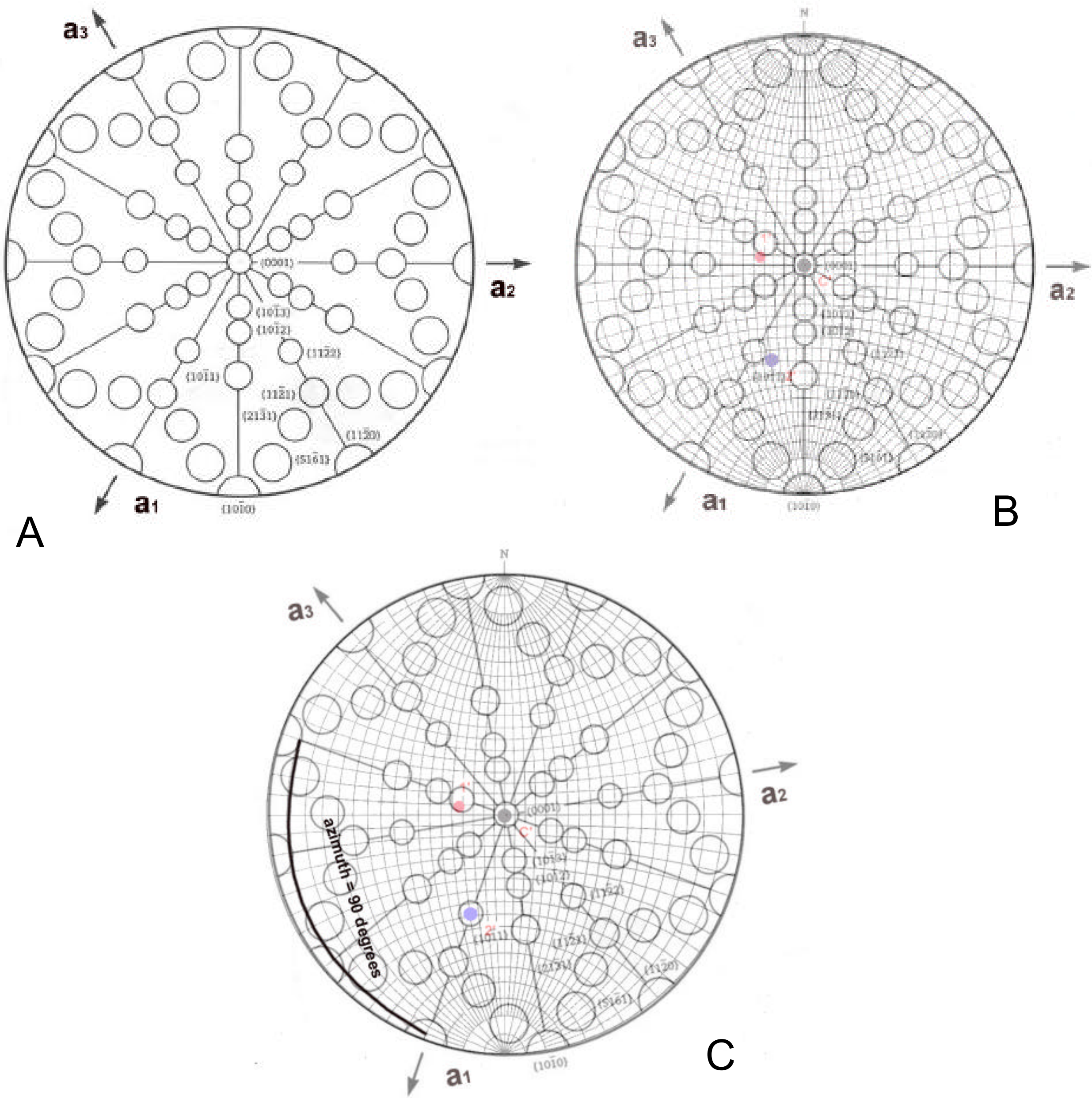

Figure 16. A) A stereographic overlay showing the poles to the low-index crystallographic planes of quartz. The circles indicate the ± 5° analytical error associated with universal stage measurements. B) The overlay is placed on the stereonet showing the positions of the poles to the planar elements after the c-axis is rotated to the center of the net. C) The overlay is rotated around the center until both measured poles lie within circles. The angles between each pole and the c-axis and the azimuth between the poles (shown) allow the planes to be indexed to rational crystallographic planes, in this case {10-13} and {11-22).

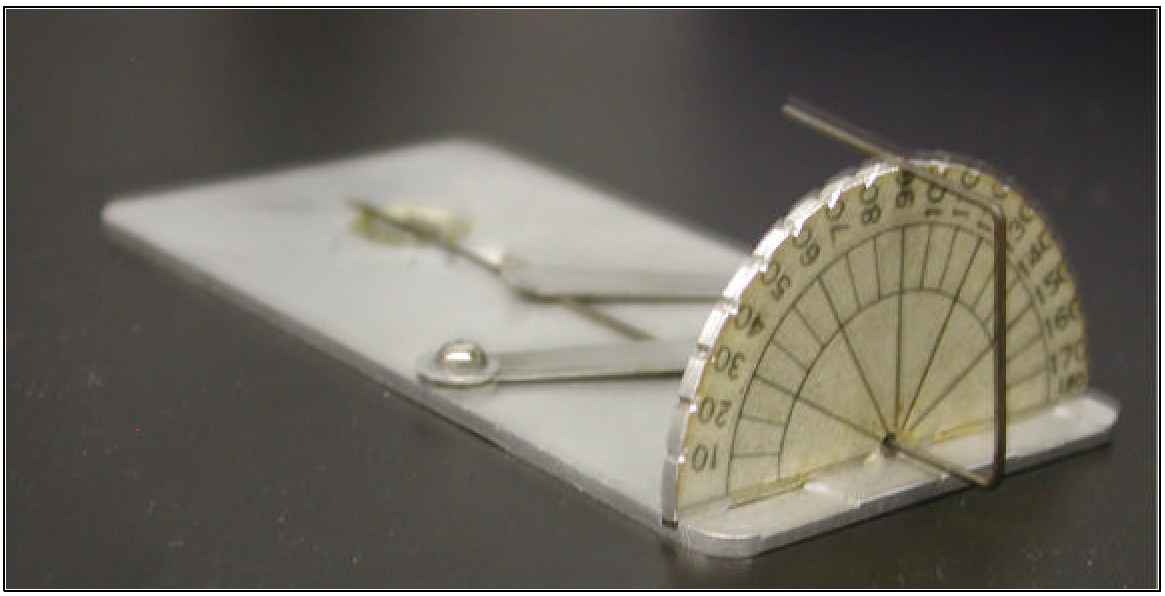

Figure 17. Photograph of a Wilcox spindle stage. A grain is mounted on the end of the spindle with a drop of glue (or thick molasses [G. Izett, personal communication, 2002]) The tip is centered in a circular well to which refractive oils are added. The entire device is positioned flat on the stage of a standard petrographic microscope. Detailed instructions on using a spindle stage may be found in Bloss (1981).

Collection and Preparation of Samples

Quartz-rich sediments were collected from a poorly-consolidated sand unit exposed at the base of the Twiggs Clay near the floor of the Purvis School Mine in Warren County and at the Hardie Mine in western Wilkinson County (see Figure 3). Prior to collecting the samples, the exposures were excavated at least 10 centimeters into the mine wall and cleared of debris from overlying units. Particular care was taken not to contaminate the sands collected from the Purvis School site (described in the next chapter) by driving a clean plastic pipe, one meter long, into the mine wall. The pipe was used to auger and funnel the sediment directly into sample bags.

In the lab, the sand fraction of the sediment was cleaned ultrasonically and wet-sieved into coarse (>500 µm), medium (250 µm to 500 µm), fine (125µm to 250µm), and very fine (63µm to 125µm) sand-size fractions. After each aliquot was dried at 70° C, a few grams of each size fraction were placed on glass plates and immersed in a film of oil (n » 1.54). Each plate was scanned under the microscope using normal reflected and transmitted light and plane and cross-polarized light. Additionally, thin section mounts in epoxy (n » 1.54) were prepared for the medium, fine, and very fine sand fractions. These mounts were ground and polished against glass plates. These mounts were used for point-counting in order to characterize the sand mineralogy, and they also were scanned for possible shocked grains. A few individual epoxy grain mounts were prepared for interesting loose grains that had been identified on the glass plates.

CHAPTER 4

RESULTS: SHOCKED QUARTZ AND OTHER EJECTA IN UPPER EOCENE SEDIMENTS

Purvis School Mine

Operated by the J.M. Huber Corporation, the Purvis School mine (Figure 18) is located along the western side of Georgia Route 17, approximately 8 kilometers north of Wrens (see Figure 3). Samples from a 10 centimeter-thick coarse sand deposit at the base of the Twiggs Clay (Figure 19) were analyzed. In the easternmost portions of the Georgia Coastal Plain the Clinchfield Sand is absent and the Twiggs Clay immediately overlies the kaolin-rich Paleocene to Middle Eocene Huber Formation, the target of lucrative mining operations. At the Purvis School mine, the basal Twiggs Clay unit is comprised of a poorly-sorted, coarse sand and gravel deposit that contains some well-rounded quartz pebbles up to 2 centimeters in diameter and large, rounded to angular smectitic and kaolin clasts up to about 8 centimeters wide. The sand-size fractions are composed primarily of very angular quartz. Similar to the Irwinton Sand and Tobacco Road Sand, higher in the succession, greater than 90 % of the fine, medium, and coarse sand is quartz. The very fine sand-size fraction contains as much as 20% complexly-twinned potassium and sodium feldspars (Figures 20 and 21) [many of which also exhibit complex extinction patterns (Figure 20)] and approximately 20% lithic components —

predominantly staurolite, chromite, and euhedral zircons with lesser abundances of brown and green amphibole, tourmaline, and kyanite. Lignite fragments locally are plentiful, and sponge spicules commonly are observed in the very fine to fine sand-size fractions. The sands are set in a matrix of light brown to lavender-gray silt and clay. The clay forms molds of bivalves that are locally abundant in the top couple of centimeters of the unit.

Approximately 1 in 250 of the quartz grains in the fine sand-size fraction exhibit possible PDF's (Figures 22 thru 24). Less than 1 in 1000 quartz grains from the medium-grained fraction contain similar features. The planes consistently appear to be 2 to 3 µm wide and spaced about 5 to 7 µm apart. For selected grains, orientations of the planar features relative to the c-axis axis were determined using a universal stage. Planar features in grains displaying at least two intersecting sets (Figures 25 thru 27) show a preference for the {10-13} and {10-11} forms. Planes corresponding to {11-22} and {51-61} also were observed.

Two grains (Figures 28 and 29) each contain a single prominent set of planar features possibly parallel to {10-12}. Universal stage measurements indicate that the poles to the planes lie 32 to 35° off the c-axis. Spindle stage measurements confirm that the pole to the planes displayed in Figure 23 is 32° from the c-axis. Those planes are 2 to 3 µm wide, 5 to 7 µm apart; and like many *bona fide* PDF's, the features fill the entire grain. Unlike Böhm lamellae, the features have the same extinction positions as the host grain. C. Koeberl (personal communication, 2002) has commented that the planes, as shown in Figure 28A, appear to be wavier than PDF's and lack their characteristic planarity.

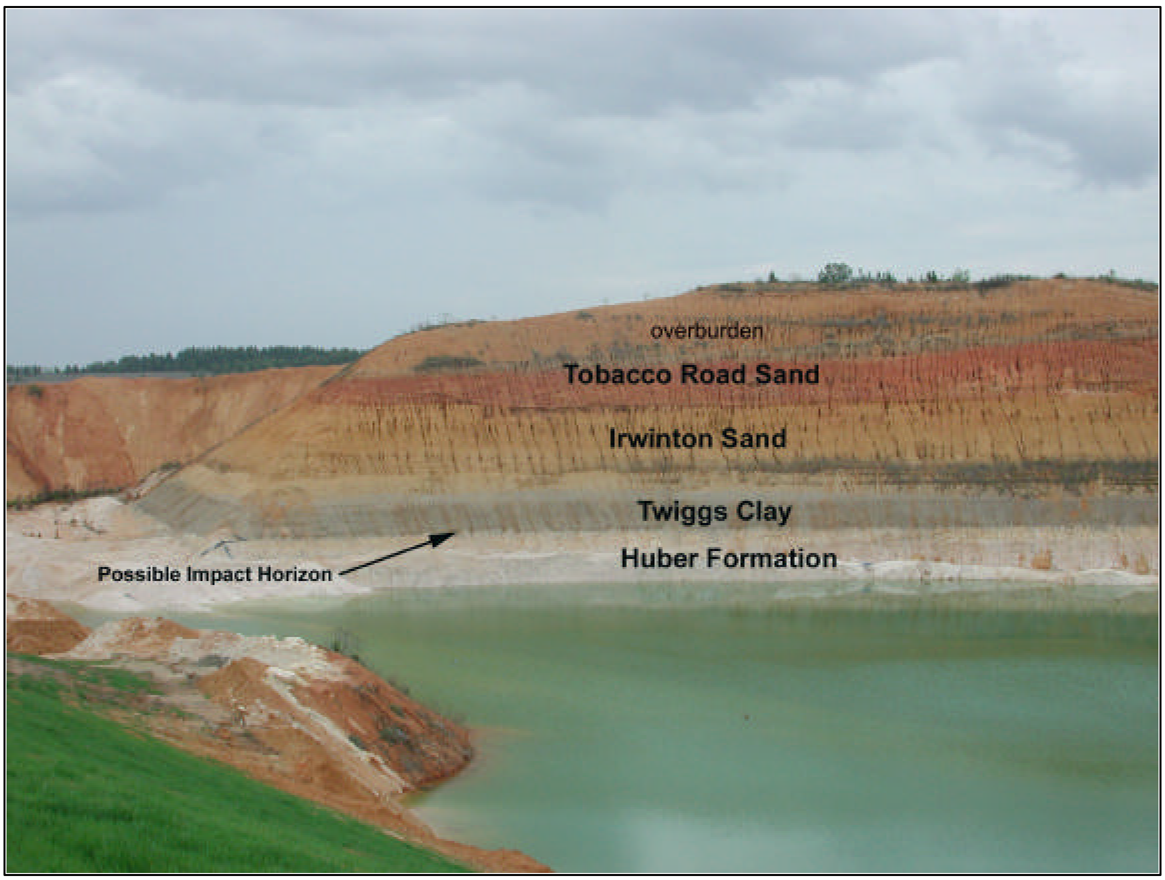

Figure 18. Photograph of the north wall of the Purvis School kaolin mine illustrating the common lithostratigraphic units exposed in the upper Coastal Plain of eastern Georgia. The arrow indicates the position of a 10 centimeter-thick coarse sand unit at the base of the Twiggs Clay that was sampled and analyzed for the presence of shocked quartz. For scale: The Twiggs Clay is 3 to 4 meters thick.

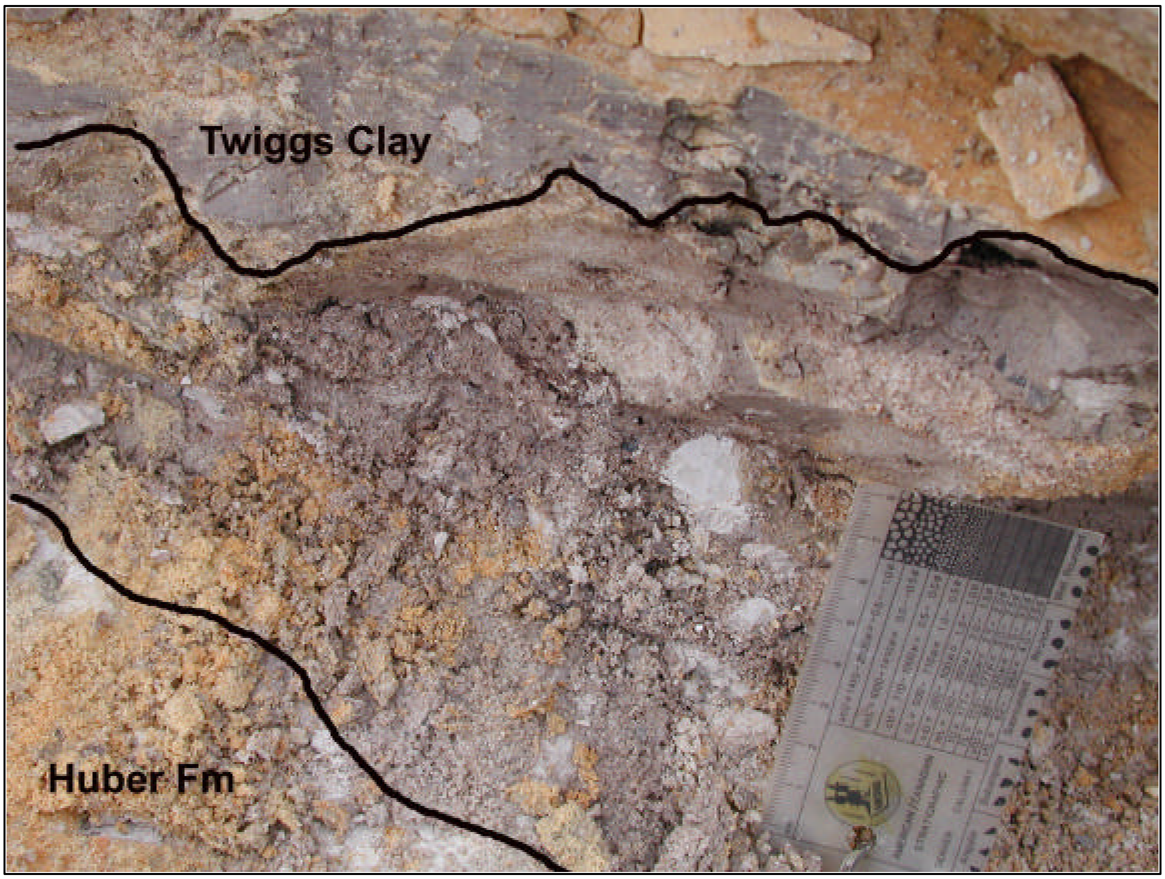

Figure 19. Photograph from the Purvis School kaolin mine showing the coarse sand unit at the base of the Twiggs Clay and overlying the Huber Formation. The shocked quartz grains were collected from this unit. The scale is 8 centimeters long.

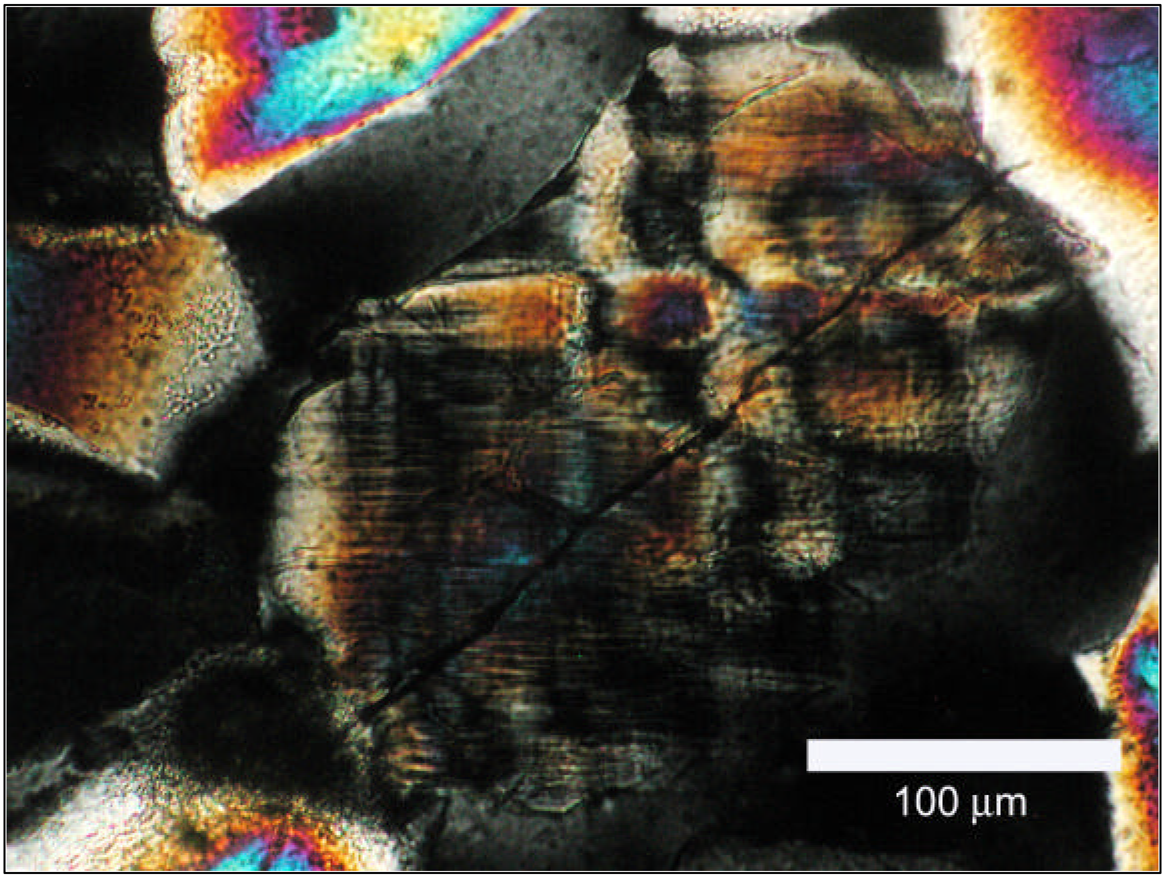

Figure 20. Photomicrograph of a complexly-twinned perthitic feldspar showing an irregular, “splotchy” extinction pattern probably resulting from intense deformation. Similar feldspars grains are relatively common in the very fine to fine sand-size fraction of the basal Twiggs Clay sand layer. Cross-polarized light (XPL).

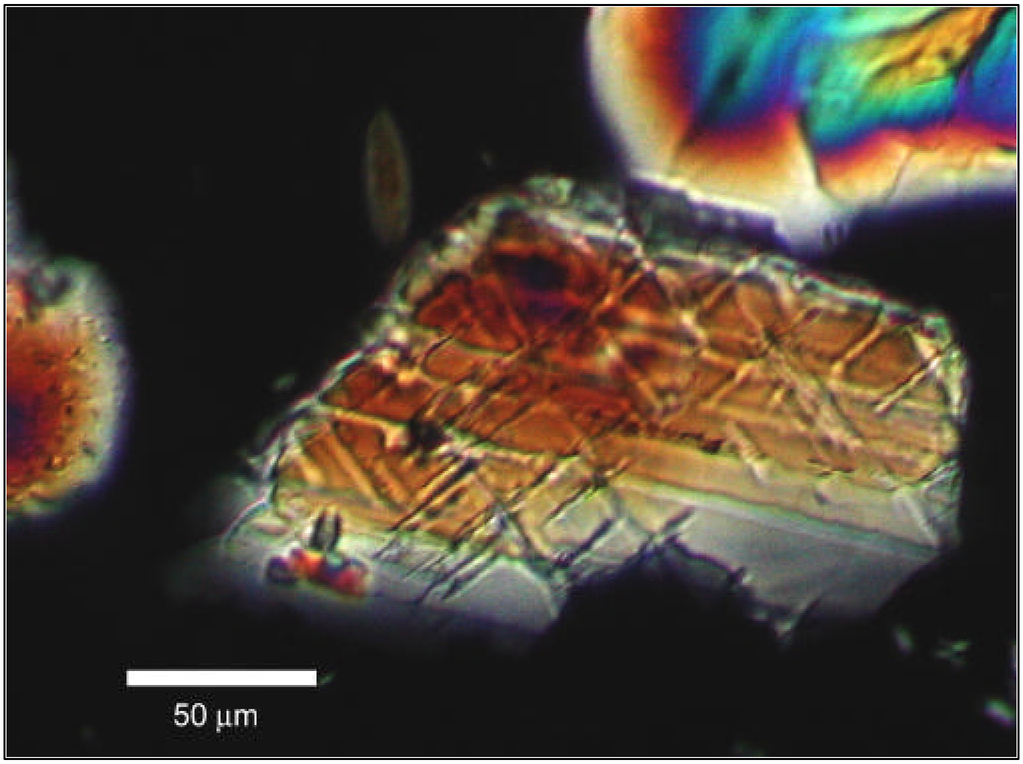

Figure 21. Photomicrograph of a twinned feldspar grain. Albite twin lamellae are oriented approximately east-west. Two sets of etched lamellae cut diagonally across the albite twins. These lamellae may represent additional twin planes (J. W. Horton, personal communication, 2003) although common feldspar twins typically form normal to albite twin planes. PDF's in feldspars frequently occur oblique to albite twins (French, 1998). It is possible that the grain represents impact ejecta. XPL.

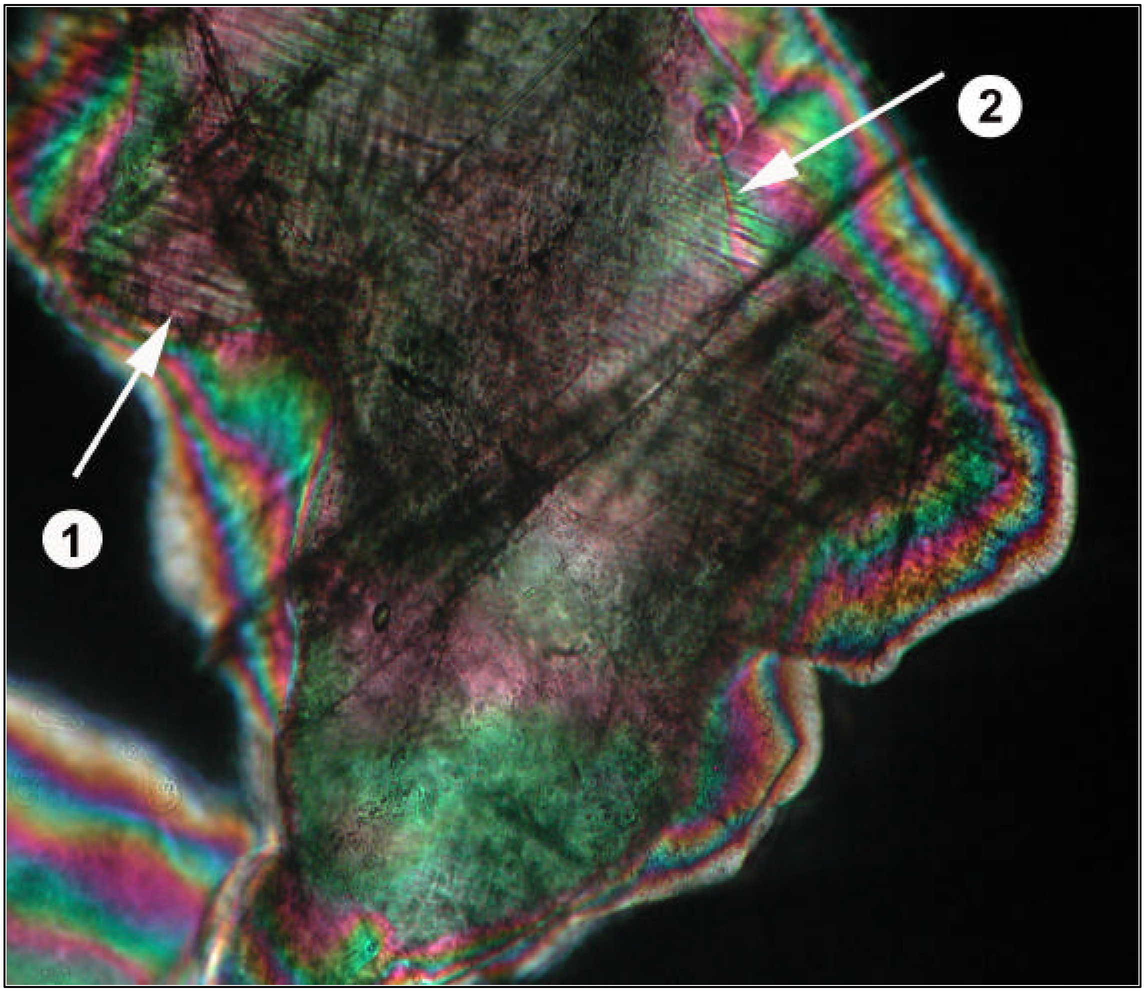

Figure 22. Photomicrograph of a fine sand grain displaying two sets of possible PDF's and two additional sets of oriented fractures that may be PF's. No orientation data is available for this grain. XPL.

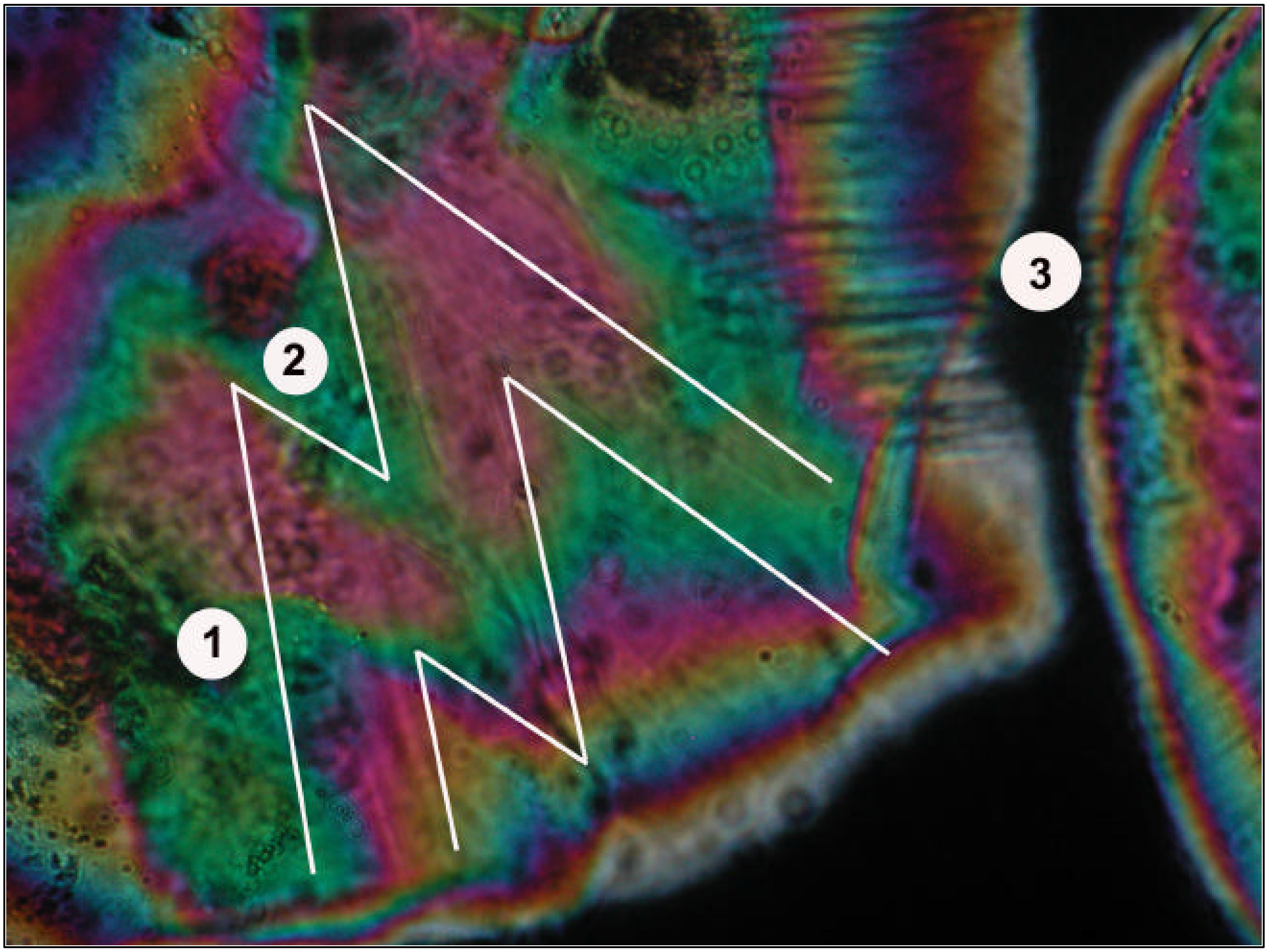

Figure 23. Photomicrograph of a fine sand grain displaying two or three sets of possible PDF's. Note the distinct chevron pattern created by the intersection of sets 1 and 2. No orientation data is available for this grain. XPL.

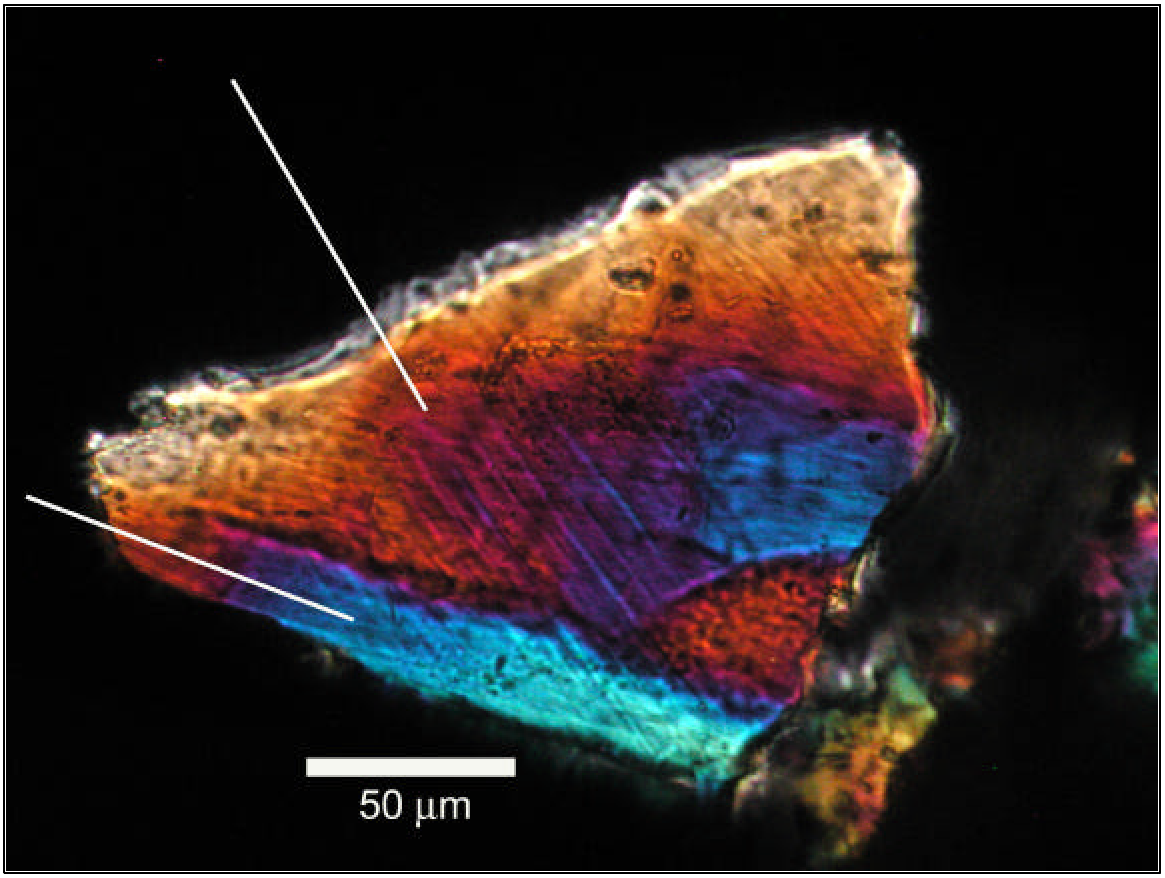

Figure 24. Photomicrograph of a fine sand grain displaying two intersecting sets of possible PDF's. XPL.

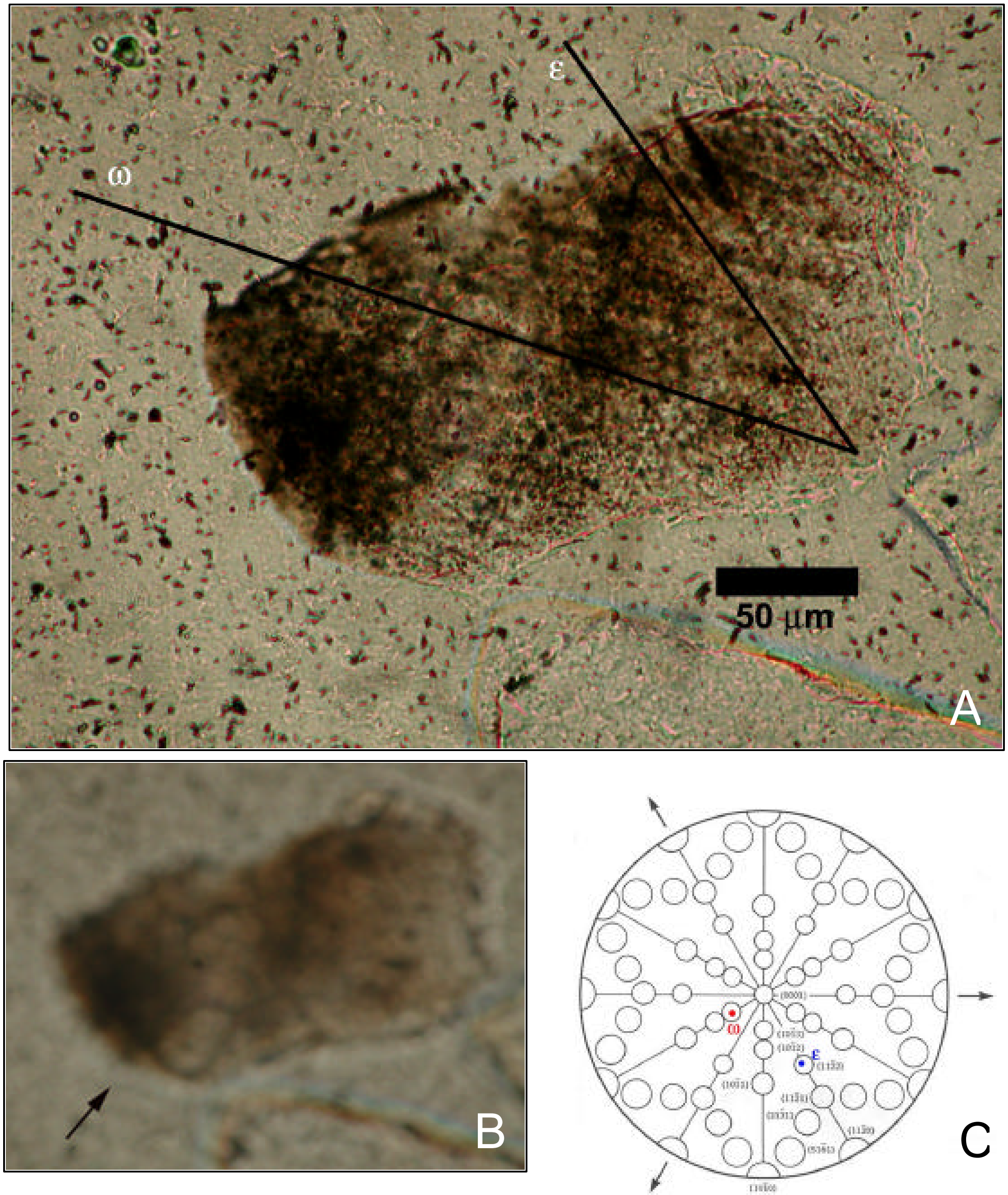

Figure 25. A) Photomicrograph of a quartz grain containing two sets of possible PDF's. PPL. B) The Becke line test indicates that the refractive index of the grain is less than 1.54. C) Stereographic plot of poles to the planar features demonstrating that they are consistent with common PDF orientations {10-13} (ω) and {11-22} (ε).

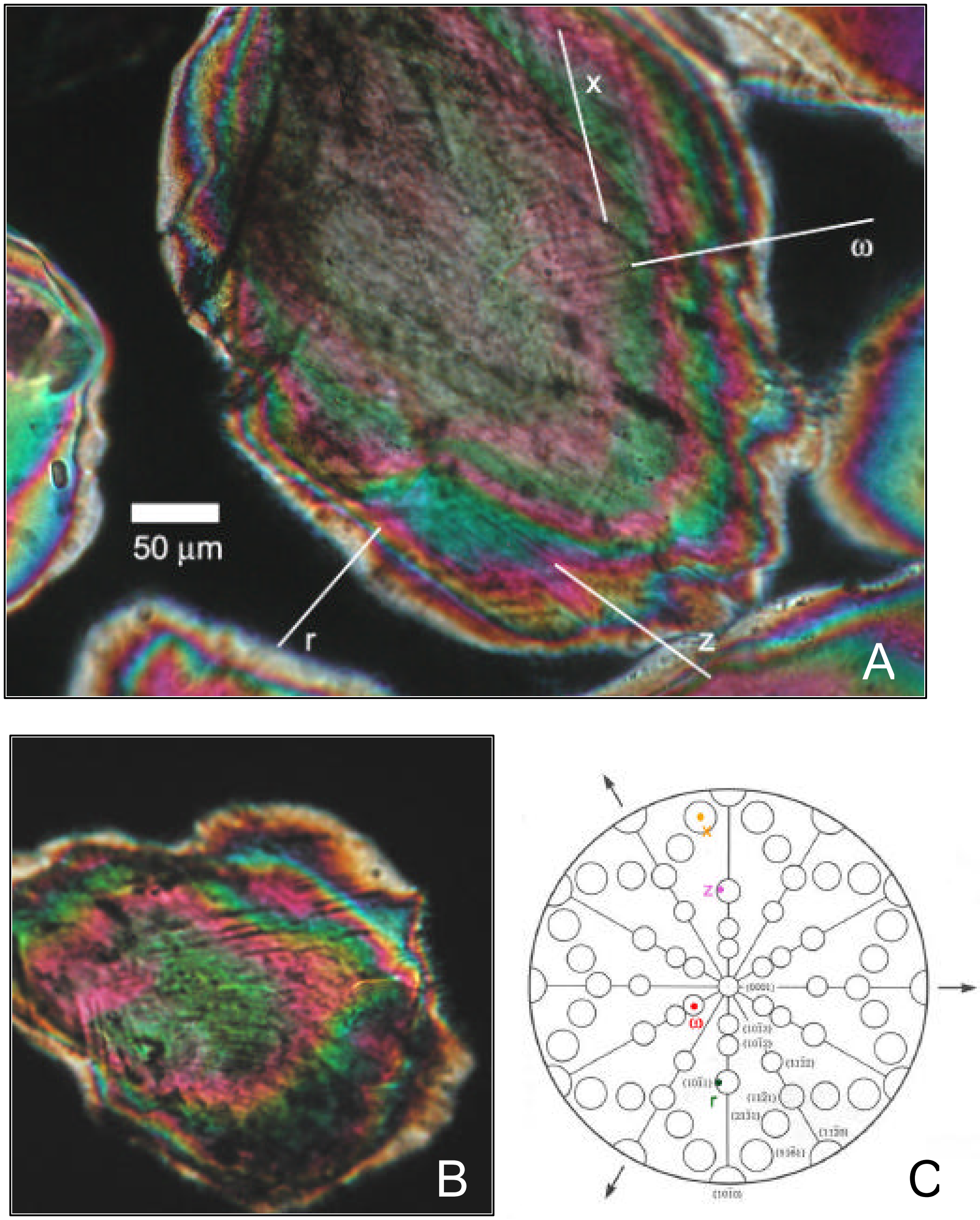

Figure 26. A) Photomicrograph of a quartz grain containing four sets of possible PDF's. XPL. B) In this orientation the grain displays three sets of possible PDF's including two sets forming a distinctive chevron pattern. C) Stereographic plot of poles to the planar features demonstrating that they are consistent with common PDF orientations {10-13} (ω), {10-11} + {-1011} (r, z), and {51-61} (x).

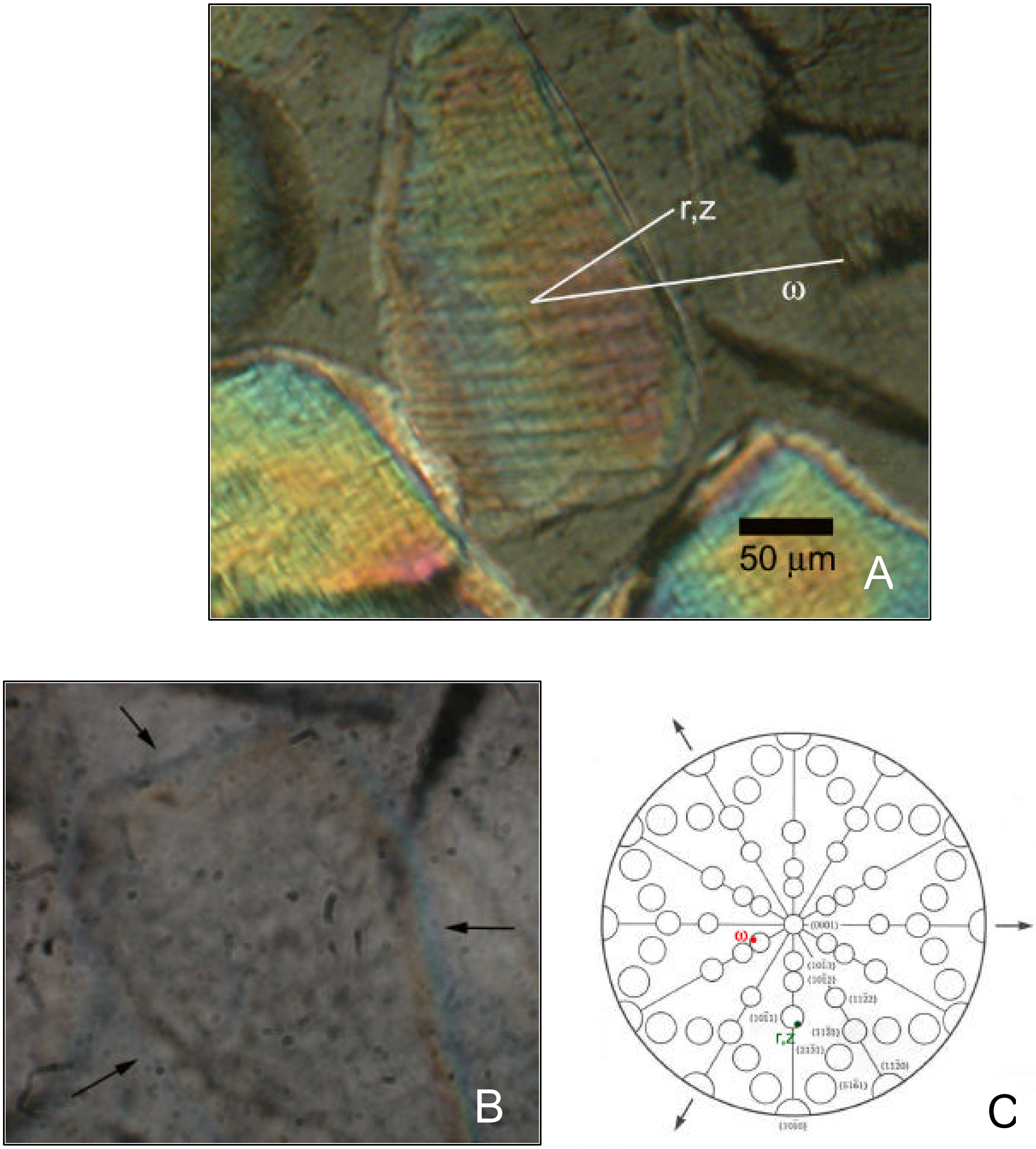

Figure 27. A) Photomicrograph of a quartz grain containing two sets of possible PDF's. XPL. B) The Becke line test indicates that the refractive index of the grain is less than 1.54. C) Stereographic plot of poles to the planar features demonstrating that they consistent with common PDF orientations {10-13} (ω) and {10-11} (r, z).

Figure 28B shows that when the grain is rotated to an optimum position on the universal stage, the features are revealed to be quite straight, planar, and parallel to one another. Further evidence that the host grain was shocked is that the refractive index of the grain appears to be less than 1.54 (Figure 28C). In fact, the grain serendipitously was immersed in refractive oil with n =1.52 and showed negative relief (demonstrating that the refractive index of the grain is less than 1.52). Shocked quartz containing PDF's parallel to {10-12} were strongly shocked and are expected to exhibit significant reductions in their refractive indices (see Figure 9). Therefore, the correspondence of possible PDF's consistent with {10-12} in a host grain with an anomalously low n supports an impact origin. Lower-angle PDF's (e.g. {10-13}) sometimes fail to form in porous sedimentary targets, probably because the shock wave initially works to close the pore spaces rather than deform the quartz lattice (Grieve et al., 1996). Consequently grains that experience pressures in excess of those required to compress the rock develop only higher-angle PDF's. Perhaps this could explain the conspicuous absence of planes parallel to {10-13} in this grain. The very high degree of rounding supports the notion that the grain may have been part of a porous sedimentary rock. Finally, it is worth noting that this grain may contain one or two additional weakly-developed sets of planar features approximately parallel to {21-31} and {22-41}.

The second grain (Figure 29) contains planar arrays of tiny brown fluid inclusions that cross the entire grain. They cut across a set of oriented fractures that run parallel to the c-axis, and the density of bubbles appears to increase where the fractures are more tightly

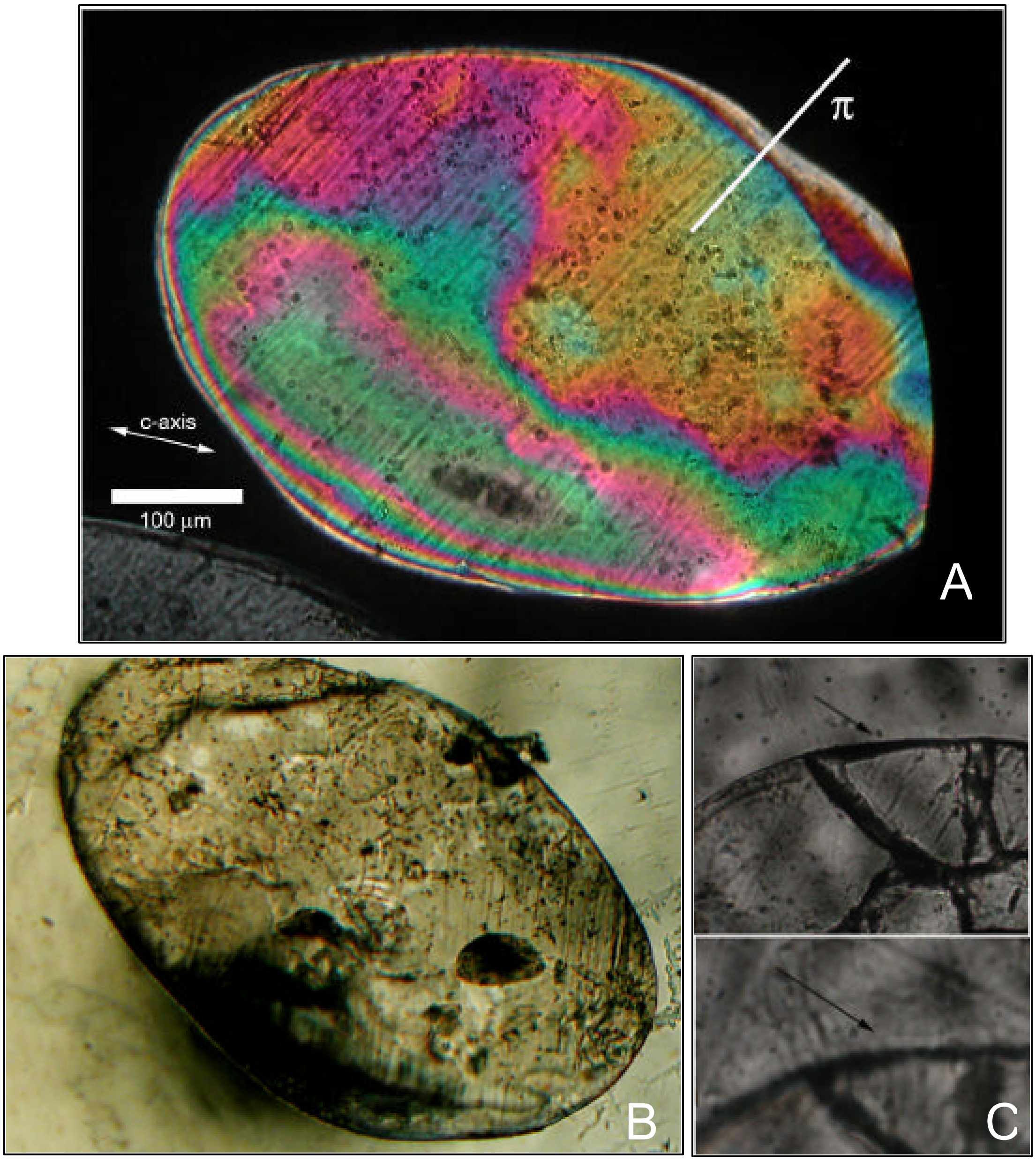

Figure 28. A) Photomicrograph of a well-rounded quartz grain containing one prominent set of planar features consistent with {10-12} (π). XPL. B) When the grain is tilted on a universal stage, the straight, parallel habit of the features is accentuated. PPL. C) The position of the Becke line is shown before (top) and after the focus is raised. The line moves out into the epoxy; therefore, the refractive index of the grain is less than 1.54.

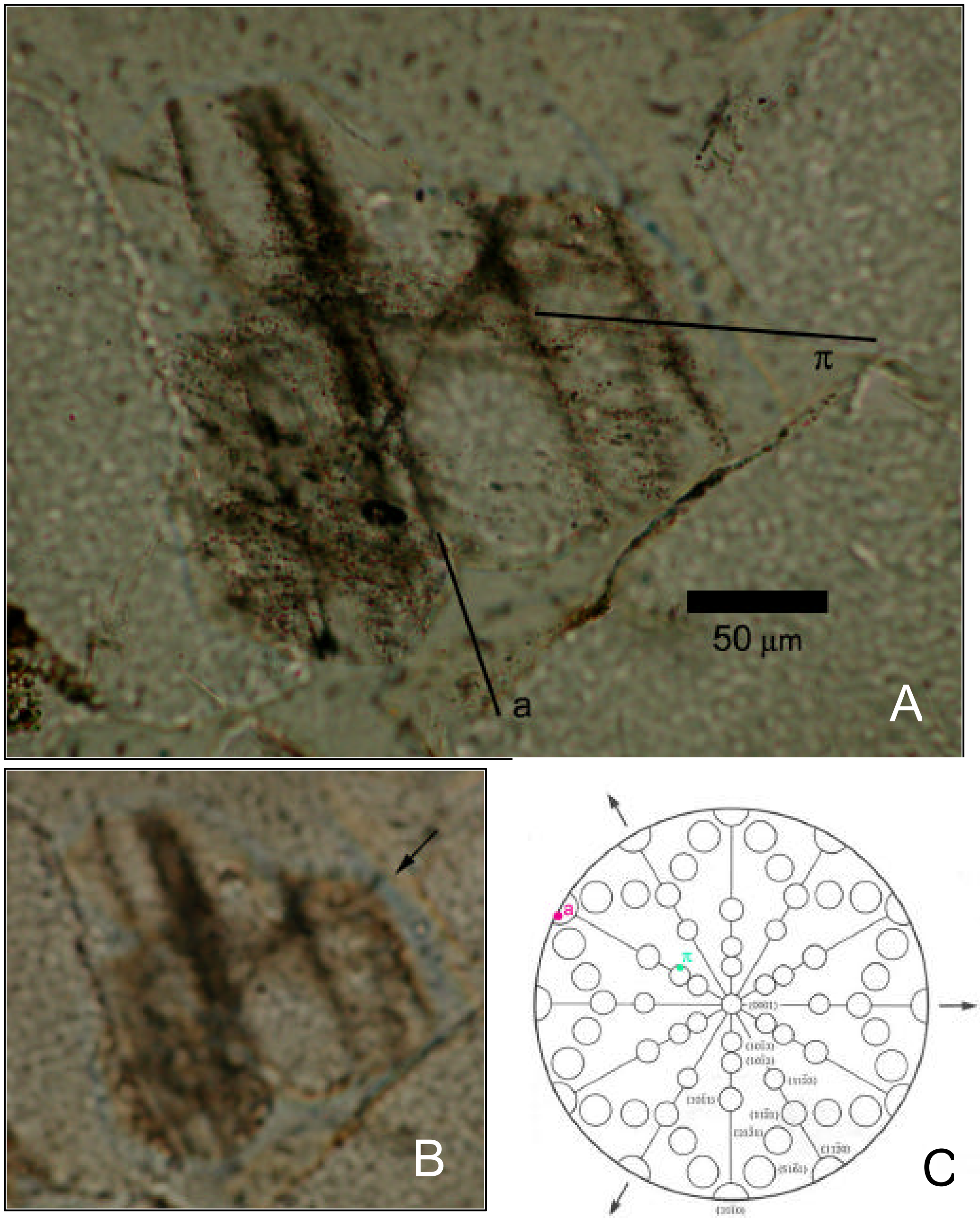

Figure 29. A) Photomicrograph of a quartz grain containing one set of planar fluid inclusion trails and one set of oriented fractures. PPL. B) The Becke line test indicates that the refractive index of the grain is less than 1.54. C) Stereographic plot of poles to the fluid inclusion arrays and the fractures suggesting that they correspond with {10-12} (π) and {11-20} (a), respectively.

spaced. Universal stage measurements suggest that the fluid inclusions follow planes parallel to {10-12}. The fractures run parallel to {11-20}. The Becke line test also suggests that this grain may have undergone shock metamorphism.

The orientations of ten planar features in five grains from the basal Twiggs Clay unit are summarized in a histogram below (Figure 30, top). The relative frequencies of planar features parallel to various lattice planes are similar to the frequencies of PDF's reported from impact craters and ejecta (Alexopoulos, et al., 1988; Grieve et al, 1996) including the Chesapeake Bay impact structure (Figure 30, bottom). The quartz grains reported here exhibit planar micro-fabrics and optical properties consistent with shocked quartz. The suite of possible PDF's suggests that these grains experienced pressures from about 18 GPa to greater than 25 GPa (Langenhorst and Clymer, 1996). These shocked grains may represent ejecta from a Late Eocene hypervelocity impact, most likely the Chesapeake Bay event, although other impacts cannot be ruled out.

Hardie Mine

The Hardie mine is located approximately 90 kilometers southwest of the Purvis School site within the town limits of Gordon (see Figure 3). The Upper Eocene Twiggs Clay and Irwinton Sand are exposed in the mine walls above the Huber Formation kaolin. About 30 centimeters to one meter of sandy sediment, commonly referred to as the Clinchfield Sand (Westgate, 2001), separates the top of the Huber Formation from the base of the Twiggs Clay (Figure 31). Along the eastern wall of the quarry, that unit is comprised of relatively thin coarse quartz-rich sand set in a dark brown to black silt and

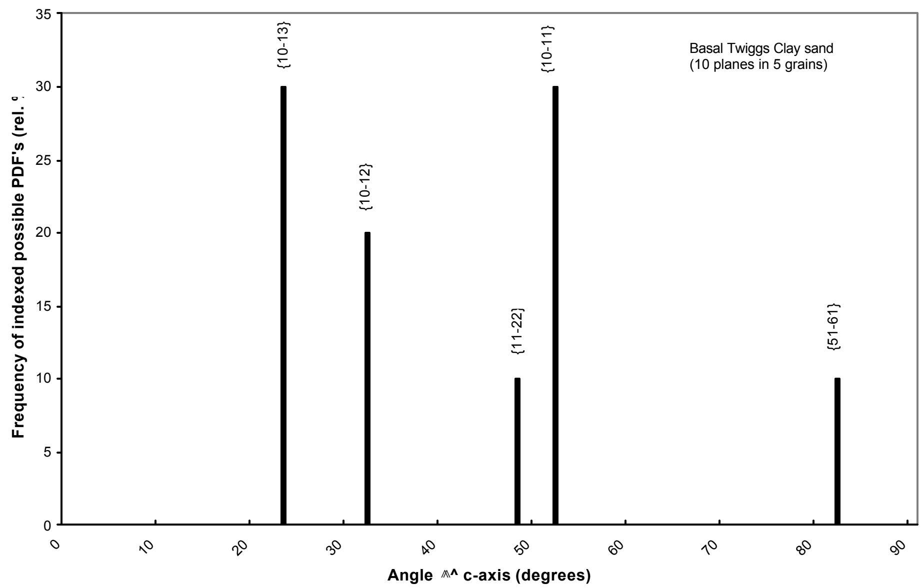

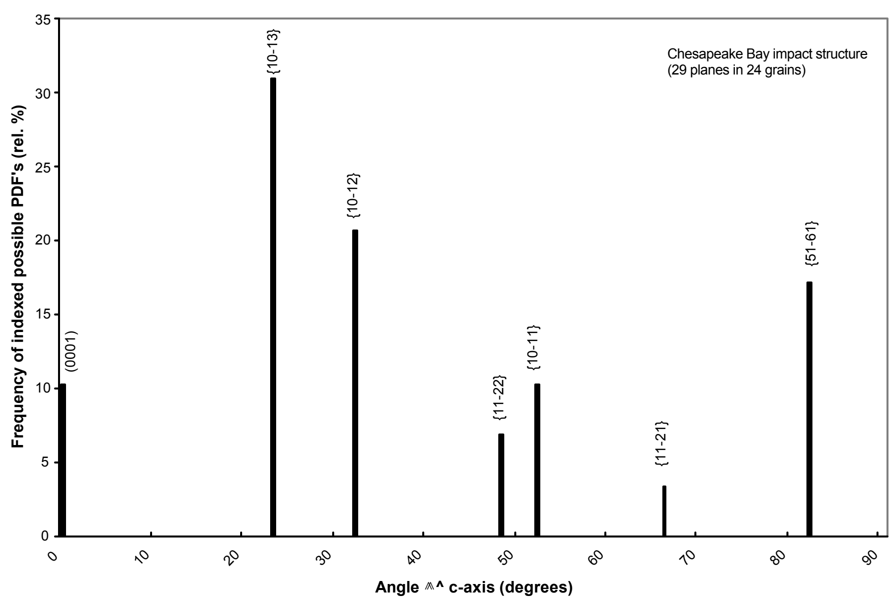

Figure 30. Histograms showing the relative frequency of PDF's indexed in shocked quartz grains from the Chesapeake Bay impact structure (bottom) [after Koeberl et al. (1996)] and possible PDF's in fine sand-size quartz grains from the sand unit at the base of the Upper Eocene Twiggs Clay at the Purvis School mine.

clay matrix. The unit is texturally and mineralogically similar to the sand described from the Purvis School mine. In the western wall of the quarry, the unit is quite different (Figure 32). There the coarse quartz-rich sand is thoroughly mixed with a hash of fine calcareous shell debris and fragments of phosphatic marine and terrestrial vertebrate fossils. The percentage of quartz sand and the size of the quartz grains both appear to increase toward the contact with the Twiggs Clay.

The Hardie mine is important to the present study because the sand unit at the base of the Twiggs Clay occupies the same stratigraphic horizon as the sand at the Purvis School mine; and as mentioned in an earlier section, L. E. Edwards (personal communication, 2003; Parmley and Holman, 2003) recently has determined a nannofossil age of 34.2 to 36.0 Ma for the unit. If the sand grains identified at the Purvis School site have been shocked, then there might be some evidence of the impact in the Clinchfield Sand at the Hardie mine — remembering, however, that the Hardie mine is significantly farther away from ground-zero.

While studying the microfossils assembled in the Chesapeake Bay crater-fill breccia, Edwards and others (Edwards and Self-Trail, 2002; Edwards et al., 2002; Edwards and Powars, 2003) observed dinoflagellates cysts with unusual surface features including folding, bubbling, and pitting. They attribute these textures to shock damage and partial melting caused by the impact. In a preliminary report (L. E. Edwards, unpublished memorandum to D. Parmley, 2002) concerning the microfossil and nannofossil assemblages in the Clinchfield Sand at the Hardie mine, Edwards suggests that some of the dinoflagellates show similar styles of damage and degradation. The possibility that

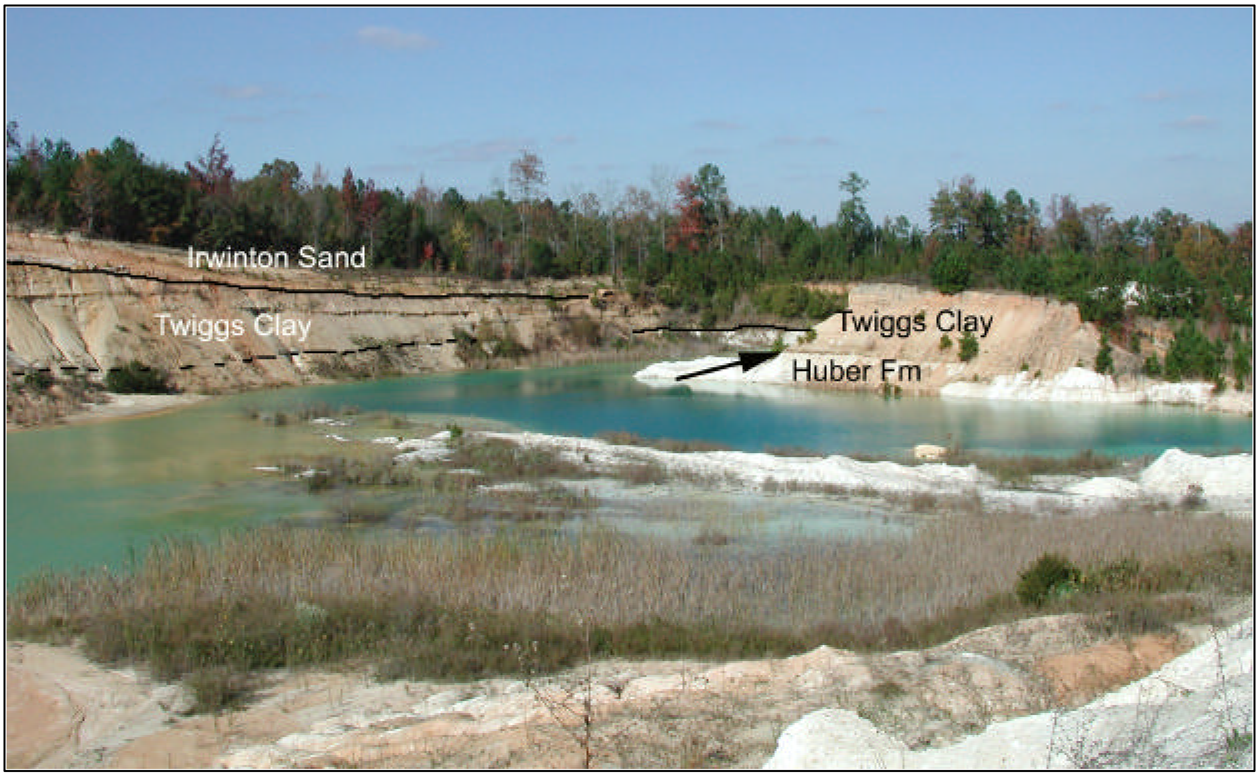

Figure 31. Photograph showing the eastern end of the Hardie mine. The arrow indicates the thin brown to black sand unit that separates the white kaolin of the Huber Formation from the gray marine shale of the Twiggs Clay. This layer, commonly referred to as the Clinchfield Sand, appears to be correlative with basal Twiggs Clay sand exposed at the Purvis School mine. The unit has been assigned a nannofossil date of 34.2 to 36.0 Ma (L. E. Edwards, personal communication, 2003; Parmley and Holman, 2003), close to the age of the Chesapeake Bay impact.

Figure 32. Photograph showing the contact between the calcareous sand and the overlying Twiggs Clay in the Hardie mine. The tip of hammer rests immediately below the contact.

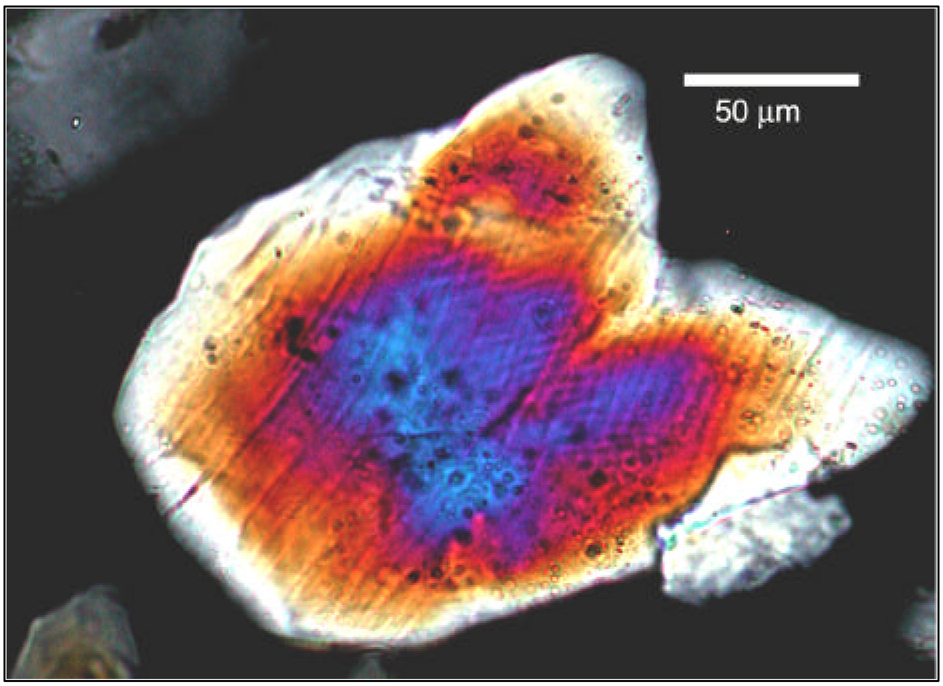

Figure 33. Photomicrograph of a quartz grain from the upper five centimeters of the Clinchfield Sand beneath the Twiggs Clay at the Hardie mine. The grain exhibits two intersecting sets of lamellae similar to PF's or PDF's. XPL.

the Hardie sediments contain impact-related microfossils, coupled with the stratigraphic context and new nannofossil age, necessitates the search for shock minerals at that location. To date, a cursory screening has resulted in the identification of a single quartz grain exhibiting a micro-fabric suggestive of shock metamorphism (Figure 33). The grain contains two intersecting sets of possible PDF's. No orientation data currently is available.

Supporting data: X-ray diffraction experiments

In addition to optical petrography, powder X-ray diffraction (XRD) experiments were conducted to test the hypothesis that certain micro-fabrics in fine sand-size quartz grains from the Purvis School site are indicative of shock metamorphism (for complete details, see Schroeder et al. (2002) and Schroeder and Harris (X-ray powder diffraction evidence for shocked quartz in an Upper Eocene sand deposit, Warren County, Georgia, U.S.A, submitted, 2003.). In short, shock-induced defects in quartz may cause peak, or line, broadening in the XRD profiles of the affected grains (Short, 1970; Schneider et al., 1984; Stöffler and Langenhorst, 1994). A powder sample was prepare from eight grains that contained possible PDF's. The grains shown in Figures 22 and 23 are representative of the grains that were used. The powder diffraction profile of these grains were compared to samples composed of *normal* metamorphic quartz, vein quartz, undeformed and random samples of quartz from the basal Twiggs Clay sand unit, and Manson impact ejecta displaying multiple sets of PDF's. Because sample sizes were very small, only the (100) and (101) reflections could be measured reliably.

These experiments support the hypothesis that the basal Twiggs Clay sand contains shocked quartz. The results show that the (100) reflection is broadened for both the Manson ejecta and those Upper Eocene grains containing possible PDF's. Similar broadening is not observed for the (101) reflections. These observations are consistent with the behavior Short (1970) observed in the XRD spectra of nuclear-shocked quartzite. At progressively higher pressures, the (100) reflection becomes broader. The intensity of the (101) peak steadily diminishes, but the peak width does not change significantly.

Shocked zircons?

The identification of additional shocked minerals or other recognizable impact debris would buttress the claim that shocked quartz exists in the basal Twiggs Clay sand unit. As noted before, the fine and very fine sand-size fractions of that unit contain abundant feldspars and euhedral zircons. No unambiguous shock features have been observed in the feldspars; however, some of the zircons appear to display uncharacteristically-low birefringence which can result from shock metamorphism (Glass et al., 2002) or, more commonly, from radiation damage (Morgan and Auer, 1941). Glass et al. (2001, 2002) have reported shocked zircons associated with Chesapeake Bay ejecta at several ODP sites and in Barbados. Recently, they discovered that some shocked zircons had transformed, at least partially, to *reidite*, a high-pressure $ZrSiO_4$ polymorph indicative of pressures greater than 30 GPa.

Consequently, reidite may be expected to occur with shocked quartz in the basal Twiggs Clay sand unit. In the refractive oils used to screen the sand samples for shock quartz, zircons are obvious because of their extremely high relief. Twenty euhedral zircons each measuring approximately 125 μm in length and displaying relatively low birefringence and a pale brownish-green hue in oil were picked by hand from the basal Twiggs Clay sand. The grains were crushed and ground for ten minutes with alcohol in a zirconium mortar. The alcohol was pipetted onto a zero-background quartz plate and the powder dried onto the surface of the plate at room temperature. The powder was analyzed by X-ray diffraction using a Scintag diffractometer, Co $K\alpha$ radiation, a 250 mm goniometer circle, 2°/4° primary and scattering slits, 0.5°/0.3° scattering and receiving slits, 40 Kv and 40 Ma, and a count time of 0.3° per minute between 5 and 70° 2θ. The resulting diffractogram is presented in Figure 34.

The XRD experiment produced a full zircon pattern. Peaks corresponding to kaolinite and quartz also are observed and probably are the result of contamination of the plate by dust in the lab. Each peak may be indexed to one of these three minerals except for the relatively strong peak at 2.824 Å. The high-intensity line for reidite in shocked zircons is reported as 2.823 Å (Glass et al., 2002).

Although the selected zircons may contain reidite, most subsidiary peaks for reidite lie so close to normal zircon peaks and have such low relative intensities (Liu, 1979; Glass et al., 2002) that unequivocal and proper indexing of the high-pressure polymorph may not be possible using this method. Single crystal diffraction or Debye-Scherrer techniques could produce less ambiguous results. Nevertheless, the appearance of a 2.824 Å reflection in the middle of a complete zircon profile suggests that reidite may be present. This observation strengthens the argument that the basal Twiggs Clay sand layer preserves ejecta from a Late Eocene impact.

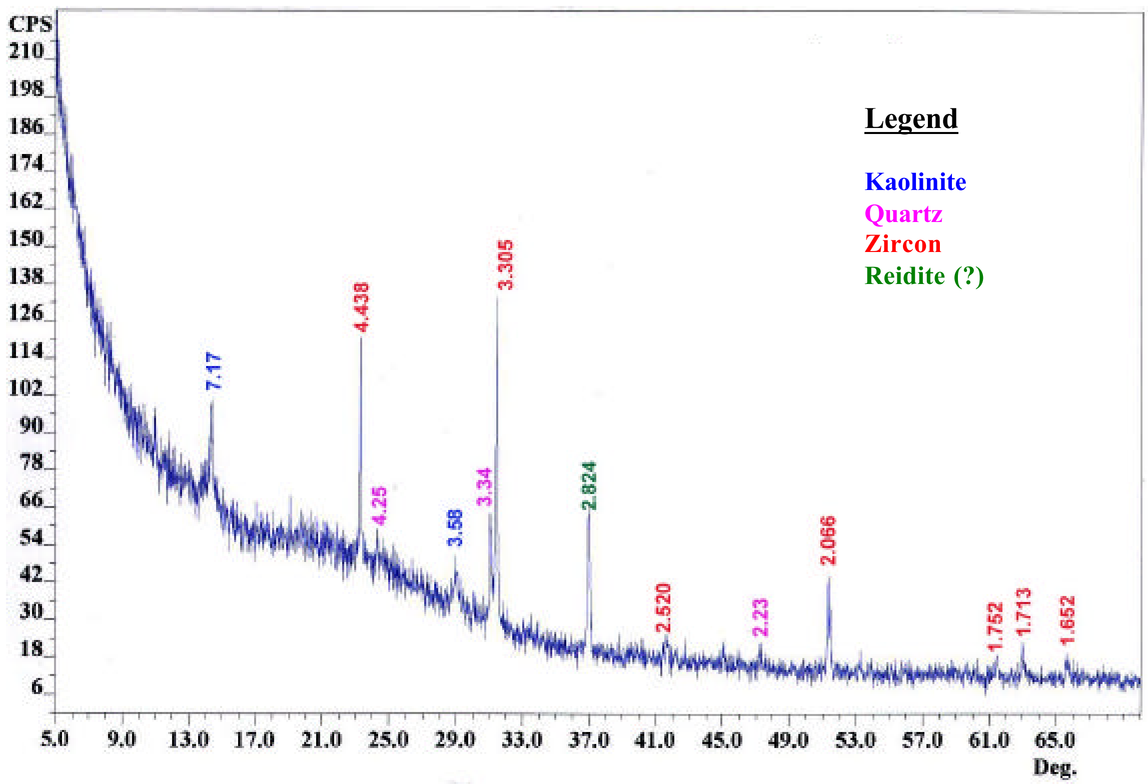

Figure 34. X-ray diffractogram of a powder ground from twenty zircons collected from the basal Twiggs Clay sand. The d-spacing (in angstroms) of each major peak is listed in the color corresponding to the mineral to which it can be indexed.

Similar to reidite, halite has a prominent diffraction maximum near 2.82 Å (Klein and Hurlbut, 1999). XRD reflections from blank slides sometimes show subtle humps near 2.81 to 2.82 Å that may be produced, in part, by contamination of the slide surfaces with skin oils bearing salt crystals; however, these reflections typically do not form sharp peaks. To test the possibility that the 2.824 Å is an artifact of contamination from salt or some other substance inherited during sample preparation, a series of control samples were run under identical experimental conditions. A clean quartz plate shows no obvious reflections. A quartz plate smeared with skin oils and immersion oils may exhibit minor reflections indicative of the silica and kaolinite dust prevalent in the lab. Samples of corundum powder (selected in order to determine if contaminants might have abraded off of the mortar and pestle) and quartz were prepared in the same manner as the zircons, using comparable masses of material. In each control, a sharp peak near 2.824 Å could not be reproduced.

If the basal Twiggs Clay sand unit contains shocked quartz from the Chesapeake Bay impact, then shocked zircons could be plentiful in the sediment. Heavy-liquid separation of zircon from the sand should be completed so that many more zircons may be studied. The identification of ejected zircons could be important because radiometric ages may be determined. Those ages may help constrain the provenance of the target material and definitively tie the distal ejecta to the Chesapeake Bay crater.

Mosaicism, ballen quartz, coesite, and diaplectic glass?

In addition to PDF's, quartz that experiences pressures between about 10 and 40 GPa may develop *mosaicism* (Stöffler and Langenhorst, 1994; Montanari and Koeberl, 2000). Mosaicism is recognized by a peculiar mottled extinction pattern. Unlike undulatory extinction (frequently observed in tectonically deformed quartz), mosaic extinction does not sweep through a grain but occurs at discrete positions as the microscope stage is rotated. At extinction, portions of a mosaic grain remain illuminated causing the grain to appear patchy (Figure 35A). Some fine sand-size quartz grains from the Purvis School site exhibit extinction patterns (Figure 35B) similar to the mosaicism observed in shocked quartz from other recognized impact ejecta.

Above about 50 GPa and 1700° C, quartz undergoes fusion to form lechatelierite (Stöffler and Langenhorst, 1994; Montanari and Koeberl, 2000). Lechatelierite is a silica glass that commonly is found as inclusions in tektites (Albin, 1997a) and may occur as inclusions in shocked quartz associated with PDF's, coesite, and diaplectic glass (Stöffler and Langenhorst, 1994; Grieve et al., 1996). Lechatelierite is metastable and reverts to cristobalite (Schuraytz and Dressler, 1997; Polsky and McHone, 1998). During devitrification the material develops a characteristic *ballen* texture (Grieve et al., 1996,; Schuraytz and Dressler, 1997; French, 1998). Ballen quartz is recognized by a distinctive "crackled" appearance (see Figure 36) and is indicative of an impact origin (Montanari and Koeberl, 2000). Several examples of possible ballen quartz have been identified in the basal Twiggs Clay sand (e.g. Figure 37).

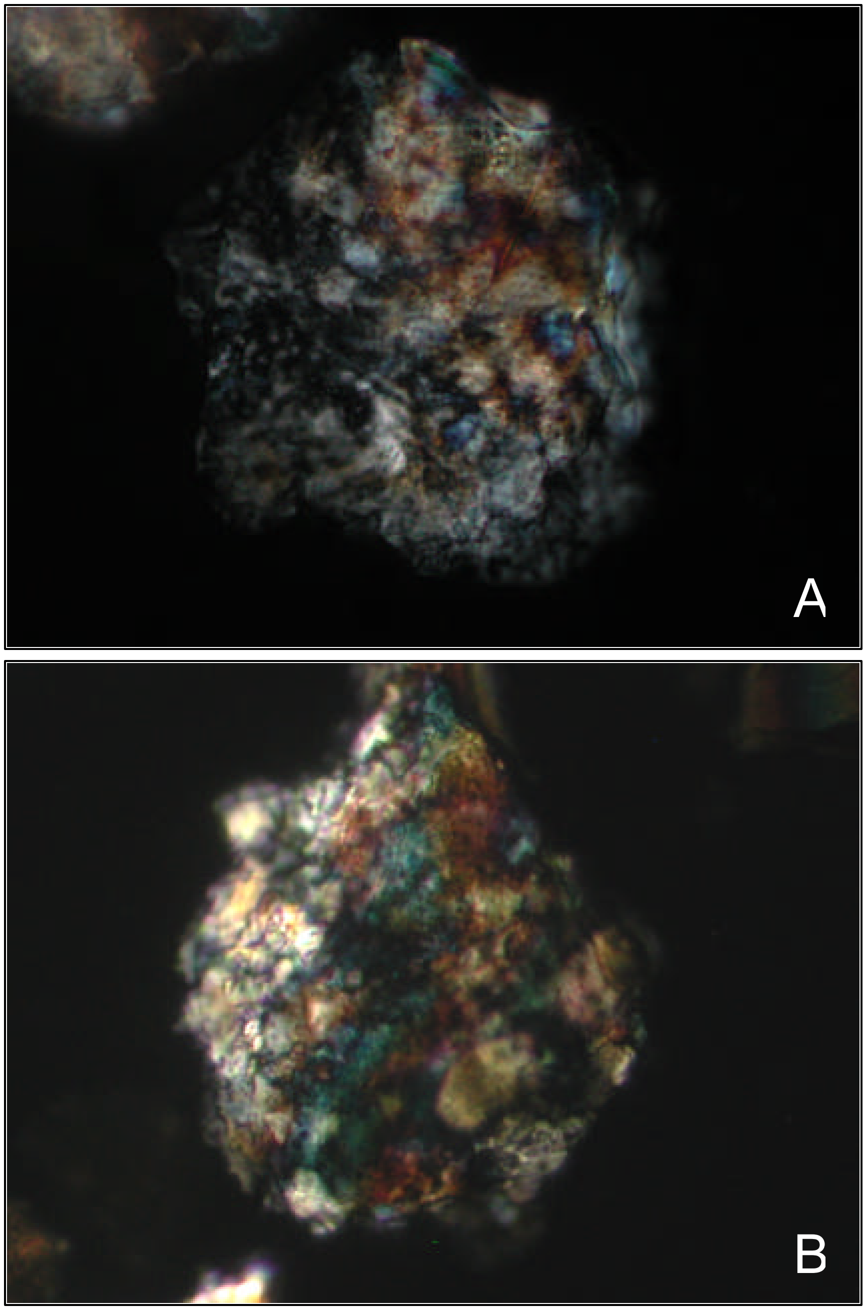

Figure 35. A) Photomicrograph of a quartz grain from the K-T boundary (Clear Creek North, Colorado) showing the mosaic extinction indicative of shock metamorphism. XPL. B) Photomicrograph of a quartz grain from the basal Twiggs Clay sand exhibiting irregular extinction similar to mosaicism. XPL. Both grains are about 200 μm wide.

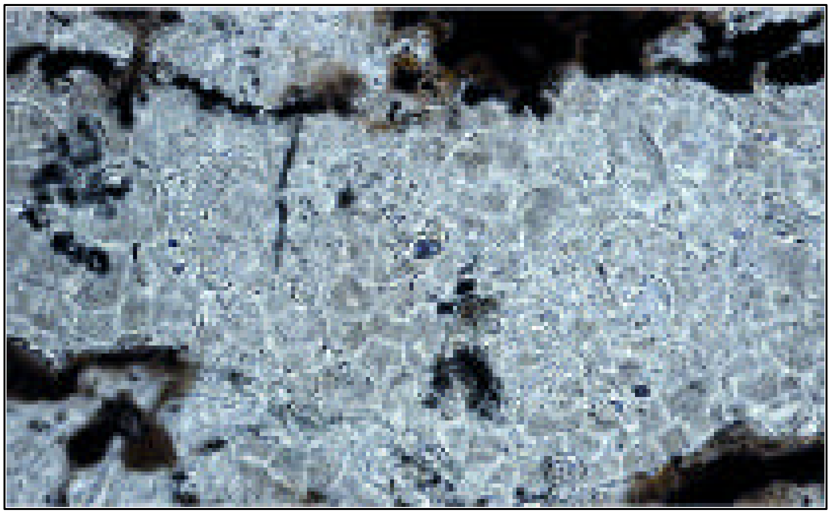

Figure 36. Photomicrograph of ballen quartz from the Chicxulub impact crater. Image is 570 μm wide. PPL. Photograph from Schmitt et al. (2003).

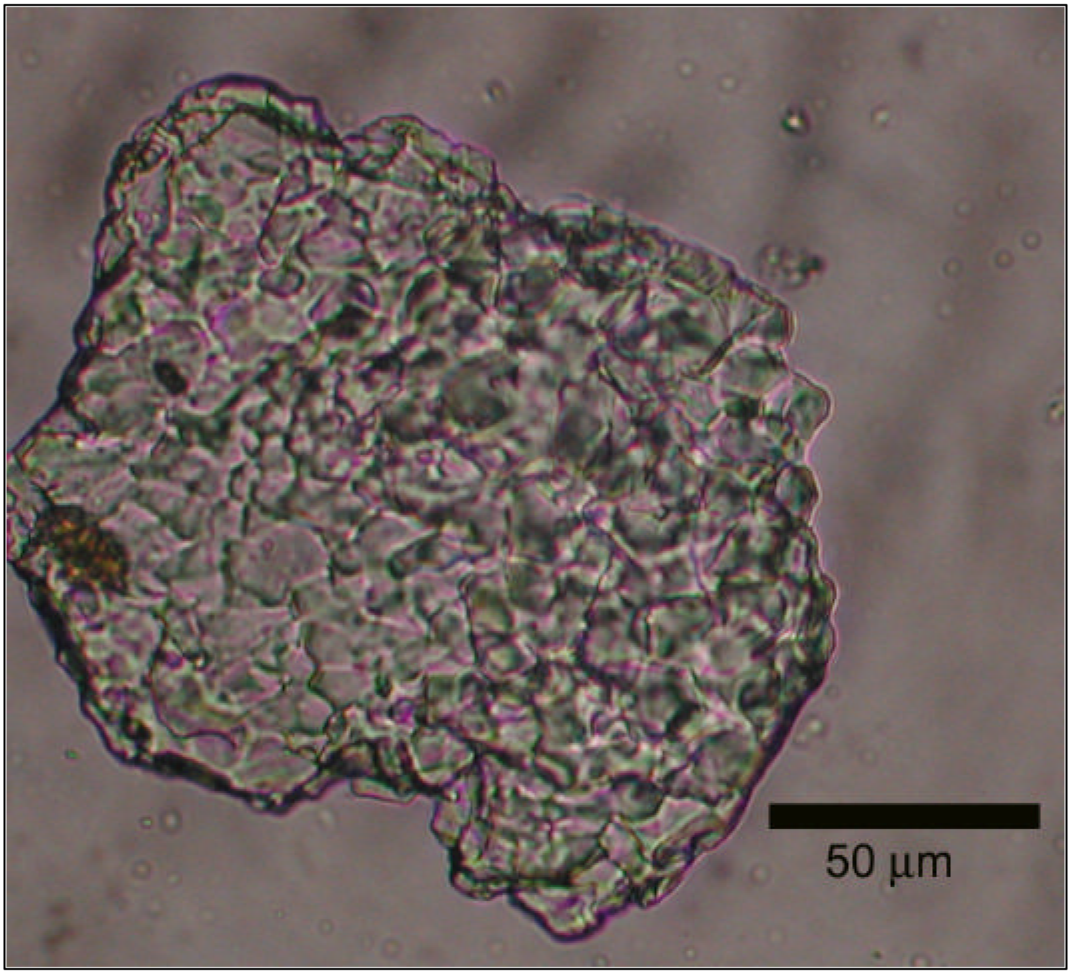

Figure 37. Photomicrograph of a grain from the basal Twiggs Clay sand layer showing the crackled texture suggestive of ballen quartz. PPL.

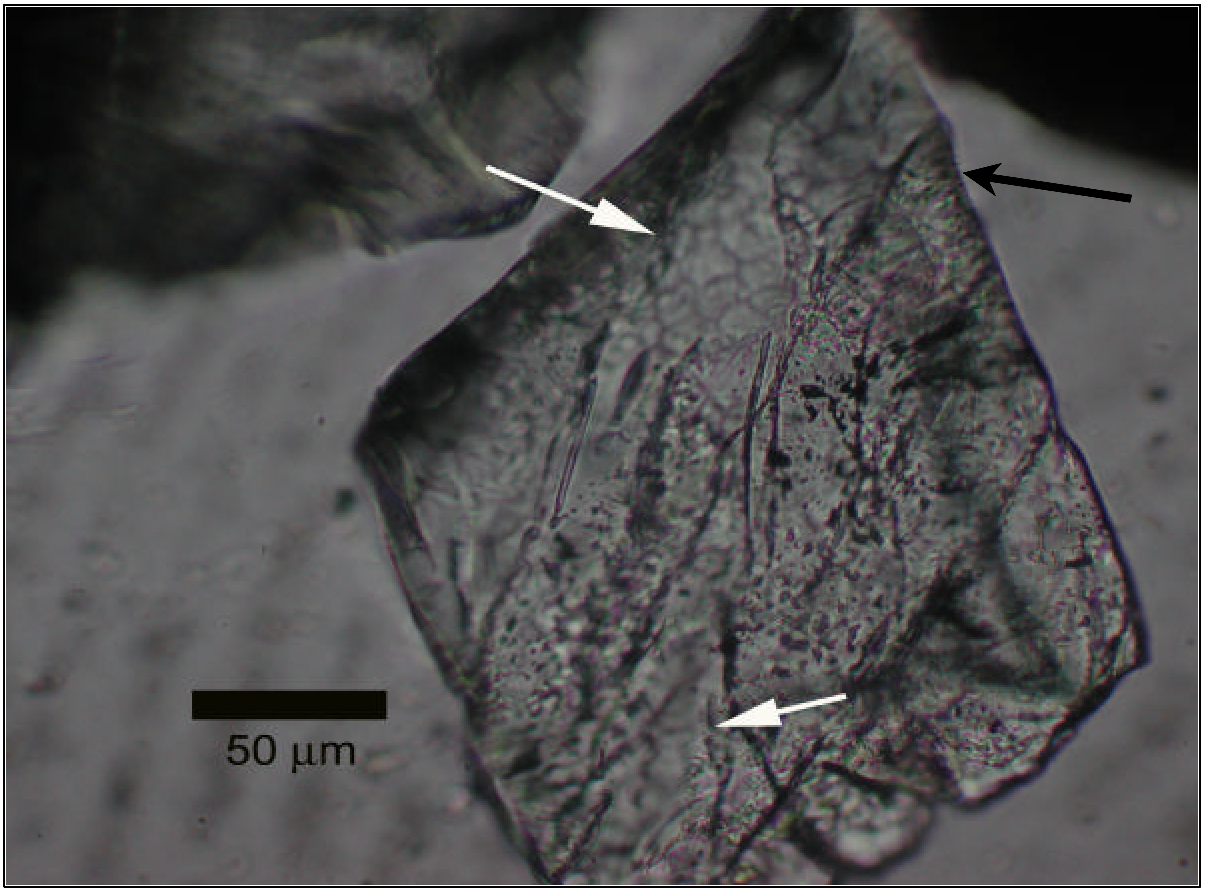

Figure 38. Photomicrograph of an SiO_2 grain that contains two regions (indicated by white arrows) that exhibit the texture indicative of ballen quartz. Note the euhedral appearance and prismatic habit of the grain. Closely-spaced planar features, possible PDF's or microfractures, also are present in portions of the grain (black arrow). PPL.

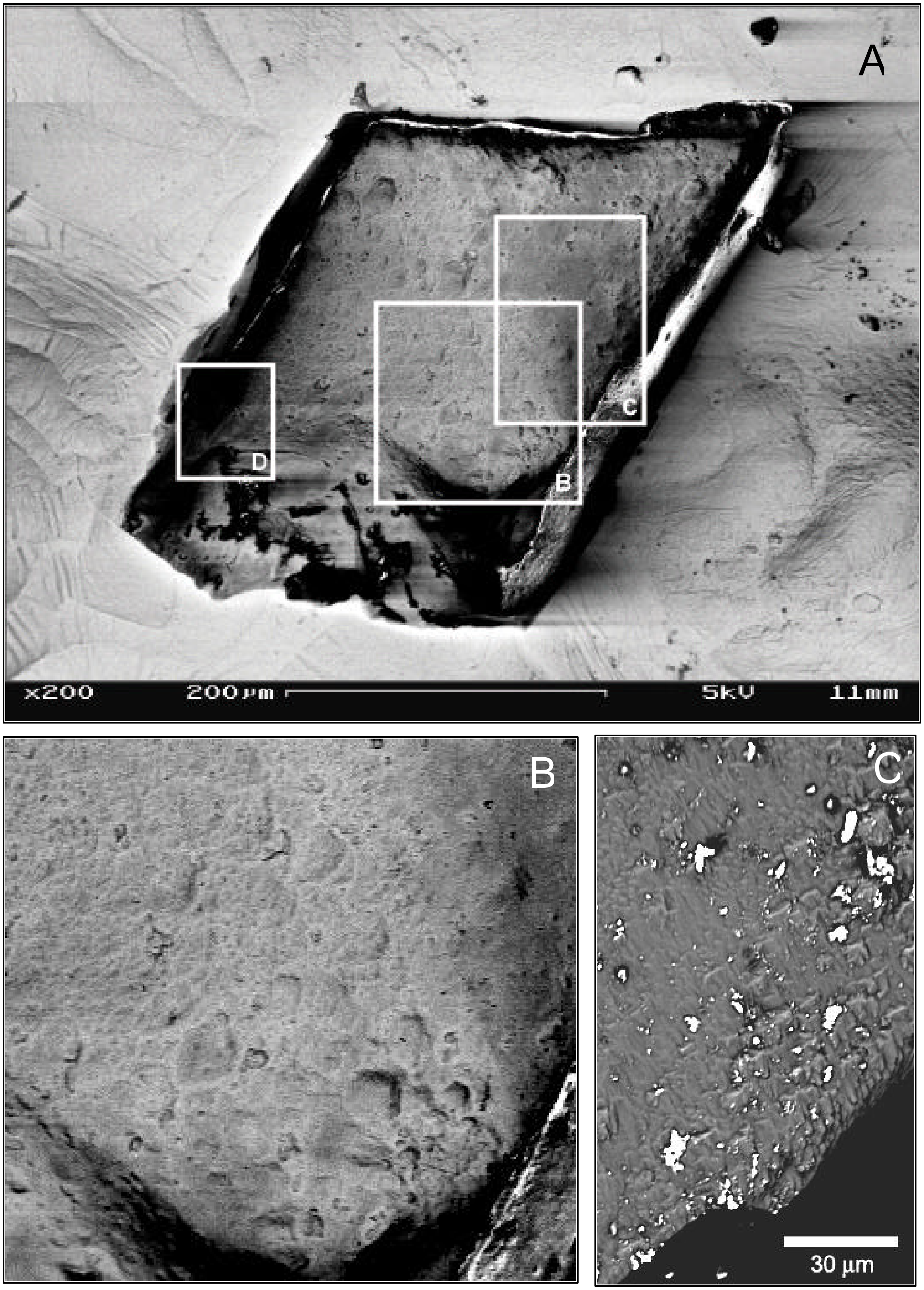
A
C
B
D
x200
200μm
5kV
11mm
B
C
30 µm

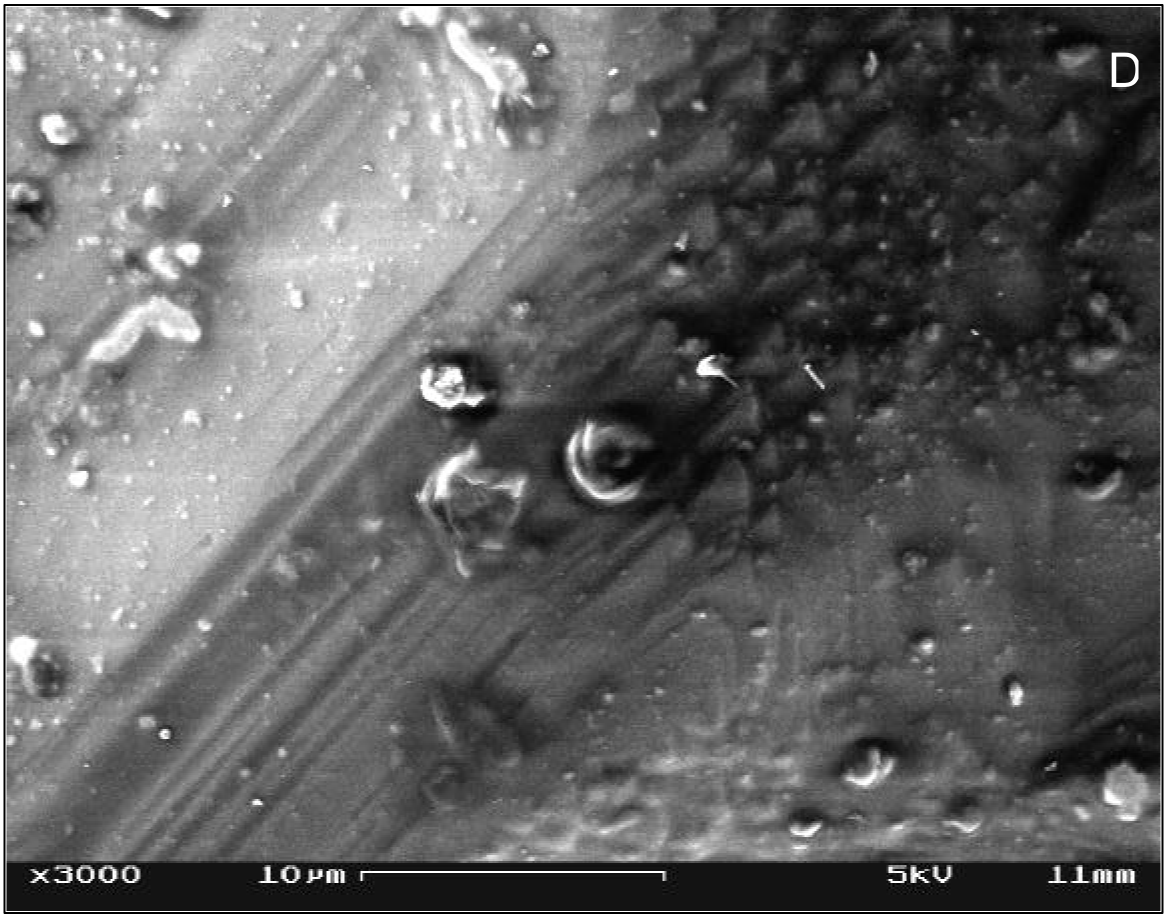

Figure 39. Electron photomicrographs of an unusual SiO_2 grain. A) Gamma-corrected secondary electron image (SEI) showing the surface texture of the entire grain. B) Close-up image of possible *ballen* quartz texture. C) Backscattered electron image (BSE) of a portion of the grain exhibiting an orthogonal pair of microfractures. (D) SEI photomicrograph of the grain edge showing the open ends of the microfractures.

The distinctive structure characteristic of ballen quartz occurs in one instance within a 250 µm-wide euhedral silica grain (Figure 38). The crystal has a prismatic shape and the dimensions are consistent with a monoclinic crystal. If the grain is a cleavage fragment, the cleavage, nevertheless, appears to be monoclinic. This is consistent with the observation that at least portions of the grain display a sharp, positive biaxial interference figure. The interference figure is inconsistent with normal quartz but should be expected for either of the monoclinic SiO_2 polymorphs, tridymite and coesite. Both polymorphs are biaxial, but tridymite has a lower refractive index than α-quartz. The refractive index of this grain is greater than about 1.54. Coesite has a relatively high refractive index (n=1.59) (Klein and Hurlbut, 1999). Electron imaging highlights the unusual ballen texture of the grain (Figure 39B) and also reveals the presence of an orthogonal pair of microfractures cutting through the grain (Figures 39C and 39D). These planar microfractures, or even possible PDF's, are also seen observed near the edge of the grain in polarized light (Figure 38). If the grain contains coesite and PF's or PDF's in addition to ballen quartz (not an uncommon situation in impact materials (Stöffler and Langenhorst, 1994; Liu et al., 2002), that would indicate that the grain must have experienced peak pressures and temperatures consistent with a large hypervelocity impact (Stöffler and Langenhorst, 1994).

Finally, a single grain has been discovered that resembles maskelynite, a glass produced by solid-state transformation of plagioclase feldspar above about 35 GPa (Koeberl, 1997). Typically maskelynite preserves the original crystal habit and defects (Koeberl, 1997). In plane-polarized light, twin lamellae are obvious in the grain (Figure

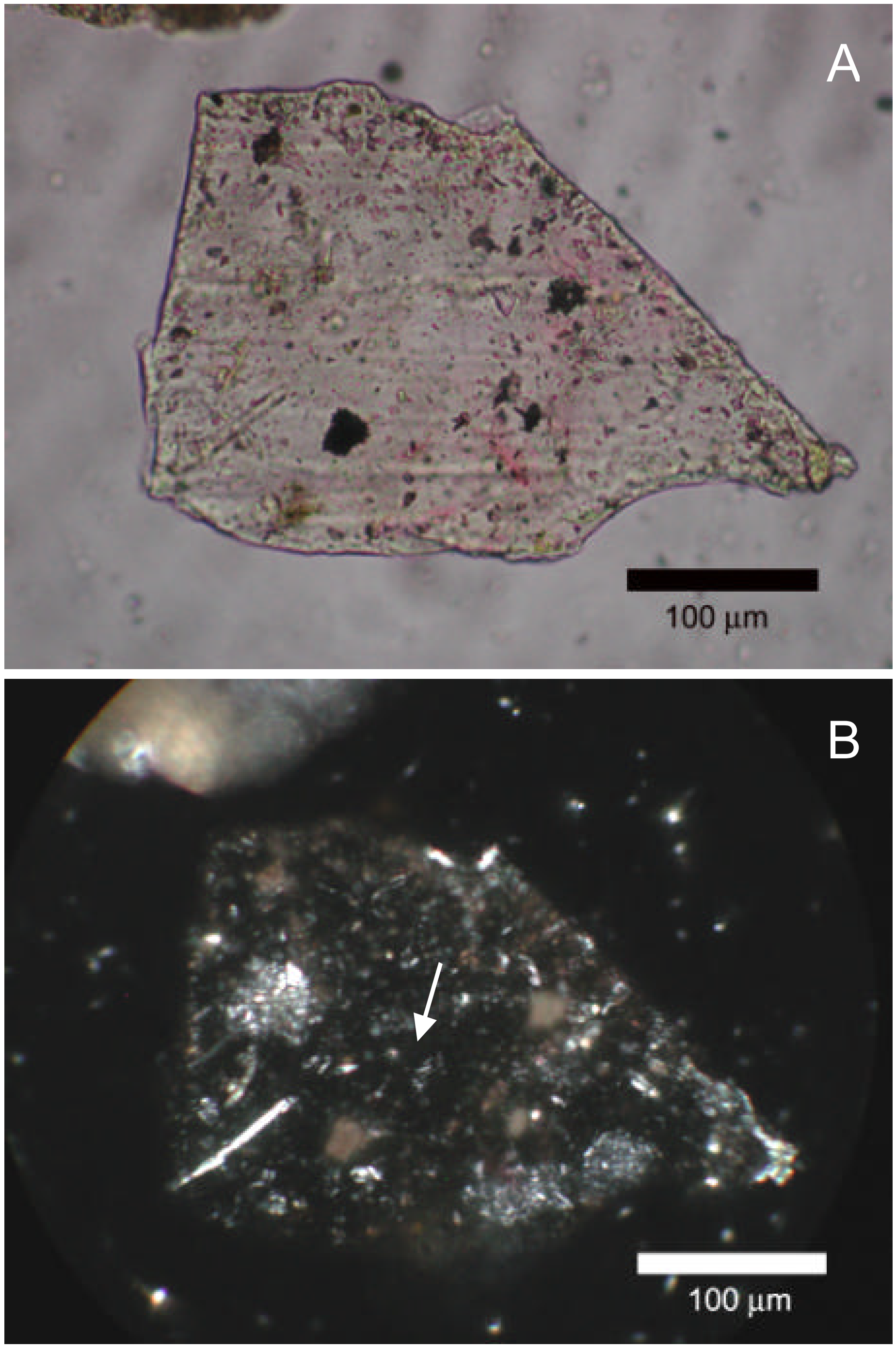

Figure 40. A) Photomicrograph of possible maskelynite grain showing preservation of albite twin planes. PPL. B) Most of the grain is composed of amorphous or microcrystalline material. Several white patches, in addition to a circular region indicated by the arrow, may be spherulites. XPL.

40A). When the nicols are crossed (Figure 40B), the grain appears to consist mostly of isotropic material. The faint outline of albite twins still may be seen. Primary maskelynite is not stable and rapidly devitrifies forming microcrystalline textures and spherulites (French, 1998). That may explain the fabric observed in this grain.

CHAPTER 5

EVIDENCE FOR AN IMPACT-GENERATED DEBRIS FLOW

The identification of possible shocked quartz and other airfall ejecta in the Upper Eocene sediments of east-central Georgia may soon lead geologists and tektite hunters to a treasure trove of georgiaites. Perhaps the grains alone can yield important information about pact dynamics and ejecta distribution. Yet the most exciting prospect of finding the Chesapeake Bay impact layer in the southeastern Coastal Plain is the possibility of following the horizon to clues concerning what devastation the impact might have wrought on geological and ecological systems up and down the eastern seaboard.

Powars and Bruce (2000) suggest that the Chesapeake Bay impact could have triggered mega-tsunamis 100's of meters high. McHugh et al. (1998) report evidence of submarine debris flows, approximately 300 kilometers northeast of the crater, probably caused by seismic shaking in the wake of the collision. Secondary cratering potentially may generate ground-hugging debris flows capable of traveling 10's to 100's of meters per second (Oberbeck, 1975; Hörz et al., 1983; Rampino, 1994). Because a significant portion of the target was water and wet sediment, there is the possibility that some debris flows could have been quite fluid (Melosh, 1989). As mentioned in Chapter 2, impacts into saturated sediments also may eject larger volumes of material farther distances from the target (Stewart et al., 2000; Melosh, 2001).

The effects of larger volumes of ejecta reaching greater distances downrange might be magnified to the southwest of the crater, if the impact was oblique. Perhaps some evidence of mega-tsunamis or extraordinary debris flows are preserved in strata correlative with sediments containing shocked quartz.

Diamictite stratigraphy and composition

Eight to ten kilometers down-dip from the Purvis School mine, and extending over an area more than 100 kilometers long from Gibson, Georgia to Aiken, South Carolina, the stratigraphic interval between the Huber Formation kaolins and the Upper Eocene Dry Branch Formation sands and clays is occupied by a 0.5 to ≥ 2 meter-thick diamictite (Figure 41). The thickest reported occurrence of the diamictite is along Windsor Spring Road in Augusta (diamictite site #3 in Figure 3) where the thickness may exceed two meters (Huddlestun and Hetrick, 1986)[3]. The lithology is unique in the Coastal Plain succession, and previous workers (Carver, 1972; Huddlestun and Hetrick, 1986) have recognized that the unit represents a fundamental change in sediment source.

The diamictite typically occurs directly above the flint, or hard, kaolin that commonly caps the Huber Formation; and where the diamictite has become indurated through recrystallization (P. A. Schroeder, personal communication, 2003) or opalization (Moskow, 1988), some authors have referred to it as the brecciated (Moskow, 1988) or mottled (Crawford et al., 1966; Sandy et al., 1966) flint kaolin. However, Huddlestun and Hetrick (1986) correctly (in this author's estimation) identify the diamictite as a

[3] Currently the thickness of the diamictite unit is difficult to determine at the Windsor Spring Road location due to excessive vegetation on the outcrop.

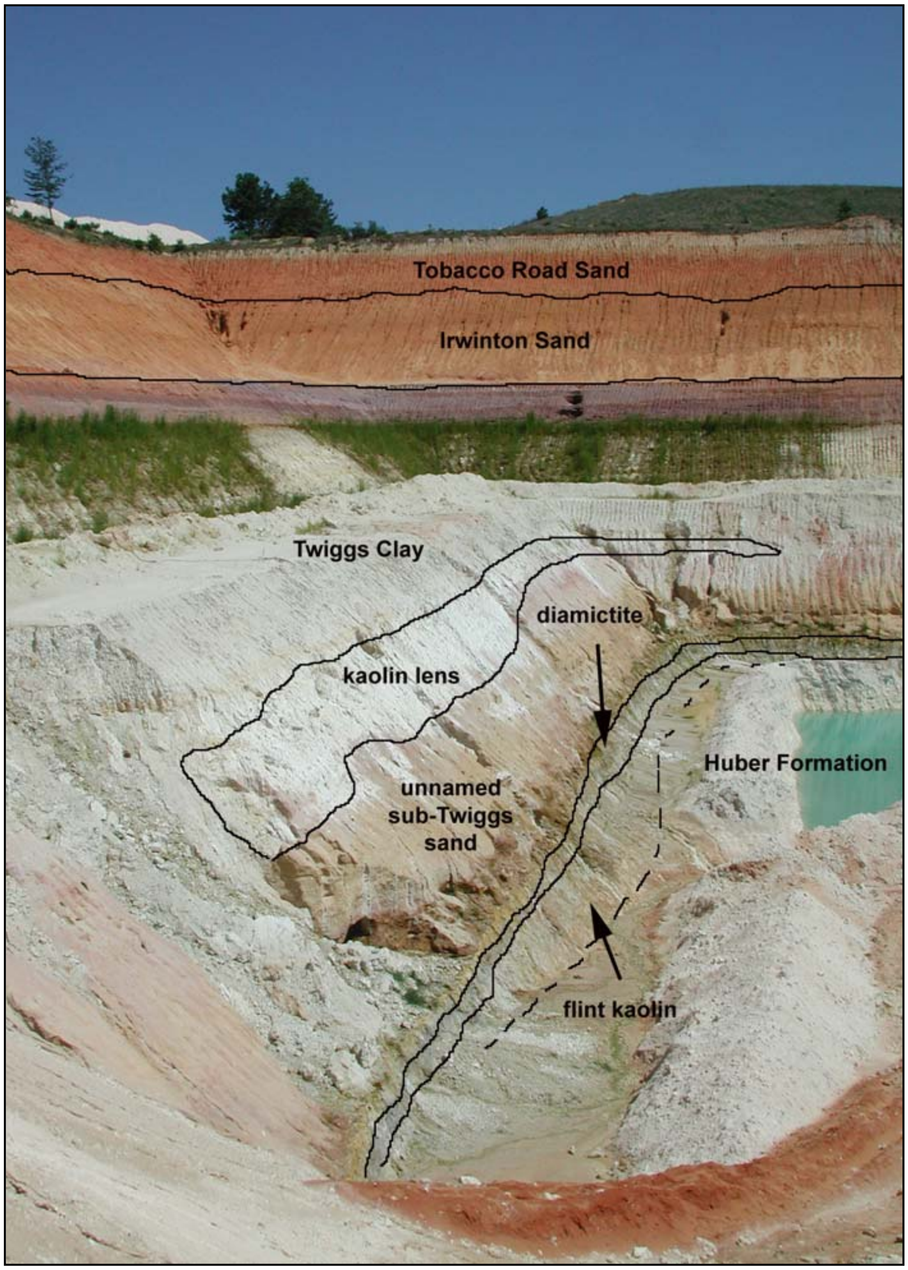

Figure 41. Photograph of the northeastern corner of J.M. Huber Corporation's Bracewell mine located near the border of Jefferson and Richmond Counties (diamictite site #2 in Figure 3). The distinctive gray-colored diamictite caps the flint, or hard, kaolin at the top of the Huber Formation. The diamictite ranges from 30 to 50 centimeters thick at this location. The unit is overlain by a thin, bright orange siltstone that contains fossilized trees.

separate unit below the Twiggs Clay and distinct from the underlying kaolins. It is sometimes overlain by, or is possibly interbedded with, a spiculitic sand, and Huddlestun and Hetrick (1986) assign the diamictite and the associated sand to the Clinchfield Sand (the Albion Member). The stratigraphic nomenclature largely is arbitrary because other units of the Clinchfield Sand do not occur where the Albion Member is exposed (Huddlestun and Hetrick, 1986); and according to Moskow (1988), other workers, including S. M. Pickering have suggested that the unit comprises the lowermost member of the Twiggs Clay. It seems plausible that the diamictite could be correlative with the proposed impact horizon.

Several authors have suggested that the diamictite is a volcaniclastic sediment (Crawford et al., 1966; Sandy et al., 1966; Carver, 1972; Huddlestun and Hetrick, 1986). Crawford et al. (1996) observed that the mottled kaolin at the Harbison-Walker mine (Diamictite site #1 in Figure 3), near Gibson, contains subangular brown masses that sometimes "show flow structure like those in volcanic glass." They proposed that the unit is an altered tuff.

Although the diamictite does appear texturally similar to weathered felsic tuffs (Figure 42), previous authors have never speculated where the Late Eocene volcanic source might have been. Gibson and Towe (1971) suggested that Mid-American or Caribbean volcanoes contributed some volcanic components to Coastal Plain sediments during the Eocene, but such distant sources seem insufficient to produce a relatively thick ($\approx$ 0.5 to 2 meters) deposit on the eastern shores of Georgia. Prior to the early 1990's, most stratigraphers were unaware of the Chesapeake Bay impact and the Late Eocene

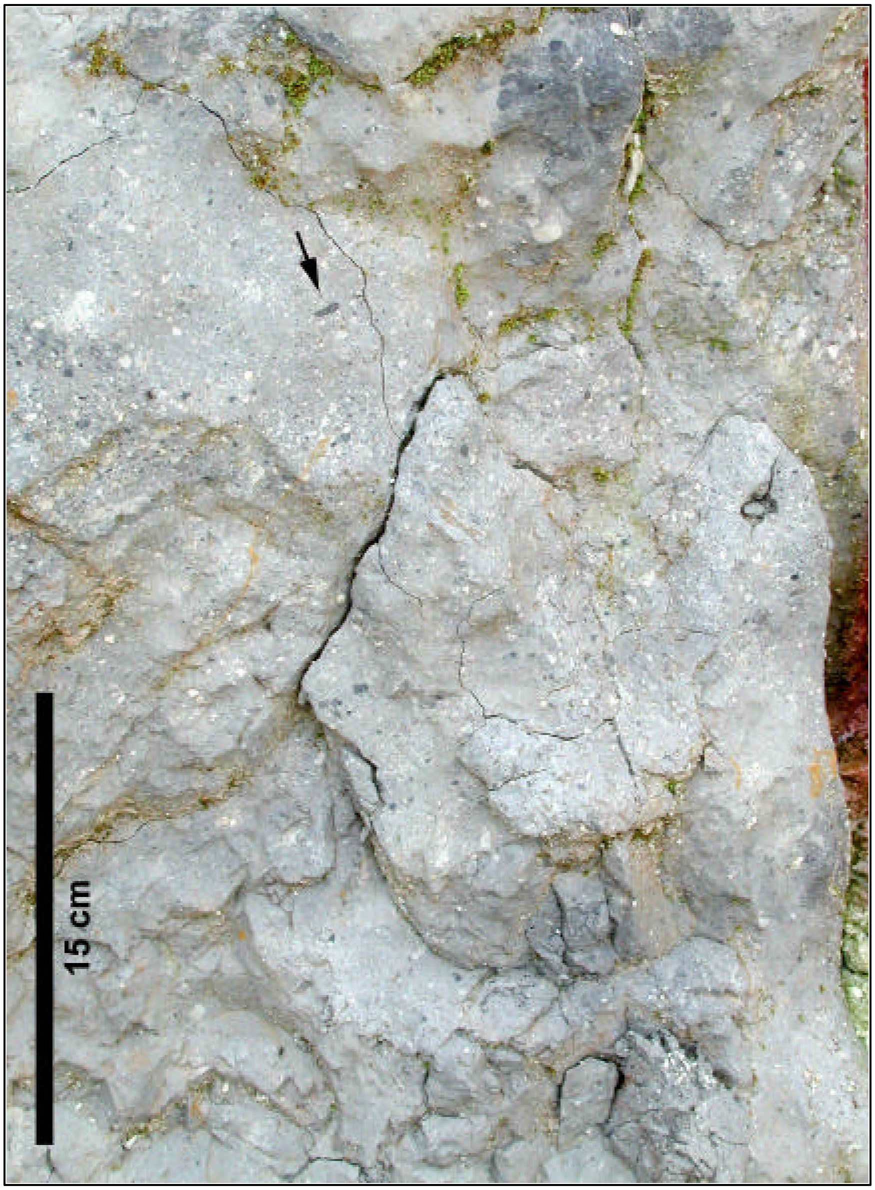

Figure 42. Photograph of the diamictite exposed at the Bracewell mine. The texture of the unit appears similar to weathered felsic volcaniclastic rocks. The white clay clasts might represent altered feldspars, and the darker smectites could be decomposed glasses. Most of the smectite clasts are well-rounded and some, including the one marked by the arrow, appear to be aligned and flattened parallel to the bedding plane.

cataclysm that must have ensued. Earlier workers could not have known to consider the potential effects of an impact on Coastal Plain geology. Today, the unusual nature of the diamictite and its special stratigraphic position suggest that its genesis should be re-evaluated to consider an impact origin (Harris, 2003).

The diamictite is composed of a gray kaolin matrix supporting cream-colored to white kaolinite clasts and dark-gray to greenish-black blebs composed of a dioctahedral smectite (determined by XRD) (Figure 43). The kaolinite clasts come in a variety of shapes from angular to rounded. They range in size from nearly 0.1 millimeter to occasionally greater than 4 centimeters wide. The smectite clasts show significantly less variation and range from less than 0.1 millimeter to rarely more than a few millimeters in diameter. Most of the smectite clasts are between 0.5 and 1 millimeter across. They have a granular texture and some of the clasts appear to be enveloped by thin, white rinds (Figure 44).

Diamictite sedimentology and emplacement

Two features of the diamictite are consistent with emplacement by a debris flow. First, the clasts are quite poorly sorted, as one would expect in a debris flow deposit (Prothero and Schwab, 1996). Second, in places the diamictite displays reverse grading (Figure 45) which may occur in debris flow deposits as a result of kinetic sieving (Hampton, 1979; Todd, 1996).

In addition to exhibiting properties consistent with debris flow, the diamictite exhibits evidence that the kaolin and smectite clasts experienced different modes of

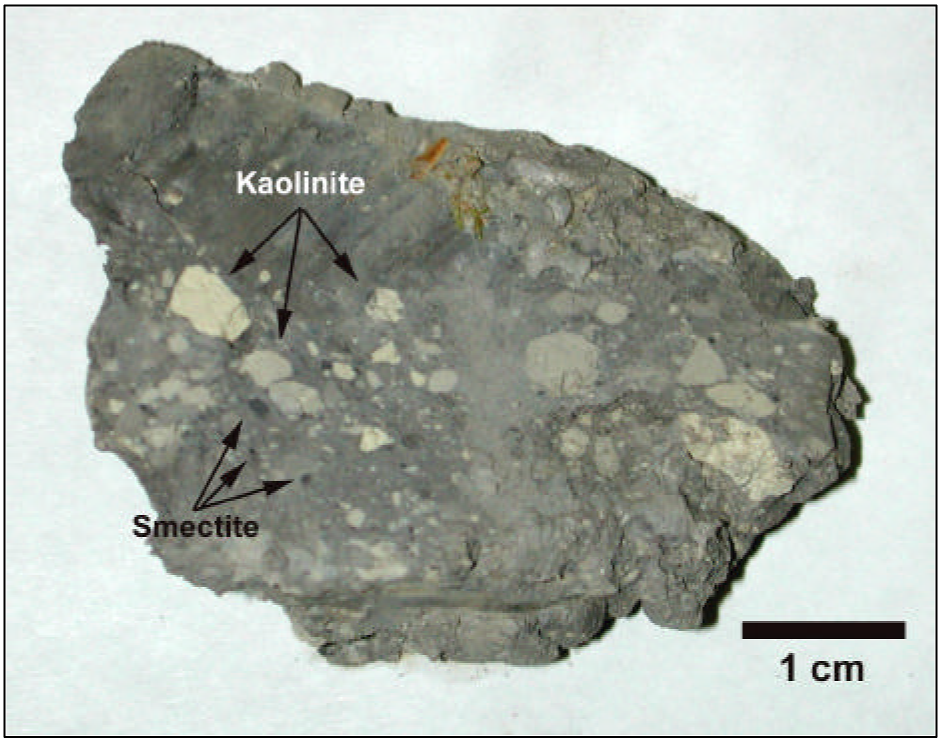

Figure 43. Photograph of a piece of the diamictite showing light-colored angular kaolinite and kaolin pebbles and smaller, rounded blebs of greenish-black smectite in a matrix of gray kaolin.

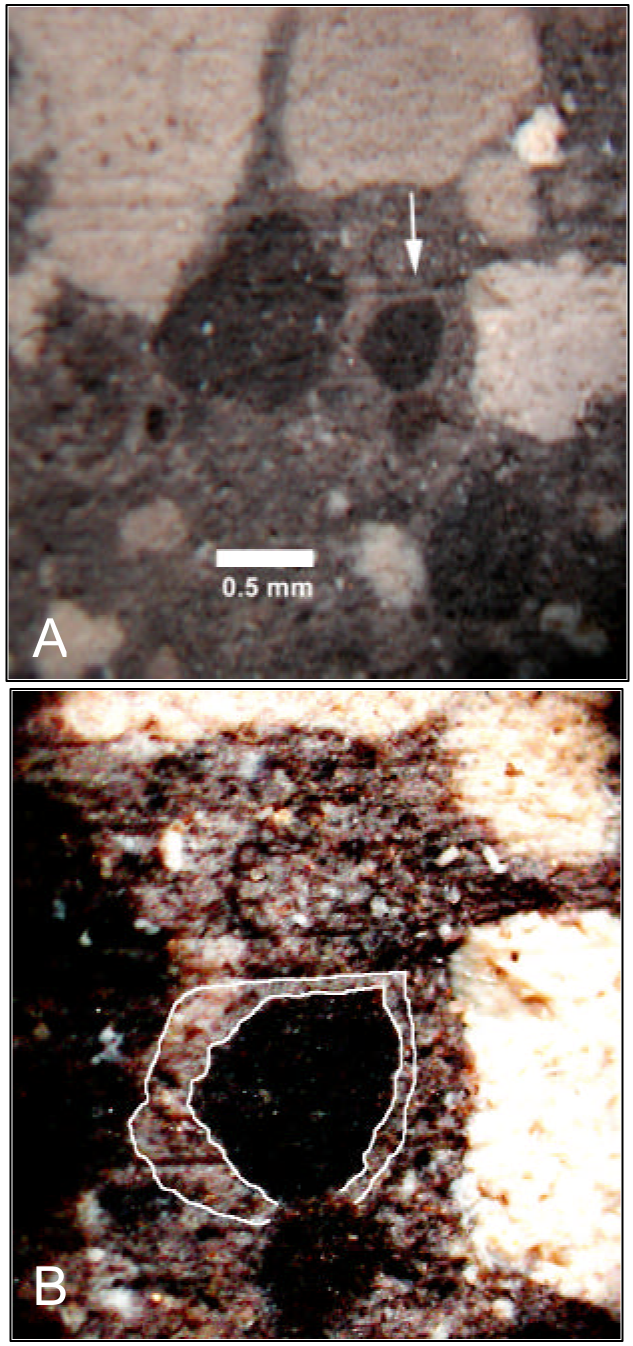

Figure 44. A) Photograph of diamictite showing several smectite clasts armored by thin white rinds. B) Close-up photograph of the clast indicated by the arrow. The image has been gamma-corrected to accentuate the rind (outlined). These clasts appear similar to volcanic or impact lapilli.

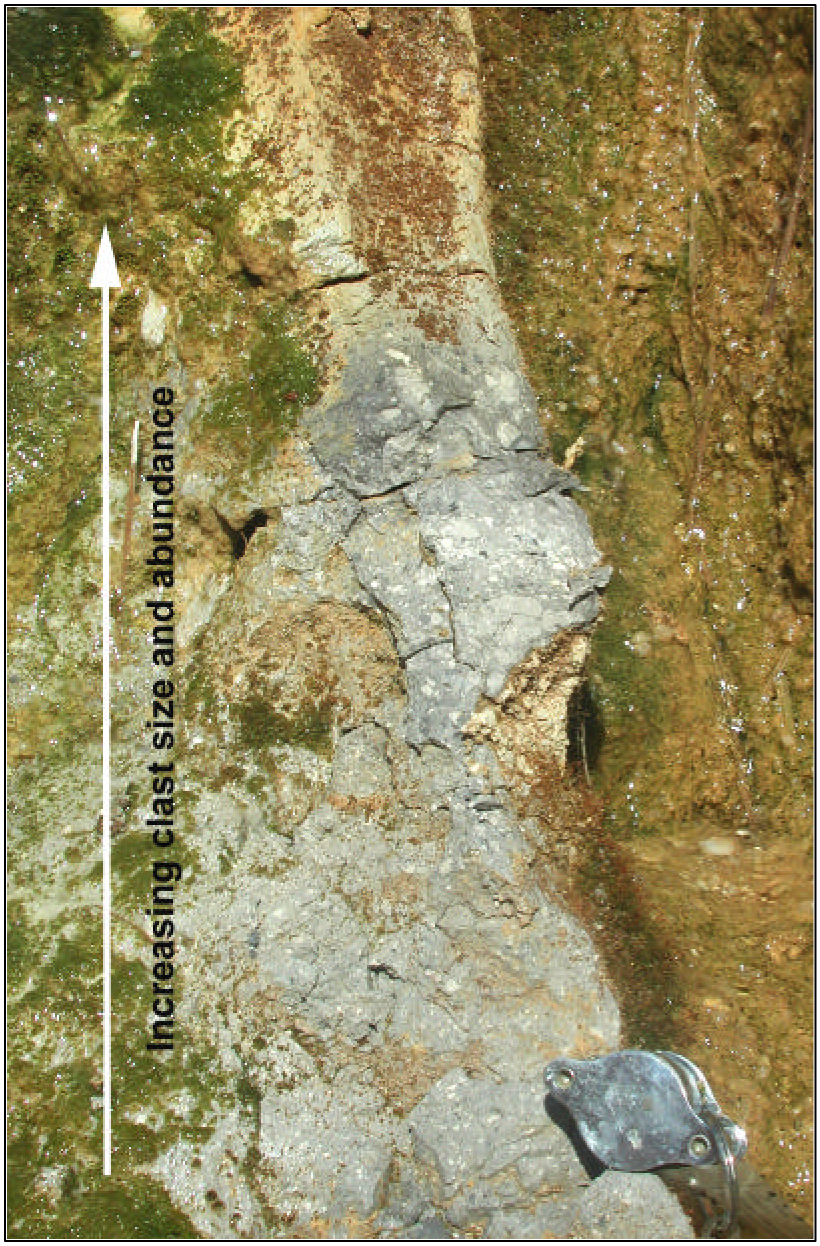

Figure 45. Photograph of the diamictite where it exhibits reverse grading. Both the abundance and size of the clasts appear to increase upward in the unit.

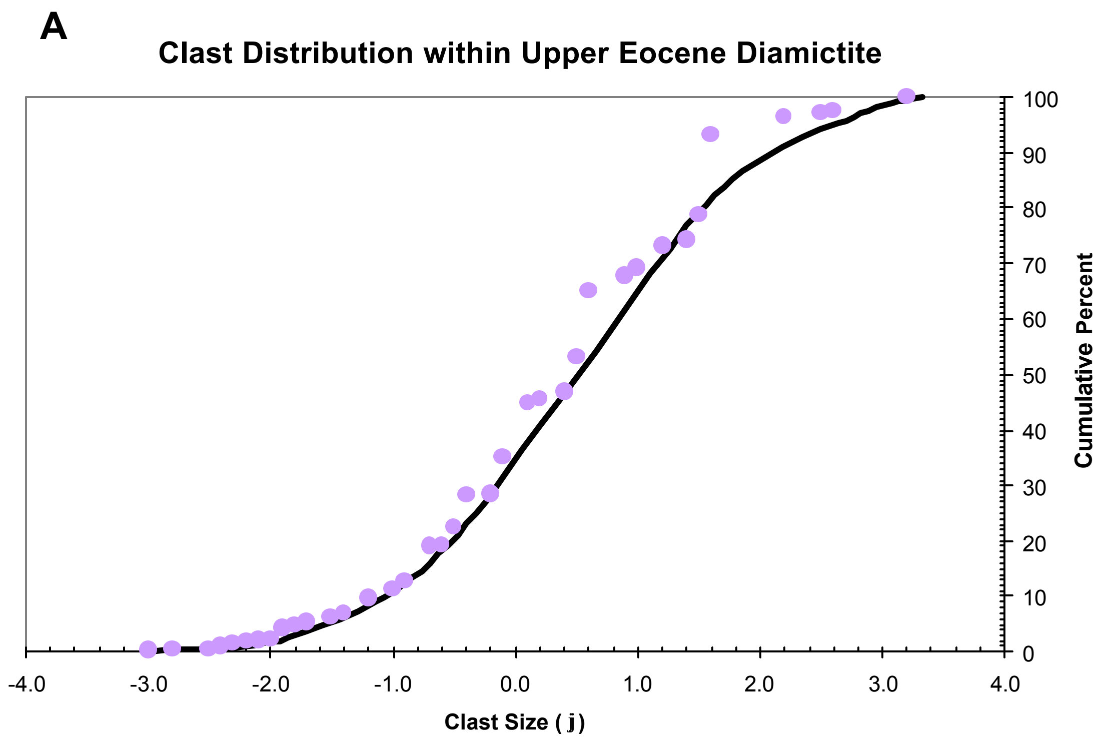
A
Clast Distribution within Upper Eocene Diamictite
100
90
80
70
60
50
40
30
20
10
0
Cumulative Percent
-4.0
-3.0
-2.0
-1.0
0.0
1.0
2.0
3.0
4.0
Clast Size (j)

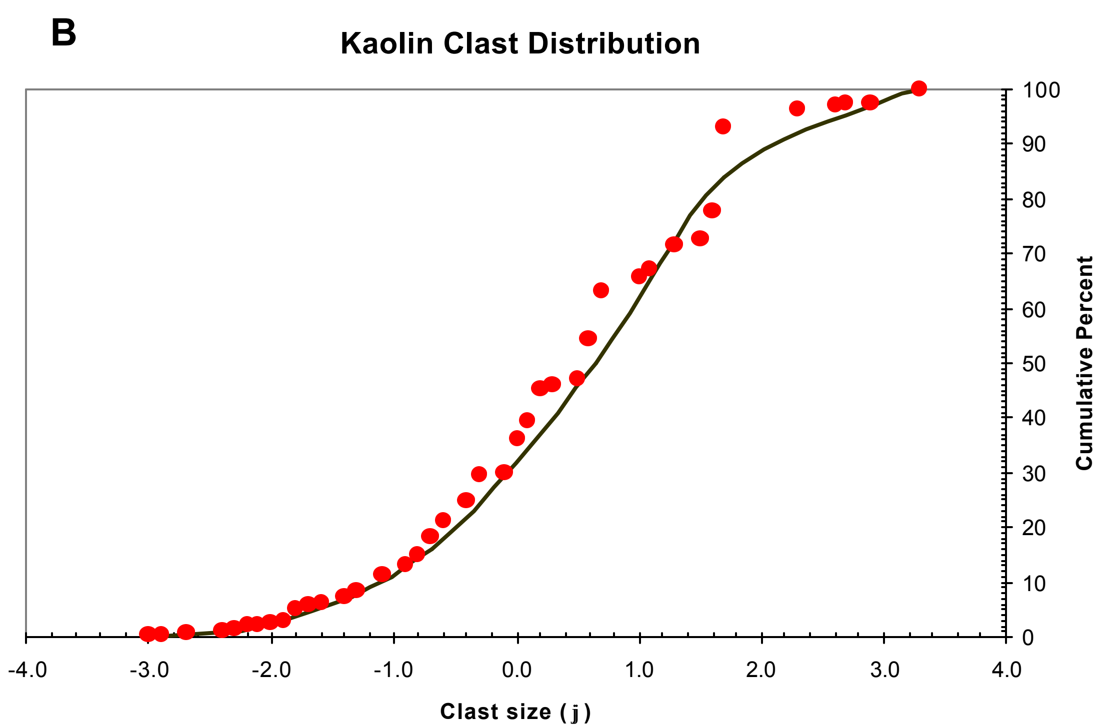
B
Kaolin Clast Distribution
100
90
80
70
60
50
40
30
20
10
0
Cumulative Percent
-4.0
-3.0
-2.0
-1.0
0.0
1.0
2.0
3.0
4.0
Clast size (j)

C

Smectite Clast Distribution

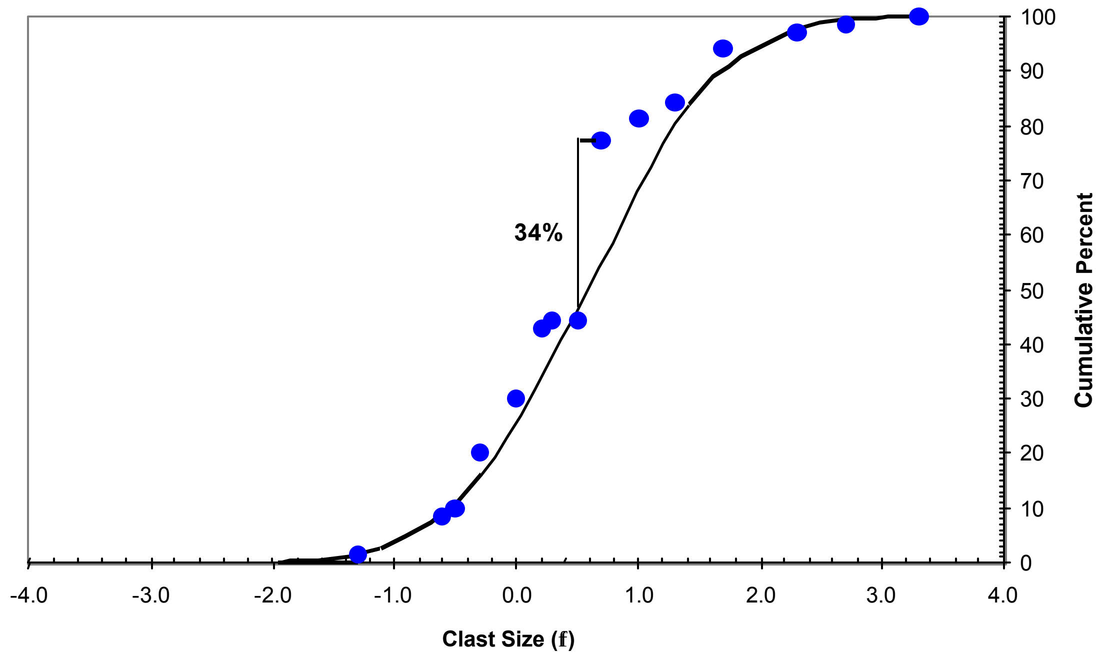

D

Comparison of Clast Distributions

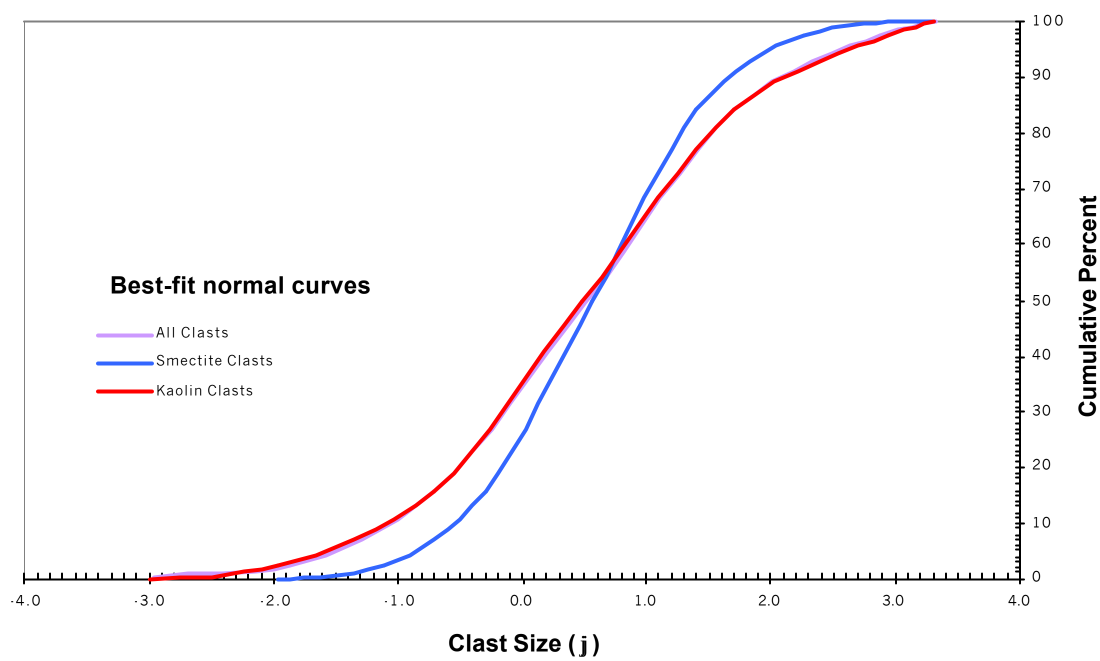

Figure 46. Clast-size-frequency plots illustrating the distribution of compositionally distinct clasts within the diamictite. A) The distribution of all clasts is approximated well by a normal distribution (solid curve) having a mean diameter of 0.53ϕ and standard deviation of approximately 0.90 ϕ, indicative of relatively poor sorting (Boggs, 1995; Prothero and Schwab, 1996). B) The distribution of kaolin clasts is approximated by a similar curve. C) A normal curve modeled to best fit the population of smectite clasts has a mean diameter of 0.60ϕ and standard deviation of approximately 0.71 ϕ, indicative of overall better sorting. Importantly, the distribution of smectite clasts close to the mean (0.60ϕ – 0.80ϕ) shows a steep departure from the model curve. 34 % of the clasts fall within that range (0.57 mm to 0.66 mm). D) Best-fit normal curves for each population displayed together for comparison.

emplacement. Photometric analyses were used to collect clast-size-frequency data. The total population of clasts (Figure 46A) can be approximated very well by a normal distribution having a mean clast diameter of 0.53ϕ (0.70 mm) and a standard deviation, or sorting coefficient, of approximately 0.90ϕ.[4] The population of kaolin casts alone (Figure 46B) can be approximated by the same distribution. The population of smectite clasts (Figure 46C), however, shows markedly better sorting. The best-fit normal distribution has a mean clast diameter of 0.60ϕ (0.66 mm) and a sorting coefficient of approximately 0.71ϕ. Moreover, the population deviates sharply from the model normal distribution between approximately 0.6ϕ and 0.8ϕ. More than one-third of the smectite clasts have diameters in that range — between 0.57 mm and 0.66 mm. In general, the smectite clasts also appear more rounded than kaolin clasts of comparable size. And as mentioned before, the diameters of smectite clasts nearly are restricted to less than two millimeters while larger, even centimeter-scale, kaolin clasts are not uncommon (see Figure 43).

Many of the kaolin clasts could have been derived directly from eroding the underlying Huber Formation. Certainly some exposures seem to show evidence that the Huber Formation clays were ripped up and entrained in the diamictite deposit (Figure 47). In addition to the noted differences in size, sorting, and roundness, the primary problem with the smectite clasts being produced in a similar manner is the location of their source. Clearly, they were not plucked from the kaolin unit, and there are no

---

[4] The mean clast size and standard deviation, or sorting coefficient, is determined graphically from the cumulative size-frequency plot following the common methods outlined by Boggs (1995, p. 86-89) and Prothero and Schwab (1996, p. 86-91).

Figure 47. Photograph of the contact between the white Huber Formation kaolin and the gray diamictite. It appears that the kaolin clasts were ripped-up from the surface of the underlying clays and entrained in the diamictite.

obvious landward or basinward deposits of extensive smectitic clays that predate the diamictite. These observations lead to the hypothesis that the smectite clasts were deposited in a fundamentally different style than the kaolin clasts from a potentially far removed and enigmatic source.

Just as puzzling is the type of depositional environment that existed when the diamictite was emplaced. One important clue may be the observation that material from the diamictite penetrates deep stump holes and root traces, at least as deep as a meter or two, into the top of the Huber Formation. Large numbers of stump holes can be seen across the floors of some kaolin mines where the dark gray breccia contrasts against the white commercial-grade kaolin (Figure 48). It seems implausible that the stump holes and root traces could have remained open, especially in such a uniform manner, for very long in a subaqueous, marine environment without collapsing or filling with sediment. Therefore, it seems likely that the trees had been absent only a short period of time before the diamictite filled the cavities. Carbonized logs also commonly are preserved along this horizon (M. Duncan, personal communication, 2003). The evidence suggests that the diamictite was emplaced rapidly into a terrestrial environment. Identifying the catalyst for a regionally extensive debris flow *landward* of the Late Eocene shoreline in Georgia is also problematic.

Goethite spherules: Evidence of impact?

The solution to each of those mysteries was suggested by the discovery of tiny goethite spherules (Figure 49) interspersed through the matrix. Typically the bright orange spherules are about 100 to 500 μm in diameter. Although some of the spherules

Figure 48. Photograph (contrast-enhanced) of large stump holes in the top of the Huber Formation uniformly filled with the diamictite breccia. Only a small number of the observed holes are outlined in the image. Note thesis advisor for scale (approximately 1.7 meters tall).

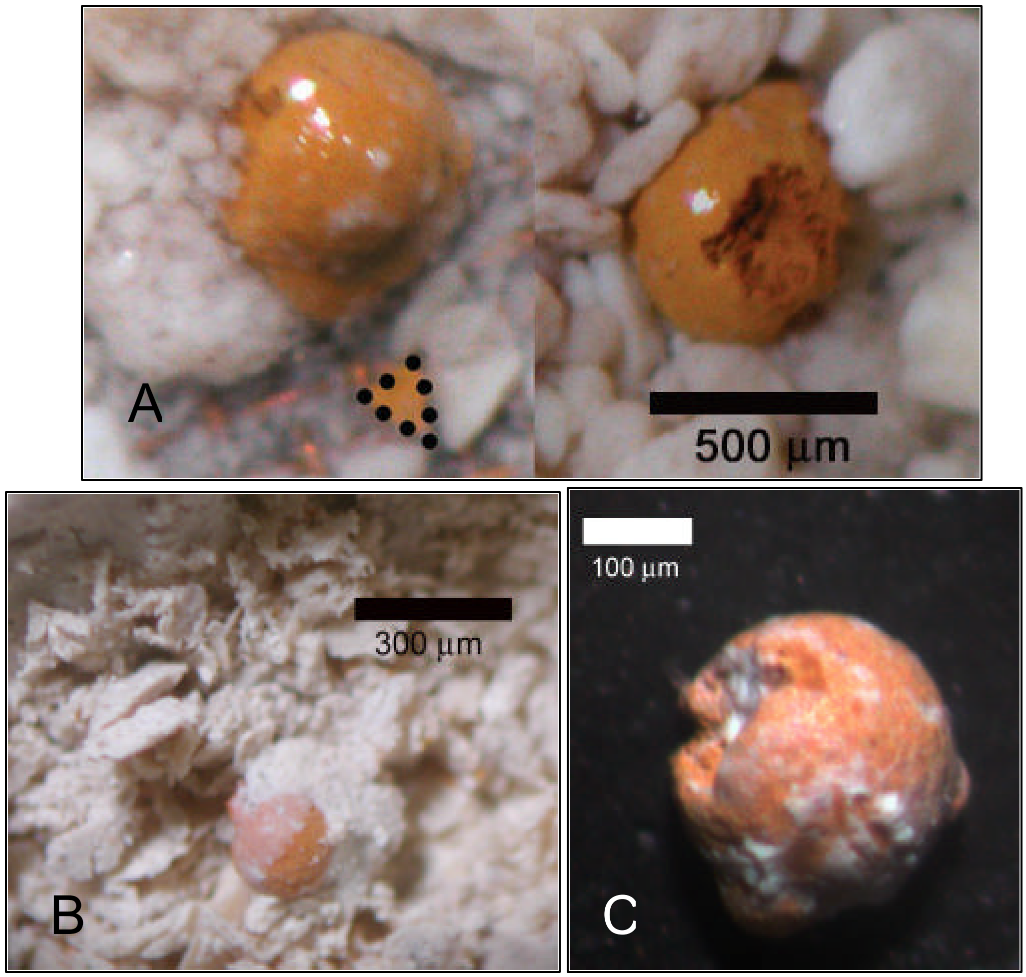

Figure 49. Photographs of goethite spherules. A) Two spherules with teardrop-like shapes. The left sphere had a delicate tapered end (outlined in dots) that has detached. The right sphere exhibits a fibroradial internal structure. B) A bulb-shaped spherule. C) A rounded spherule with several bulbous protrusions.

are quite round, most have tapered ends (Figure 49A) or bulb-like protrusions (Figures 49B and 49C). Spherules are common in marine clays (Berner, 1970), including the Twiggs Clay (Horwath, 1990), where iron oxides have replaced framboidal pyrite. However, the spherules found within the diamictite do not have obvious framboidal textures (compare Figures 50A and 50B). Internally, they appear to be constructed of fibrous blades of goethite arranged in radial patterns (Figure 50C). Similar textures may result from the rapid crystallization of silicate melts (Montanari et al., 1983). The teardrop morphologies of many of the goethite spherules are reminiscent of tektites and microtektites. They are very similar, internally and externally, to goethite spherules found within the K-T boundary clay at Agost, Spain (Figure 51). The common "wart-like" protrusions, observed in both groups of spherules, also are a ubiquitous feature of altered K-T impact spherules in Belize (Pope et al., 1999).

The Agost spherules are believed to have formed as the result of condensation from a vapor plume associated with the Chicxulub impact (Martinez-Ruiz et al., 1997). Texturally, the Agost spherules are similar to clinopyroxene (cpx) spherules found in Upper Eocene deep-ocean sediments, and they may have originally condensed as pyroxene (Martinez-Ruiz et al., 1997). If the Spanish spherules are altered cpx spherules, or microkrystites, the goethite spherules associated with the diamictite also might be altered microkrystites. Perhaps they represent a portion of the Upper Eocene cpx spherule strewn field. B. P. Glass (personal communication, 2003) agreed that the goethite spherules appear similar to some microkrystites.

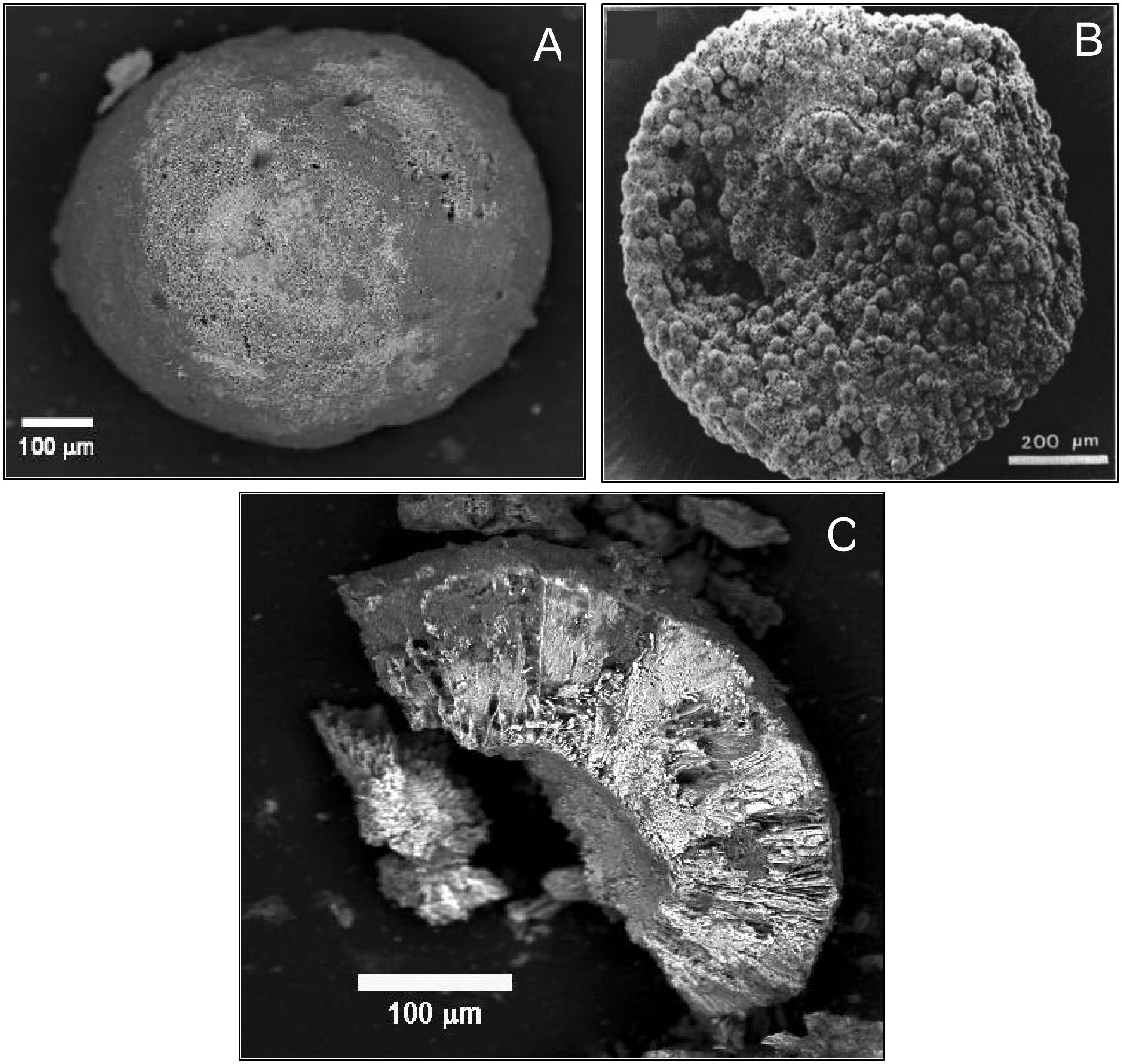

Figure 50. A) Backscattered electron photomicrograph of goethite spherule showing a smooth surface dominated by patches of clay (dark) and tiny crystals (bright). B) For comparison, a scanning electron photomicrograph of framboidal pyrite replaced by iron oxides (from Martinez-Ruiz et al., 1997). C) Backscattered electron photomicrograph revealing the radial habit of fibrous crystals inside the spherules.

Figure 51. Photograph of several goethite spherules from the K-T boundary at Agost, Spain. These spherules are believed to be altered microkrystites (Martinez-Ruiz et al., 1997) related to the 65 Ma Chicxulub impact. The original material, probably pyroxene, is believed to have condensed from the impact vapor plume (Montanari et al, 1983; Martinez-Ruiz et al., 1997). These spherules are very similar to those found in the Upper Eocene diamictite.

Commonly Upper Eocene cpx spherules are found in fused forms with one or more small blebs attached to the surface of a larger spherule (Figure 52A) (Glass et al., 1985). Similar morphologies are observed in the diamictite spherules (Figure 52B). The fused form shown in Figure 52B is embedded in a larger concretion containing multiple spherules. Agost spherules typically are found cemented together in the same fashion by iron oxides and clay. Although additional geochemical data is needed to prove an impact origin, it seems plausible by comparison with other occurrences of impact-generated goethite spherules that the diamictite spherules could be related to an Upper Eocene impact.

Argument for impact and implications

The evidence suggests that the diamictite was emplaced, at least in some locations, as a subaerial debris flow composed largely of very fine material that was able to entrain blocks and pebbles of the substrate as it moved across the surface. This depositional model is inconsistent with conventional models for deposition on the Late Eocene coast of Georgia. It is understandable that early workers suggested a volcanic hypothesis because the mechanisms required to generate the deposit are atypical of local sedimentary processes. Yet there is no plausible volcanic source for the deposits during the Late Eocene. There was, however, a large hypervelocity impact about 700 kilometers to the northeast. Texturally, the diamictite resembles some known impact surge deposits and debris flows, including the Bunte breccia (Hörz, 1983), the lapilli bed of the Alamo breccia (Warme et al., 2002), and the spheroid bed at the base of the K-T Albion diamictite in Belize (Pope et al., 1999; D. A. King, personal communication, 2003).

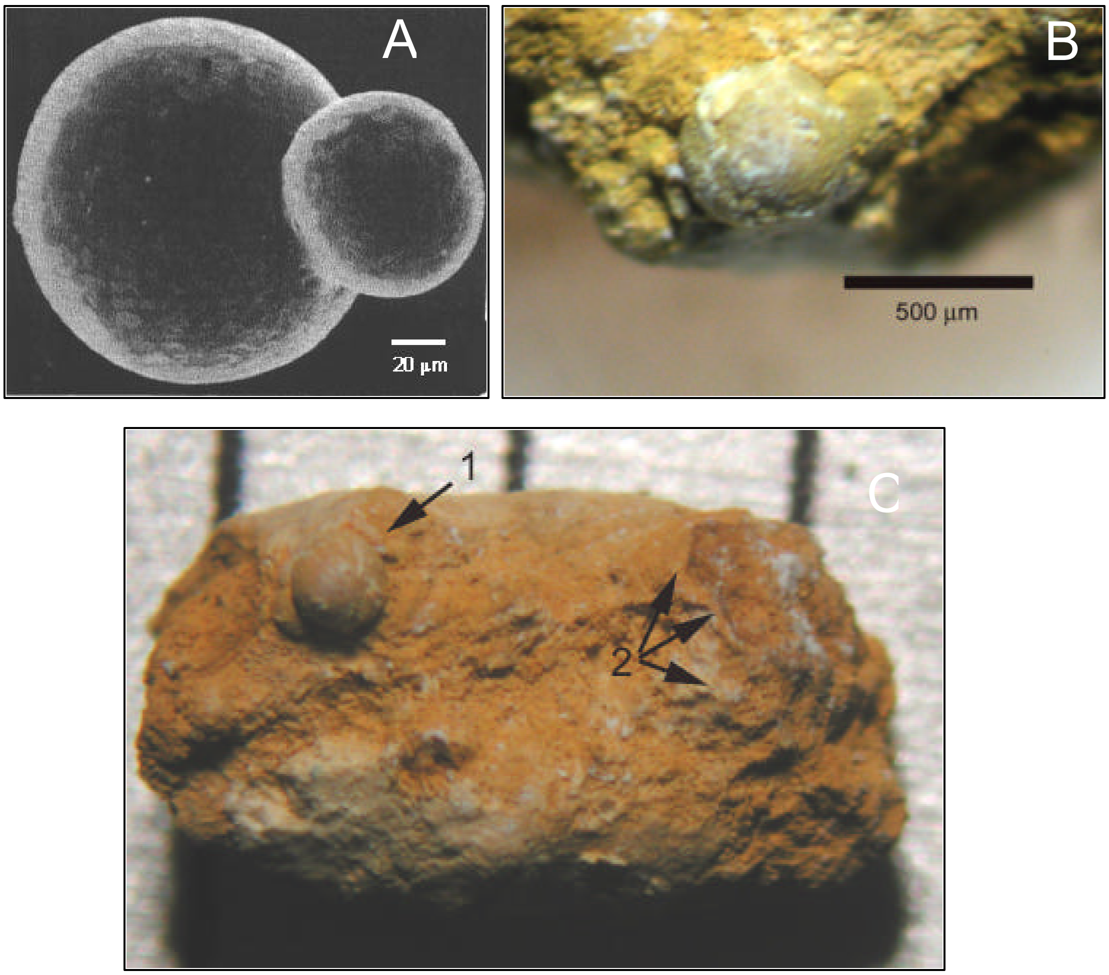

Figure 52. A) Photograph of fused Upper Eocene cpx spherules from the Pacific Ocean (from Keller et al., 1987). B) Possible fused goethite spherules from the Upper Eocene diamictite in east-central Georgia. C) A concretion composed of numerous goethite spherules. The fused pair shown in B (above) is indicated by #1. The outlines of three other spherules are indicated by #2.

Perhaps a ground-hugging debris flow generated by secondary cratering from the Chesapeake Bay impact could have swept south along the shores of South Carolina and Georgia and overrun coastal swamps and forests. Alternatively, seismic shaking or tsunamis associated with the impact would have been capable of triggering mass flows (Claeys et al., 2002).

As it advanced, airfall ejecta would have rained down into the debris flow (Rampino, 1994). The size of the ejecta would have been limited by the distance from the target and by atmospheric sorting (King et al., 2003). If the smectite clasts represent the altered remnants of tektite glass, that could explain why they are relatively well sorted and why they have an upper size limit significantly smaller than the other clasts.

Impacts into wet targets, such as the Chesapeake Bay impact, may produce accretionary lapilli (Figure 53) as the moist debris collides within the impact plume (Masaitis, 2001). These lapilli are known from many wet-target impacts but none have been reported with Chesapeake Bay ejecta. The armored smectite clasts shown in Figure 44 resemble those lapilli. They have a very fine outer shell surrounding a granular clay core that might have been a mixture of impact glass and other debris.

If the diamictite does represent an impact-generated debris flow deposit, it would have important implications regarding the environmental effects of the impact on southeastern North America. It also could have important consequences for understanding the origin of the cpx spherules. The cpx spherules generally are believed to have been produced by the Popigai (Siberia) impact (Whitehead et al., 2000) no more than 100,000 years (Keller et al., 1987), and as little as three to five thousand years (Glass and Koeberl, 1999), before the Chesapeake Bay collision. In the Pacific, they are found at least 15

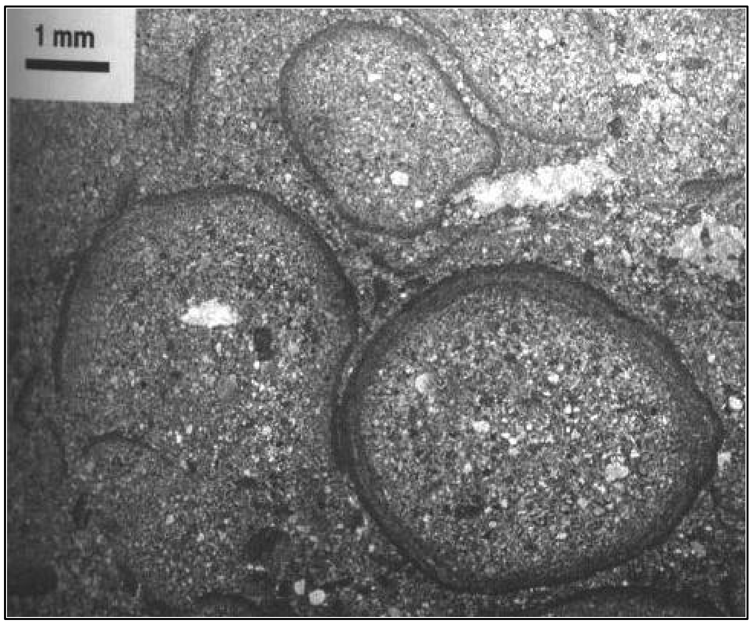

Figure 53. Accretionary lapilli from the Alamo breccia formed by an impact into a marine environment (from Warme et al., 2002).

centimeters below the Chesapeake Bay horizon. However in the North Atlantic, specifically at ODP Site 612, the cpx spherules are found in the bottom few centimeters of a submarine debris flow that contains Chesapeake Bay ejecta (McHugh et al., 1998). McHugh et al. (1998) suggest that the cpx spherules were reworked into the base of a younger debris flow caused by the Chesapeake Bay event. Yet if the goethite spherules in the diamictite represent the cpx spherules, it seems unlikely that they would have survived on the land surface very long before they had to have been incorporated into the debris flow. This suggests the possibilities that either the cpx spherules are not associated with Popigai, that cpx spherules were produced by both impacts, or that the Popigai and Chesapeake Bay impacts were much more closely spaced in time than most authors suggest.

Farley et al. (1998) have argued, based on anomalously high abundances of ^{3}He in pelagic sediments, that the Late Eocene was marked an episode of increased cometary activity in the inner solar system that may have persisted three million years. During that time, the earth could have been bombarded by numerous large bolides in addition to those that formed the Chesapeake Bay and Popigai structures. Therefore, it also is possible that the diamictite and the goethite spherules, if they have an impact origin, are related to as yet undiscovered craters.

CHAPTER 6

CONCLUSION

The discovery of quartz grains exhibiting micro-fabrics consistent with planar deformation features, or PDF's, indicative of shock metamorphism, along with other possible impact ejecta, in a sand deposit at the base of the Upper Eocene Twiggs Clay and Irwinton Sand (Dry Branch Formation) in east-central Georgia suggests that the horizon preserves the record of a major hypervelocity impact. Although several major impacts occurred during the Late Eocene (Whitehead et al., 2000) and an as yet undiscovered crater cannot be ruled out as the source of the debris; the Chesapeake Bay impact is the closest to the southeastern Coastal Plain and probably produced the majority of ejecta reaching the shores of Georgia. The horizon likely represents the elusive source stratum for Georgia tektites and its identification finally may lead to the recovery of *in situ* georgiaites. Considerable work remains to be done to fully characterize the shocked quartz and other possible ejecta deposits including an unusual diamictite which may represent an impact-generated debris flow. Future results may lead to significant strides in understanding the dynamics of the Chesapeake Bay impact and marine impacts in general. Stratigraphers and paleontologists should now attempt to correlate the impact layer throughout the Coastal Plain and characterize the ecological and sedimentological changes that occur across the horizon.

Concluding comment regarding the "Age Paradox"

If as this study suggests, the Chesapeake Bay impact horizon does lie at the base of the Twiggs Clay and Irwinton Sand, someone may question why no tektites have been found in or "on" sediments deposited between the impact horizon and the Tobacco Road Sand. The solution rests in the nature of the units directly overlying the impact horizon. Both the Twiggs Clay and Irwinton Sand were deposited in marine basins (Huddlestun and Hetrick, 1986). These units generally would have covered and protected the impact horizon rather than excavating materials from it. When sea level fell near the beginning of the Oligocene (Prothero, 1994), the post-impact units would have been exposed to significant fluvial erosion for the first time. Only then could significant numbers of tektites have been eroded. Therefore, it should not be alarming that tektites, or other impact materials, are not found within the Twiggs Clay or Irwinton Sand. McCall (2001) eloquently explains why, for similar reasons, the "Age Paradox" associated with many strewn fields should not be a mystery.

Large water-worn pebbles, deep channels, and lateral accretion surfaces are common features in the Tobacco Road Sand and probably indicate that those units were deposited during the Oligocene regression. It is not inconceivable that some Oligocene rivers cut down into the impact horizon and that the Tobacco Road Sand actually contains some redeposited georgiaites. However, it appears that more-modern river systems have been most effective at excavating below the Twiggs Clay (Albin, 1997b). That would explain why most georgiaites are found in recent alluvium. Even now the total area of natural Eocene exposures along the walls of most major drainage systems is quite small (see Figure 3). That is probably why georgiaite finds remain relatively rare.

Addendum

The recent publication of magnetostratigraphic results by Poag et al. (2003) necessitates a brief update to this thesis. They conclude that the Chesapeake Bay impact took place during Chron C16n.2n. Therefore, the impact occurred between 35.7 and 36.3 Ma, according to the Berggren et al. (1995) timescale (Edwards and Powars, 2003). That would mean that the average ages reported for georgiaites [35.2 Ma (Albin, 1997a)] and other North American tektites [35.5 Ma (Glass et al., 1986)], assuming that they were produced by the Chesapeake Bay event, are slightly too young. However, the discrepancy would be consistent with the loss of some radiogenic argon while the glasses have been buried (Albin, 1997a), or it may simply reflect the accuracy limits inherent to the radiometric dating techniques.

The Chesapeake Bay event must have occurred toward the more recent end of the 35.7 to 36.3 Ma range because the fall-back breccia matrix within the impact structure (Poag and Aubry, 1995; Poag et al., 2003; L. E. Edwards, personal communication, 2003) and the microtektite-bearing layer in deep-sea cores (Albin, 1997a; Kyte, 2000; Poag et al., 2003) both contain nannofossils indicative of zone NP19-20. That zone correlates to 34.2 to 36.0 Ma on the Berggren et al. (1995) timescale (Parmley and Holman, 2003). Therefore, the impact occurred between approximately 35.7 and 36.0 Ma.

It then follows from the biostratigraphic and radiometric age constraints summarized in Chapter 1 that the impact most likely occurred during or shortly before deposition of the upper part of the Clinchfield Sand. That timeline is consistent with the discovery of impact ejecta in the coarse sands immediately below the base of the Twiggs Clay in east-central Georgia.

REFERENCES

Albin, E.F, Georgiaites tektite geochemistry and stratigraphic occurrence in east-central Georgia, Ph.D. dissertation, 302 pp., Univ. of Georgia, Athens, 1997a.

Albin, E.F., Redistribution of Georgia tektites as channel lag deposits (abstract), *Lunar Planet. Sci., 28*, Abstract #1274, 1997b.

Albin, E.F., M.D. Norman, M.F. Roden, Major and trace element compositions of georgiaites: Clues to the source of North American tektites, *Meteor. Planet. Sci., 35*, 795-806, 2000.

Albin, E.F. and J.M. Wampler, New potassium-argon ages for georgiaites and the upper Eocene Dry Branch Formation (Twiggs Clay Member): Inferences about tektite Stratigraphic occurrence (abstract), *Lunar Planet. Sci., 27*, 5-6, 1996.

Alexopoulos, J. S., R.A.F. Grieve, and P.B. Robertson, Microscopic lamellar deformation Features in quartz: Discriminative characteristics of shock-generated varieties, *Geology, 16*, 796-799, 1988.

Alvarez, W., F. Asaro, H.V. Michel, and L.W. Alvarez, Iridium anomaly approximately synchronous with terminal Eocene extinctions, *Science*, *216*, 886-888, 1982.

Alvarez, W., F. Asaro, and M. Montanari, Iridium profile for 10 million years across the Cretaceous-Tertiary boundary at Gubbio (Italy), *Science*, *250*, 1700-1702, 1990.

Barnouin-Jha, O. S. and P.H Schultz, Lobateness of impact ejecta deposits from atmospheric interactions, *J. Geophys. Res., 103*, 25,739-25,756, 1998.

Bauluz, B., D.R. Peacor, and W.C. Elliot, Coexisting altered glass and Fe-Ni oxides at the Cretaceous-Tertiary boundary, Stevns Klint (Denmark); direct evidence of meteorite impact, *Earth. Planet. Sci. Letters, 182*, 27-136, 2000.

Berggren, W.A., D.V. Kent, M-P. Aubry, and J. Hardenbol, *Geochronology, time scales and global stratigraphic correlation*, 386 pp., SEPM (Society for Sedimentary Geology), Tulsa, Oklahoma, 1995.

Berner, R. A., Sedimentary pyrite formation, *Am. J. Sci., 268*, 1-23, 1970.

Bice, D.M., C.R. Newton, S. McCauley, P.W. Reiners, and C.A. McRoberts, Shocked quartz at the Triassic-Jurassic boundary in Italy, *Science, 255*, 443-446, 1992.

Boggs, S., *Principles of Sedimentology and Stratigraphy*, 774 pp., Prentice-Hall, Inc., Englewood Cliffs, New Jersey, 1995.

Bloss, F.D., *The spindle stage: principles and practice,* 340 pp., Cambridge University Press, New York, 1981.

Bohor, B.F., Shocked quartz and more; Impact signatures in cretaceous/Tertiary boundary clays, in *Global Catastrophes in Earth History: Geol. Soc. Am., Special Paper247*, edited by V.L. Sharpton and P. D. Ward, 335-347, 1990.

Boslough, M.B, Shock modification and chemistry and planetary geologic processes, *Ann. Rev. Earth Planet. Sci, 19,* 101-130, 1991.

Boslough, M.B. and R.T. Cygan, Shock-enhanced dissolution of silicate minerals and chemical weathering on planetary surfaces, *Proc. Lunar Planet. Sci. Conf. 18th,* 443-453, 1988

Bourgeois, J., T.A. Hansen, P.L. Wieberg, and E.G. Kauffman, A tsunami deposit at the Cretaceous-Tertiary Boundary in Texas, *Science*, *241*, 567-569, 1988.

Carter, B.D., J.P. Manker, and J.R. Bryan, Facies and Paleogeography in Paleogene Carbonate Facies and Paleogeography of the Dougherty Plain Region, in *Ga.Geol. Soc.Guidebook* , *15*, pp. 29-51, 1995.

Carver, R.E., Stratigraphy of the Jackson Group in eastern Georgia, *Southeast. Geol., 14*, 153-181, 1972.

Claeys, P., W. Kiesslin, and W. Alvarez, Distribution of Chicxulub ejecta at the Cretaceous-Tertiary boundary, in *Catastrophic Events and Mass Extinctions: Impacts and Beyond, Geol. Soc. Am. Special Paper 356*, edited by C. Koeberl and K.G. MacLeod, pp. 55-68, 2002

Cordier, P., S. Vrana, and J. C. Doukhan, Shock metamorphism in quartz at Sevetin and Susice (Bohemia)?; a TEM investigation, *Meteoritics, 29*, 98-99, 1994.

Crawford, T. J., V.J. Hurst, and L.D. Ramspott, Extrusive volcanics and associated dike swarms in east-central Georgia, in *Geol. Soc. Am. Southeast. Sect, Guidebook, Fieldtrip 2*, pp. 35-47, 1966.

Edwards, L.E., N.O. Frederiksen, J.M. Self-Trail, and W.C. Poag, Paleontology of crater-fill deposits, Chesapeake Bay impact structure, Virginia (abstract), *GSA Abstracts with Programs, Abstract # 204-5*, 2002.

Edwards, L.E. and D.S. Powars, Impact damage to dinocysts from the Late Eocene Chesapeake Bay event, *Palaios*, *18*, 275-285, 2003

Edwards, L.E. and J.M Self-Trail, Shocking news — Impact effects on marine microfossils, Chesapeake Bay impact structure, Virginia (abstract), *Eos. Trans. AGU, 83(19), Spring Meet. Supp.,* Abstract # T21A-04, 2002.

Engelhardt, W. v and W. Bertsch, Shock induced planar deformation structures in quartz from the Ries crater, *Contrib. Min. Petrol., 20*, 203-234, 1969.

Farley, K.A., A. Montanari, E.M. Shoemaker, and C.S. Shoemaker, Geochemical evidence for a comet shower in the Late Eocene: *Science*, *280*, 1250-1253, 1998.

French, B.M., *Traces of Catastrophe*, 120 pp., Lunar and Planetary Institute, Houston 1998.

Furcron, A.S., Geologic age of the tektite shower and its associated rocks of the Georgia Coastal Plain, Ga. Min. Newl., 14, 115-119.

Georgia Geologic Survey, *Digital Geologic Map of Georgia*, Georgia Department of Natural Resources, Atlanta, 1999.

Gibson, T. G. and K. M. Towe, Eocene volcanism and the origin of horizon A, *Science, 172*, 152-154, 1971.

Glass, B. P., C. A. Burns, J. R. Crosbie, and D. L. Du Bois, Late Eocene North American microtektites and clinopyroxene bearing spherules, *Proc. Lunar Planet. Sci. Conf. 16th, J. Geophys. Res., 90*, D175-D196, 1985.

Glass, B.P., C.M. Hall, and D. York, $^{40}Ar/^{39}Ar$ laser probe dating of North American tektite fragments from Barbados and the age of the Eocene – Oligocene boundary, *Chem. Geol*., *59*, 181-186, 1986.

Glass, B.P. and C. Koeberl, Ocean Drilling Project Hole 689B spherules and upper Eocene microtektite and clinopyroxene-bearing spherule strewn fields, *Meteor. Planet. Sci*., *34*, 185–196, 1999.

Glass, B.P., C. Koeberl, J.D. Blum, and C.M.G. McHugh, Upper Eocene tektite and impact ejecta layer on the continental slope off New Jersey, *Meteor. Planet Sci., 33*, 229-241, 1998.

Glass, B.P., S. Liu, and P.B. Leavens, Discovery of a naturally-occurring, shock-produced, high-pressure zircon polymorph (abstract), *Lunar Planet. Sci,* 32, Abstract # 1155, 2001.

Glass, B.P., S. Liu, and P.B. Leavens, Reidite; an impact-produced high-pressure polymorph of zircon found in marine sediments, *Am. Mineralogist, 87*, 562-565, 2002.

Glass, B.P. and J. Wu, Coesite and shocked quartz discovered in the Australian and North American microtektite layers, *Geology*, *21*, 435-438, 1993.

Goltrant, O., H. Leroux, J.C. Doukhan, and P. Cordier, Formation mechanisms of planar deformation features in naturally shock quartz, *Phys. Earth Planet. Inter*., 74, 219-240, 1992.

Grieve, R.A.F., F. Langenhorst, and D. Stöffler, Shock metamorphism of quartz in nature and experiment: II. Significance in geoscience*, Meteor. Planet. Sci, 31*, 6-35, 1996.

Hampton, M.A., Buoyancy in debris flows, *J. Sed. Petrol.*, *49*, 753-758, 1979.

Harris, R.S., Re-evaluating the origin of an Upper Eocene diamictite in the Coastal Plain of east-central Georgia: An impactoclastic layer? (abstract) , *Lunar. Planet. Sci., 34*, Abstract # 1965, 2003.

Harris, R.S., M. Duncan, S. M. Holland, M. F. Roden, and P. A. Schroeder, Probable shocked quartz as evidence for an Upper Eocene impact horizon in Coastal Plain strata, Warren County, Georgia, U.S.A. (abstract), *Geol. Soc. Am. Abstr. Programs,* Abstract #41931*,* 2002.

Horwath, R.M., Late Eocene and early Oligocene calcareous nannofossils and search for microtektites from central Georgia, M.S. Thesis, 127 pp., Univ. of Georgia, Athens, 1990.

Hörz, F., R. Ostertag, and D.A. Rainey, Bunte breccia of the Ries: Continuous deposits of large impact craters, *Rev. Geophys. And Space Phys., 21*, 1667-1725., 1983.

Huddleston, P.F. and J.H. Hetrick, Upper Eocene stratigraphy of central and eastern *Georgia, Ga. Geol. Sur. Bull, 95*, 78pp., 1986.

Hurst, V.J. and S.M. Pickering, Cretaceous-Tertiary strata and kaolin deposits in the inner Coastal Plain of Georgia, in Upper Cretaceous and Cenozoic Geology of the southeastern Atlantic Coastal Plain, in *28th Internat. Geol. Cong., Field Trip Guidebook T172*, edited by W.B. Harris, V.J. Hurst, P.G. Nystrom, and L.W. Ward, pp. 2-22, 1989.

Izett, G.A., W.A. Cobban, J.D. Obradovich, and M.J. Kunk, The Manson Impact Structure: Ar/Ar age and its distal impact ejecta in the Pierre Shale in south-eastern South Dakota, *Science*, *262*, 729-731, 1993.

Keller, G., S. L. D'Hondt, C. J. Orth, J. S. Gilmore, P. Q. Oliver, E. M. Shoemaker, and E. Molina, Late Eocene impact microspherules: Stratigraphy, age, and geochemistry, *Meteoritics, 22*, 25-60, 1987.

King, D.T., L.W. Petruny, K. O. Pope, and A.C. Ocampo, The Albion impactoclastic breccia (Albion diamictite bed): Cumulative grain-size frequency curves and possible modes of emplacement (abstract), *Lunar. Planet. Sci., 34*, Abstract # 1995, 2003.

King, E.A., Field investigation of Georgia tektites and description of new specimens, *Ga. Min. Newl., 15*, 84-89.

Klein, C. and C.S. Hurlbut, *Manual of Mineralogy*, 681 pp., John Wiley and Sons, New York, 1999.

Koeberl, C., New estimates of area and mass for the North American tektite strewn field, *Proc. Lunar Planet. Sci. Conf. 19th,* 745–751, 1989.

Koeberl, C., Impact cratering: The mineralogical and geochemical evidence, in *Proceedings: The Ames Structure and Similar Features, Oklahoma Geological Survey Circular 100*, edited by K. Johnson and J. Campbell, pp. 30-54, 1997.

Koeberl, C., C.W. Poag, W.U. Reimold, and D. Brandt, Impact origin of the Chesapeake Bay structure and the source of the North American tektites, *Science, 271*, 1263-1268, 1996.

Kyte, F.T., Identification of late Eocene impact deposits at ODP Site 1090, in *Proc. OPD, Sci. Results, 177,* edited by R. Gersonde, D.A. Hodell, and P. Blum, pp.1-9, 2001.

Langenhorst, F. and Clymer, A.K., Characteristics of shocked quartz in late Eocene impact ejecta from Massignano (Ancona, Italy): Clues to shock conditions and source Crater, *Geology, 24*, 487-490, 1996.

Leroux H., W.U. Reimold, and J.C. Doukhan , A TEM investigation of shock metamorphism in quartz from the Vrederfort dome, South Africa, *Tectonophysics, 230*, 223-239, 1994.

Liu, L.G., High-pressure phase transformations in baddeleyite and zircon, with geophysical implications, Earth *Planet. Sci. Letters, 44*, 390-396, 1979.

Liu, S., F.T. Kyte, and B.P. Glass, Discovery of coesite and shocked quartz associated with the Upper Eocene cpx spherule layer (abstract), *Meteor. Planet. Sci*, *37,* Abstract #5040, 2002.

Martinez-Ruiz, F., M. Ortega-Huertas, I. Palomo, and P. Acquafredda, Quench textures in altered spherules from the Cretaceous-Tertiary boundary layer at Agost an Caravaca, SE Spain, *Sed. Geology, 113*, 137-147, 1997.

Masaitis, V. L., Impact ejecta containing accretionary lapilli (abstract), in *Bolide Impacts on Wet Targets*, *Geol. Soc. Am. Field Forum*, 2001.

McCall, G.J.H., *Tektites in the geological record: showers from the sky*, 256 pp., Geological Society, London, 2001.

McGetchin, T.R., M. Settle, and J.W. Head, Radial thickness variation in impact crater ejecta: implications for lunar deposits, *Earth Planet. Sci. Lett., 20*, 226-236, 1973.

McHugh, C.M.G., S.W. Snyder, and K.G. Miller, Upper Eocene ejecta of the New Jersey continental margin reveal dynamics of Chesapeake Bay impact, *Earth Planet. Sci. Letters, 160,* 353-367, 1998.

Melosh, H.J., *Impact Cratering: A geologic process*, 245 pp., Oxford University Press, New York, 1989.

Melosh, H.J., The physics of crater collapse in saturated media (abstract), in *Bolide Impacts on Wet Targets*, *Geol. Soc. Am. Field Forum*, 2001.

Montanari, A., F. Asaro, H. Michel, and J. Kennett, Iridium anomalies of Late Eocene age at Massignano (Italy), and ODP Site 689B (Maud Rise, Antarctic), *Palaios, 8*, 420-437, 1993.

Montanari, A., R.L. Hay, W. Alvarez, F. Asaro, H. V. Michel, L. W. Alvarez, and J. Smit, Spheroids at the Cretaceous-Tertiary boundary are altered impact droplets of basaltic composition, *Geology, 11*, 668-671, 1983.

Montanari, A. and C. Koeberl, *Impact Stratigraphy: The Italian Record*, 364 pp., Springer-Verlag, Berlin, 2000.

Morgan, J.H. and M.L. Auer, Optical, spectroscopic, and radioactivity studies of zircon, *Am. J. Sci*., *239*, 3405-311, 1941.

Moskow, M.G., Flint Kaolins in the Georgia Coastal Plain, M.S. thesis, 79 pp., Univ. of Georgia, Athens, 1988.

Mossman, D.J., R.G., Grantham, and L. Langenhorst, A search for shocked quartz at the Triassic-Jurassic boundary in the Fundy and Newark basins of the Newark Supergroup, *Can. J. Earth Sci., 35*, 101-109, 1998.

Oberbeck, V.R., The role of ballistic erosion and sedimentation in lunar stratigraphy, *Rev. Geophys. Space Phys.,* 13, 337-362, 1975.

Parmley, D. and J. A. Holman, *Nebrakophis* HOLMAN from the Late Eocene of Georgia (USA), the oldest known North American colubrid snake, *Acta zoologica cracoviensia*, *46*, 1-8, 2003.

Phillips, W.R., *Mineral Optics: Principles and Techniques*, 249 pp., W. H. Freeman and Company, San Francisco, 1971.

Poag, C.W., The Chesapeake Bay bolide impact: a convulsive event in Atlantic coastal plain evolution, *Sedimentary Geology*, *108*, 45-90, 1997.

Poag, C.W., The Chesapeake Bay bolide: modern consequences of an ancient cataclysm, Woods Hole Field Center, United States Geological Survey (http://woodshole.er.usgs.gov/epubs/bolide/index.html), 1998.

Poag, C.W. and M. Aubry, Upper Eocene impactites of the U.S. east coast: Depositional origins, biostratigraphic framework, and correlation, *Palaios, 10*, 16-43, 1995.

Poag, C.W., E. Mankinen, and R.D. Norris, Late Eocene impacts: geologic record, correlation, and paleoenvironmental sequences, in *From Greenhouse to Icehouse: The Marine Eocene-Oligocene Transition*, edited by D.R. Prothero, L.C. Ivany, and E. Nesbitt, pp. 495-510, 2003.

Poag, C.W., J.B. Plescia, and P.C. Moler, Scientific and Technical Abstracts- 1997, Woods Hole Field Center, United States Geological Survey, (http://woodshole.er.usgs.gov/bibliographies/1999/56.html), 1997.

Poag, C.W., D.S. Powars, L.J. Poppe, and R.B. Mixon, Meteoroid mayhem in Ole Virginny: Source of the North American tektite strewn field, *Geology*, *22*, 691-694.

Polsky, C.H. and McHone, J.F., Raman spectroscopic confirmation of metastable cristobalite in melt samples from the Wanapitei impact structure (abstract), *Lunar Planet. Sci. 29*, Abstract # 1471, 1998.

Pope, K. O., A. C. Ocampo, A. G. Fischer, W. Alvarez, B. W. Fouke, C. L. Webster, F. J. Vega, J. Smit, A. E. Fritsche, and P. Claeys, Chicxulub impact ejecta from Albion Island, Belize, *Earth Planet. Sci. Letters, 170*, 351-364, 1999.

Povenmire, H.R., A Georgia tektite worked by local aborigines? *Earth Sci., Sept.-Oct.,* 241, 1975.

Povenmire, H., The parent stratum and distribution of the Georgia tektites, *Meteoritics*, *20,* 795-799, 1985.

Povenmire, H.R., The Georgia tektite strewn field (abstract), *Lunar. Planet. Sci., 26*, 1131-1132, 1995.

Povenmire, H., The distribution of Georgia tektites (abstract), 65th Meeting of the Meteoritical Soc., #5121, 2002.

Povenmire, H., *Tektites: A cosmic enigma*, Self-published, 2003.

Powars, D.S. and T.S. Bruce, The effects of the Chesapeake Bay impact crater on the geological framework and correlation of hydrogeologic units of the lower York-James Peninsula, Virginia, *U.S. Geol. Surv. Prof. Paper.1612*, 33 pp., 2000.

Powars, D.S., C.W. Poag, and R.B. Mixon, The Chesapeake Bay "impact crater," stratigraphic and seismic evidence (abstract), *Geol. Soc. Am. Abstr. Programs*, *25*, A-378, 1993.

Prothero, D.R., *The Eocene-Oligocene transition: Paradise lost*, Columbia Univ. Press, New York, 291 pp., 1994.

Prothero, D.R. and F. Schwab, *Sedimentary Geology*, 575 pp., W.H. Freeman, New York, 1996.

Rampino, M.R., Tillites, diamictites, and ballistic ejecta of impact ejecta, *J. Geol., 102*, 439,-456, 1994.

Sandy, J., R. E. Carver, and T. J. Crawford, Stratigraphy and economic geology of the Coastal Plain of the Central Savannah River area, Georgia, in *Geol. Soc. Am. Southeast. Sect, Guidebook, Fieldtrip 3*, pp. 1-29, 1966.

Schneider, H., R. Vasudevan, and U. Hornemann, Deformation of experimentally shock-loaded quartz powders: X-ray line broadening studies, *Phys. Chem. Min., 1*0, 142-147, 1984.

Schroeder, P. A., R. S. Harris, M. F. Roden, S. M. Holland, and M. Duncan, X-ray diffraction evidence for shocked quartz in Atlantic Coastal Plain deposits, Warren County, Georgia, U.S.A. (abstract), *Geol. Soc. Am. Abstr. Programs,* Abstract #38959*,* 2002.

Schultz, P.H., Atmospheric effects on ejecta emplacement, *J. Geophys. Res., 97*, 11,623-11,662, 1992.

Schuraytz, B.C. and B.O. Dressler, Ballen-structured quartz in glasses of the Wanapitei Impact structure, Ontario, Canada (abstract), *Lunar Planet. Sci*. *28*, 1265-1266, 1997.

Short, N.M, Progressive shock metamorphism of quartzite ejecta from the Sedan nuclear explosion crater*, J. Geol., 78*, 705-732, 1970.

Smith, J.J., A.M. Therriault, and Y. Pan, Ballen quartz from the Deep Bay impact structure, *Meteor. Planet. Sci*, *34* , 110-111, 1999.

Schmitt, R.T., D. Stöffler, and A. Whittman, Shock metamorphism of impactite lithologies of the ICDP Chicxulub drill core YAX-1 (abstract) , *Lunar. Planet. Sci., 34*, Abstract # 1327, 2003.

Spry, A., R. G. Turner, and R. C. Tobin, Optical phenomena associated with Brazil-twin boundaries in quartz, *Am. Mineralogist, 54*, 117-133, 1969.

Stöffler, D. and F. Langenhorst, Shock metamorphism of quartz in nature and experiment: I. Basic observation and theory*, Meteoritics, 29*, 155-181, 1994.

Stöffler, D., J. Wedekind, and G. Polkowski, Experimental hypervelocity impact into quartz sand: distribution and shock metamorphism of ejecta*, J. Geophys. Res., 80*, 4062-4077, 1975.

Stewart, S.T., J.D. O'Keefe, and T.J Ahrens, The role of subsurface ice and water in rampart crater formation (abstract), *AGU Fall Meeting Abstracts*, 2000.

Storzer, D., G.A. Wagner, and E.A. King, Fission track ages and stratigraphic occurrence of Georgia tektites, *J. Geophys. Res., 78*, 4915-4919, 1973.

Todd, S. P., Process deduction from fluvial sedimentary structures, in *Advances in Fluvial Dynamics and Stratigraphy*, edited by P. A. Carling and M. R. Dawson, pp. 299-350, 1996.

Vrana, S., The Sevetin astrobleme, southern Bohemia, Czechoslovakia, *Geologische Rundschau, 76*, 505-528, 1987.

Wampler, J.M., C.W. Elliott, B.W. White, and K.A. Pajewski, The character of glauconite in the Twiggs Clay Member along Elko Road, Houston County, Georgia (abstract), *Geol. Soc. Am. Abstracts*, 2001.

Ward, L.W., Tertiary Stratigraphy of the central Virginia Coastal Plain, in Upper Cretaceous and Cenozoic Geology of the southeastern Atlantic Coastal Plain, in *28th Internat. Geol. Cong., Field Trip Guidebook T172*, edited by W.B. Harris, V.J. Hurst, P.G. Nystrom, and L.W. Ward, pp. 63-100, 1989.

Warme, J. E., M. Morgan, and H-C. Kuehner, Impact-generated carbonate accretionary lapilli in the Late Devonian Alamo Breccia, in *Catastrophic Events and Mass Extinctions: Impacts and Beyond, Geol. Soc. Am. Special Paper 356*, edited by C. Koeberl and K.G. MacLeod, pp. 489-504, 2002.

Westgate, J., Paleoecology and biostratigraphy of marginal marine Gulf Coast Eocene Vertebrate localities, in *Eocene Biodiversity, Unusual Occurrences and Rarely Sampled Habitats: Topics in Geology, 18*, edited by G.F. Gunnell, pp. 263-297 , Kluwer Academic/Plenum, New York, 2001.

Whitehead, J., D A. Papanastassiou, J. G. Spray, R. A.F. Grieve, and G. J. Waaerburg, Late Eocene impact ejecta: geochemical and isotopic connections with the Popigai impact structure, *Earth Planet. Sci. Letters., 181*, 473-487, 2000.

Zwart, P. A., An investigation of the stratigraphic occurrence of Georgia tektites, M.S. Thesis, 87 pp., Univ. of Delaware, Newark, 1978.